EXPERIMENTAL AND THEORETICAL INVESTIGATIONS ON FLUID FLOW IN TWO DIMENSIONS.

by

A. Thom, B.Sc., Ph.D., A.R.T.C.

ProQuest LLC.
789 East Eisenhower Parkway
P.O. Box 1346
Ann Arbor, MI 48106 – 1346

I N D E X.

Introduction.

During 1924 and 1925 the writer carried out a series of experiments on the lift and drag forces experienced by a cylinder rotating in an air stream. In some of these experiments, notably those in which the cylinder formed the core for a series of disks, certain peculiarities were obtained, perhaps the most noteworthy being the very high lift/drag ratio at certain speeds. This work formed part of a thesis presented for the Ph.D. degree in 1926 and none of it appears in this report, but the above-mentioned results indicated the possibilities of the subject.

The most obvious objection to the use of a rotating cylinder instead of an aerofoil is the high drag of the former, but it appears that this drag decreases at the higher rotational speeds. At any rate the profile drag decreases, and if the lift coefficient can be made greater than 2π it will probably become very small.

To advance the problem it seemed necessary to find out how the plain rotating cylinder produces a circulation and so a lift force. The first point tackled was a determination of the pressure distribution round such a cylinder for a variety of speeds. The work was published by The Aeronautical Research Committee (R. & M. No.1082) and forms Part 8 of the present paper. Considerable difficulties beset these experiments and were it necessary to repeat the work it would appear advisable to adopt the indirect method of placing a small static tube or plate near the surface as

was done in the experiments described in Part 10. As it seems certain that it is the boundary layer (stable or unstable) which controls the circulation this was the next region to be investigated. The results are given in Part 10. Measurements were also made in the boundary layer on a stationary cylinder (Part 1) and a study of these led to the boundary layer theory given in Part 2. Parts 1 and 2 have also been published by the A.R.C. (R. & M. No.1176). The arithmetical method developed in Part 2 to solve the boundary layer equations seemed capable of extension, and when, as a result of such an extension, a method of solving the general two-dimensional equations of steady viscous flow had been developed it was natural to try it out on the case of flow past a stationary cylinder. The method seems to be applicable to any continuous boundaries with the exception of multiply connected unsymmetrical regions. The flow past a rotating cylinder belongs to this category and so far a solution for this case has not been achieved. It is hoped, however, that it will be possible to obtain solutions for this and other problems in the near future, but applications of these will necessarily be confined to low values of Reynold's Number. Meanwhile, the experiments on the boundary layer on a rotating cylinder described in Part 10 give an indication of the conditions close to the surface.

The process of solution as described in Part 5 was laborious in the extreme, but it is hoped that it will be possible to obtain solutions for the cylinder for neighbouring values of Reynold's Number with much less labour by a method which is being tried out now by the writer.

To check the solution obtained in Part 5 it was decided to measure the pressure distribution round a cylinder at as low a value of Reynold's Number as possible. Using air it was found impossible to get lower than R = 28 and even this involved a cylinder diameter of 0.025 inches and a wind speed of 2 ft./sec. so that the experimental errors are of necessity large. With considerable trouble a hole about 0.003 inch diameter was drilled in the cylinder, but the throttling effect was so great as to render measurements of pressure impossible. Hence much larger holes had to be used - holes large in comparison with the cylinder diameter-and this necessitated a study of the effect of the size of hole on the pressure. This had to be done on larger cylinders, so that altogether a large range of Reynold's Number was covered (Part 6). The results for the various cylinders form an interesting series in themselves and it was decided to combine them with those obtained elsewhere. To obtain the necessary corrections for the channel walls in order to include results on large cylinders, a brief study of the wall effect has been made in Part 7. Parts 3, 4, 5, 6 and 7 are being published by the Aeronautical Research Committee (T 2680).

The above gives an idea of the order in which the experiments were carried out. It seemed better, however, to connect up the various sections of the work in the manner adopted in the body of the paper.

For the facilities placed at his disposal the writer is deeply indebted to Professor J.D. Cormack whose interest and encouragement have rendered possible the carrying out of this and other work of a like nature.

PART 1.

EXPERIMENTS ON THE BOUNDARY LAYER OF A CYLINDER.

A large amount of information is now available regarding the flow of water or air past a cylinder placed across the stream so far as the behaviour of the main body is concerned; but the conditions in the layer close to the surface of the cylinder seem to be largely unknown.

Accordingly the present experimental and theoretical investigation was undertaken. The work deals mainly with the front portion and it appears that in the first 60° or so the boundary layer is stable. About the same time Mr. Fage at the N.P.L. carried out an investigation on the conditions in the region where the boundary layer breaks down and eddying commences.[1] By this fortunate coincidence the conditions are fairly well established throughout the whole boundary layer.

The cylinder used by the writer for these experiments was of brass 4.5 inches in diameter, turned and ground true. The resulting surface was smooth but was not polished. The cylinder extended across the wind channel which is approximately 2 ft. square. As it is the boundary layer which is under consideration the relative largeness of the cylinder compared to the channel dimensions can hardly affect the results. Since the boundary layer theory assumes a knowledge of the pressures and velocities outside the skin the pressure distribution was first obtained by drilling a small hole in the central section of the cylinder. As the cylinder could

1. R & M No.1179.

be rotated to any position a comparison of the pressure in this hole with that in a similar hole in a plate on the channel wall, for various positions of the hole, gave the required pressure distribution. This was done for channel speeds of 12.3 and 36 ft./sec.

The results are given in Table 2 and shown plotted in fig. 1. No corrections have been applied to these figures and subsequent experiment showed that they are referred to a pressure which is $0.02\,\rho\,V^2$ below the undisturbed static pressure in the channel. The values given for K_D at the foot of Table 2 were obtained by integrating the drag component of the pressure round the cylinder.

A small static tube about 0.6 mm. diameter was used to test the constancy of the static pressure through the boundary layer. As was to be expected the results showed that the static pressure over distances of the order of 1 or 2 mm. is practically constant and equal to the pressure on the surface at the point considered. This simplifies the measurement of velocity as it is now only necessary to measure the total head at a point near the surface to obtain the velocity, the static head being taken from the distribution of pressure as given on fig. 1.

The method used to measure the total head was as follows:-

A small open-ended or Pitot tube was mounted on a micrometer arrangement so that the end of the tube could be traversed along the normal. Provision was made for mounting the arrangement in any position round the cylinder. The pressures were measured on an ordinary tilting gauge manometer

detecting pressure changes of about 0.0003 inches of water. The Pitot tubes were made by drawing a glass tube down to a diameter of about 1⅓ mm., and then drawing a section of this down to the required diameter. The tube was then broken off and the ends ground square on a fine stone. As the diameters used varied from about 0.23 mm. upwards, this was a delicate operation.

It was found desirable to fill the tube with wax before attempting to grind the end, thus preventing the bore becoming choked with chips, etc., which cannot afterwards be removed. A great many of these tubes were made and tested. It was found that if the bore was less than about 0.1 mm., the damping effect produced was so great that the tube was practically useless when used in conjunction with the usual tilting manometer. With care, the wall thickness can be controlled and made about 0.05 mm., so that the overall diameter has a lower limit of about 0.2 mm. If the tube is made oval a slight advantage is gained as the centre can then be brought slightly nearer the surface for a given area of bore. The most useful tube of all those made, measured 0.36X 0.45 mm. externally. This permitted the velocity to be measured at 0.18 mm. from the surface.

It was necessary to find if these small tubes gave an accurate measure of total head. This point has already been investigated by Miss M. Barker (Mrs. Glauert)[1] using a small pitot in water but it was considered advisable to test the actual tubes being used in air. Accordingly, a number were

1. Proc. Roy. Soc. A. 101.

compared at various velocities with a larger pitot tube about 5 mm. diameter. It was found that at low velocities the smaller tubes tended to give higher pressures than the large tube.

Let H = pressure in small pitot tube.

p = the static pressure at the point and

d = tube diameter.

Then $H - p = f(vd/\nu) \times \rho v^2$

The large tube is assumed to give a pressure of $\frac{1}{2}\rho v^2$ above static pressure. Hence if the tubes are connected to opposite sides of the manometer the latter will read $H - p - \frac{1}{2}\rho v^2$ or

$$\rho v^2 \left\{ f(vd/\nu) - \frac{1}{2} \right\} \text{ so we get}$$

$$f(vd/\nu) - \frac{1}{2} = (\text{Manometer reading}) \div \rho v^2$$

It is only at low values of vd/ν that $f(vd/\nu)$ will differ from $\frac{1}{2}$. It is difficult to get this low vd because reducing v reduces the pressures being dealt with and reducing d introduces the damping trouble already mentioned, so that no great accuracy is possible in the determination of $f(vd/\nu)$ by this method. About 40 readings were taken with different tubes at various velocities. The individual readings are scattered and uncertain and the mean results as presented in Table 1 are only given to show the corrections applied to the subsequent measurements of total head.

TABLE 1.

Mean vd ft. ^{2}/sec.	Mean vd/ν	Mean $f(vd/\nu)$
0.004	25	0.64
0.006	38	0.61
0.009	56	0.58
0.013	81	0.54
0.018	113	0.52
0.025	157	0.50

When a Pitot is placed with its end in a field where the total head is varying rapidly along the normal it may not be correct to assume that the pressure given by the tube corresponds to the total head at the centroid of the end. Involved with this question is that of the effect of the proximity of the surface when the tube is very close to the latter. These points were investigated by exploring the same normal section with tubes of different sizes. (See Table 3 and fig. 4, $\theta = 60^{\circ}$.).

It appears that the error, if any, due to assuming the pressure in the tube equal to the total head at the position occupied by its centre is smaller than the experimental errors except when the tube is practically touching the surface when it perhaps reads a trifle high.

The total head was measured along the normals at 10 degree intervals from $\theta = 10^{\circ}$ to $\theta = 90^{\circ}$ with a channel speed of 12.3 ft./sec. In each case the tube was placed parallel to the surface. In all about 180 measurements were made with

tubes varying in diameter from 0.36 to 0.9 mm. The results are given in Table 3, practically all the tabulated values being means of two or more readings. Table 3 also gives additional measurements made at $\theta = 50^{\circ}$ with wind speeds of 5.4 and 22.5 ft./sec. Where necessary, all these results have been corrected for the scale effect already mentioned (Table 1). In most cases the correction brought the results obtained from different tubes into closer agreement. The figures tabulated for $n = 0$ in each case are taken from the measures of surface pressures (Table 2) since at the surface the static pressure and the total head are equal, the velocity being zero. Table 3 also gives the velocities corresponding to the measured pressures.

PART 2.

THEORY OF THE BOUNDARY LAYER ON THE FRONT PORTION OF A CYLINDER AND A COMPARISON WITH THE EXPERIMENTS DESCRIBED IN PART 1.

In a paper to the Royal Aeronautical Society in January 1925 Bairstow gives the boundary layer equations as

$$q_1 \frac{\partial q_1}{\partial s} + \omega \frac{\partial q_1}{\partial n} = -\frac{1}{\rho} \frac{\partial p}{\partial s} + \nu \frac{\partial^2 q_1}{\partial n^2} \qquad (1)$$

$$0 = \frac{1}{\rho} \frac{\partial p}{\partial n} \qquad (2)$$

$$\frac{\partial q_1}{\partial s} + \frac{\partial \omega}{\partial n} = 0 \qquad (3)$$

where n and s are measured normal and tangential to the surface, the component velocities being ω and q_1.

The solution thereafter given for a flat plate is based on the fact that $\partial p/\partial s$ can be neglected. In the case of the flow over the surface of a cylinder this assumption is no longer permissible in fact $\partial p/\partial s$ turns out to be the controlling factor in the solution later presented.

A step by step method of solution was used first as follows :- Let A, B, C and D be four points on the corners of a small rectangle in the boundary layer and O the centre point

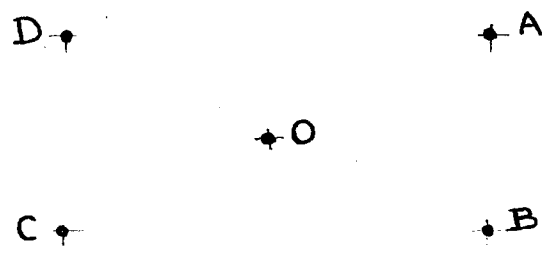

Let q, ω etc., be the values of the quantities at O, and q_m be the average of q_A, q_B, q_C and q_D. Then

$$\left.\begin{aligned} q_A &\doteqdot q + s\frac{\partial q}{\partial s} + \frac{s^2}{2}\frac{\partial^2 q}{\partial s^2} + n\frac{\partial q}{\partial n} + \frac{n^2}{2}\frac{\partial^2 q}{\partial n^2} + ns\frac{\partial^2 q}{\partial n\,\partial s} \\ q_B &\doteqdot q + \quad + \quad - \quad + \quad - \\ q_C &\doteqdot q - \quad + \quad - \quad + \quad + \\ q_D &\doteqdot q - \quad + \quad + \quad + \quad - \end{aligned}\right\} \qquad (4)$$

where, for the moment, s and n are the co-ordinates of A relative to O. Adding and re-arranging we get

$$q = q_m - \frac{n^2}{2}\left(\frac{\partial^2 q}{\partial n^2} + \frac{s^2}{n^2}\frac{\partial^2 q}{\partial s^2}\right) \quad -- \quad (5)$$

We have from (1) a value of $\partial^2 q/\partial n^2$ to substitute in (5). If s^2/n^2 is of the order unity we are justified in neglecting $\partial^2 q/\partial s^2$ since it is neglected in forming (1). By suitable combinations of (4) we obtain the obvious expressions

$$\partial q/\partial s = (q_A + q_B - q_C - q_D) \div 4s$$

$$\partial q/\partial n = (q_A + q_D - q_B - q_C) \div 4n$$

Making these substitutions in (5) it becomes

$$q = q_m - k_1 q(q_A + q_B - q_C - q_D) - k_2 \omega (q_A + q_D - q_B - q_C) + k_3 \qquad (6)$$

where

$$k_1 = n^2/8\nu s \,, \quad k_2 = n^2/8\nu n \,, \quad k_3 = -\frac{n^2}{2\nu\rho}\frac{\partial p}{\partial s}$$

If a velocity distribution is assumed throughout the boundary layer and the assumed field divided into rectangles then the velocity at the centre of each rectangle can be calculated from the assumed values at the corners by means of (6). A second approximation can then be obtained by using the calculated central velocities to compute new "corner" velocities. The process is repeated until identical values are obtained on succeeding repetitions. Strictly speaking the velocity ω at each corner should be calculated from (3) at each cycle of operations. For this purpose write (3)

$$d\omega = - \partial q/\partial s \; dn$$

and integrate graphically or mechanically. In practice the ω term had so little effect on (6) (throughout the region tried) that the integration had only to be performed once in several cycles.

The above method was applied to obtain an approximate solution for the front portion of the cylinder. For this purpose the radius was taken as unity (1 ft.) and the channel velocity 100 ft./sec. As VD/ν for the experiment already described was about 28,000, a value of ν was used which would give the same Reynold's number. The intervals used for s correspond to 2 degrees and the n intervals are 0.002. The pressures round the cylinder are shown in fig. 1. For present purposes a good approximation to these values from $\theta = 0$ to $\theta = 35^0$ is $p - p_o = \frac{1}{2}\rho V^2(1 - 3.5 \sin^2\theta)$ against $p - p_o = \frac{1}{2}\rho V^2(1 - 4 \sin^2\theta)$ for a perfect fluid. Then, the velocity outside the boundary layer is

$$v = \sqrt{3.5}\, V \sin\theta \quad , \text{ and } \frac{1}{\rho}\frac{\partial p}{\partial s} = - \frac{V^2}{r}\, 3.5 \sin\theta \cos\theta$$

It follows that

$$k_1 = 1/500, \quad k_2 = 1/28.6, \quad k_3 = 999 \sin\theta \cos\theta$$

A start was made by assuming that on the surface $q = 0$, and at $n = 0.008$, $q = v$.

Many cycles were calculated, the last two being shown in Table 4 up to $\theta = 20^\circ$. The upper figures in the squares at $\theta = 4^\circ$, 8°, 12°, etc., are assumed values of q obtained from previous trials. Values of $k_2\omega$ at $\theta = 0$ and $\theta = 20^\circ$ as obtained by graphical integrations are given in the outer columns. From these figures the values of q at $\theta = 2^\circ$, 6°, etc., were computed and then from these the lower values in the other squares were obtained. The agreement with the assumed values indicates that the process has been carried far enough. The solution was not extended far round the cylinder since a new method of attack suggested itself as a result of an examination of the figures obtained in the first 20 degrees.

It will be noticed that q/v at any definite value of n is nearly independent of θ., i.e., of s.

Assume then as a first approximation that we can write $q = vx$ where v is the velocity outside the boundary layer and x is a function of n only. Also in the first approximation neglect the term $\omega\, \partial q/\partial n$. (Corrections are made at a later stage for the errors introduced by these assumptions.) Then we have

$$\left.\begin{aligned} q &= vx \quad , \quad \partial q/\partial n = v\, \partial x/\partial n \\ \partial^2 q/\partial n^2 &= v\, \partial^2 x/\partial n^2 \quad , \quad \partial q/\partial s = x\, \partial v/\partial s \end{aligned}\right\} \quad (7)$$

We also have

$$p + \tfrac{1}{2}\rho v^2 = p_0 + \tfrac{1}{2}\rho V^2 \qquad (8)$$

where V = channel speed, which on differentiation yields

$$\frac{dv}{ds} = -\frac{1}{\rho v}\frac{dp}{ds} \qquad (9)$$

Substituting these values in (1) and dividing by v we get

$$\frac{dv}{ds}x^2 - \frac{dv}{ds} = \nu\frac{d^2x}{dn^2} \qquad (10)$$

Multiply through by $2\,dx/dn$ and integrate obtaining

$$\frac{2}{3}\frac{dv}{ds}x^3 - 2\frac{dv}{ds}x = \nu\left(\frac{dx}{dn}\right)^2 + C \qquad (11)$$

When

$$x = 1\,,\quad dx/dn = 0 \quad \text{giving} \quad C = -\frac{4}{3}\frac{dv}{ds}$$

Hence,

$$\frac{dn}{dx} = \sqrt{\left(\frac{3\nu}{2\,dv/ds}\right)} \div \sqrt{(x^3 - 3x + 2)} \qquad (12)$$

or

$$n = \sqrt{\left(\frac{3\nu}{2\,dv/ds}\right)} \int \frac{dx}{(1-x)\sqrt{(x+2)}} \qquad (13)$$

Performing the integration and noting that when $n = 0$, $x = 0$ gives

$$n = \sqrt{\left(\frac{3\nu}{2\,dv/ds}\right)} \cdot \frac{2}{\sqrt{3}} \log \frac{(\sqrt{3} - \sqrt{2})\sqrt{(1-x)}}{\sqrt{3} - \sqrt{(x+2)}} \qquad (14)$$

This can be compared with the previous mechanical solution directly, but it is perhaps better to put it in a form with the dimensional and non-dimensional parts separated

as follows :

Put

$$p_1 = (p - p_0) \div \tfrac{1}{2}\rho V^2$$

then we have from (8)

$$v = V\sqrt{1 - p_1} \qquad \ldots \qquad \ldots \qquad \ldots \qquad (15)$$

so that dv/ds can be written

$$\frac{dv}{ds} = -\frac{1}{\rho v}\frac{dp}{ds} = -\frac{V}{2\sqrt{(1-p_1)}}\frac{dp_1}{ds}$$

$$= -\frac{V}{2r\sqrt{(1-p_1)}}\frac{dp_1}{d\theta} = \frac{Vh}{r}$$

where r = radius of cylinder and

$$h = -\frac{1}{2\sqrt{(1-p_1)}}\frac{dp_1}{d\theta} \qquad \ldots \qquad \ldots \qquad \ldots \qquad (16)$$

Hence (14) becomes

$$n = \sqrt{\left(\frac{r\nu}{Vh}\right)} \cdot \sqrt{2}\log\frac{(\sqrt{3}-\sqrt{2})\sqrt{(1-x)}}{\sqrt{3}-\sqrt{(x+2)}} \qquad \ldots \qquad \ldots \qquad \ldots \qquad (17)$$

For comparison with forms to be developed later it is convenient to write this

$$n = \sqrt{\left(\frac{r\nu}{Vh}\right)}\, F(x) \qquad \ldots \qquad \ldots \qquad \ldots \qquad (18)$$

The advantage of using h instead of dv/ds is that for a given value of θ, h is constant and independent of VD/ν so long as the pressure curve (fig. 1) is unaltered.

A comparison of theory and experiment is given in fig. 3.

The experimental values of fig. 3 have been reduced by putting $x = q/v$ and $F(x) = n\sqrt{(Vh/rv)}$, v and h being the appropriate values for the section as given by (15) and (16). (See Table 5.)

The full line represents the above approximate solution, that is

$$F(x) = \sqrt{2}\ \log \frac{(\sqrt{3}-\sqrt{2})\sqrt{(1-x)}}{\sqrt{3}-\sqrt{(x+2)}}$$

while the values obtained by the mechanical method (Table 4) are shown by arrows. It is evident that the mechanical solution gives better agreement with the observed values than (17). This is only to be expected considering the assumptions made in deducing (17).

A brief examination will now be made of the terms neglected in the previous theory, using where necessary the results of the first approximation.

The Term $\omega\, \partial q/\partial n$:- From (3) and (7) we have

$$\omega = -\int \frac{dq}{ds}\, dn \doteqdot -\frac{dv}{ds}\int x\, dn \quad \text{and} \quad \frac{\partial q}{\partial n} = v\frac{dx}{dn}$$

Re-writing (12) as

$$\frac{dn}{dx} = \sqrt{\left(\frac{rv}{Vh}\right)}\, F'(x)$$

where

$$F'(x) = \sqrt{\frac{3}{2(x^3-3x+2)}}$$

and substituting these values leads to

$$\omega\,\frac{\partial q}{\partial n} \doteqdot -v\,\frac{dv}{ds}\,\frac{1}{F'(x)}\int x\,F'(x)\,dx = (\text{say}) - v\,\frac{dv}{ds}\,\varphi(x)$$

where

$$\varphi(x) = \int x\, F'(x)\, dx \div F'(x)$$

Retaining this value of $\omega\, \partial q/\partial n$ in (1), equation (10) becomes

$$\frac{d\omega}{ds} x^2 - \frac{d\omega}{ds} \varphi(x) - \frac{d\omega}{ds} = \nu \frac{d^2x}{dn^2}$$

Treating this as (10) was previously treated yields

$$\frac{dn}{dx} = \sqrt{\left(\frac{3\nu}{2\, d\omega/ds}\right)} \div \sqrt{\left\{x^3 - 3x + 2 + 3 \int_{x=x}^{x=1} \varphi(x)\, dx\right\}} \quad \cdots \quad (19)$$

The integral in (19) is easily evaluated graphically or by mechanical quadrature and once done it applies to all sections. This has come about because $\omega\, \partial q/\partial n$ is linear with $\partial\omega/\partial s$ (see above). In the term to be dealt with next, this does not hold necessitating a separate integration for every section.

The term $\partial x/\partial s$:- In the analytical solution above it was assumed that $\partial q/\partial s$ was equal to $x\, d\omega/ds$. This can only be regarded as a crude approximation. We shall now write:-

$$\frac{\partial q}{\partial s} = x \left(\frac{d\omega}{ds}\right)_n + \nu \left(\frac{dx}{ds}\right)_n$$

the subscript indicating the variable to be considered constant. Considering n as a function of s and x we have

$$\left(\frac{dx}{ds}\right)_n = - \frac{\left(\frac{dn}{ds}\right)_x}{\left(\frac{dn}{dx}\right)_s}$$

From the first approximate solution we have

$$n = \sqrt{(\nu r/Vh)}\, F(x)$$

Differentiating this and recalling that h is a function of S only leads to

$$\left(\frac{dn}{ds}\right)_x = -\frac{1}{2} F(x) \sqrt{\left(\frac{\nu r}{Vh^3}\right)} \frac{dh}{ds}$$

and

$$\left(\frac{dn}{dx}\right)_s = F'(x) \sqrt{\left(\frac{\nu r}{Vh}\right)}$$

so that

$$\left(\frac{dx}{ds}\right)_n = \frac{1}{2h} \frac{F(x)}{F'(x)} \frac{dh}{ds}$$

and the second approximation for $\partial q/\partial s$ is given by

$$\frac{\partial q}{\partial s} = x \frac{dw}{ds} + \frac{\nu}{2h} \frac{F(x)}{F'(x)} \frac{dh}{ds}$$

Inserting this value in the original differential equation and proceeding as in the previous solution leads to the result :-

$$\frac{dn}{dx} = \sqrt{\left(\frac{\nu r}{Vh}\right)} \div \sqrt{\frac{2}{3}(x^3 - 3x + 2 + M + N)}$$

$$= (\text{say}) \sqrt{\left(\frac{\nu r}{Vh}\right)} F_2'(x)$$

where

$$M = 3\int_x^{1.0} \varphi(x)\,dx \quad : \qquad f(x) = x \frac{F(x)}{F'(x)}$$

and

$$N = -\frac{3}{2}\frac{\sqrt{(1-p_1)}}{h^2}\frac{dh}{d\theta}\int_x^{1.0} f(x)\,dx$$

so that the final result is

$$n = \sqrt{\left(\frac{\nu r}{Vh}\right)}\,F_2(x)$$

$$\text{and} \quad F_2(x) = \sqrt{\left(\frac{3}{2}\right)}\int \frac{dx}{\sqrt{(x^3 - 3x + 2 + M + N)}} \qquad (20)$$

Table 6 shows the details of the numerical calculation for various values of θ . The data used is given in Table 5 along with a list of the formulae used. The values obtained by calculation in Table 6 are compared with the experimental values in fig. 4 (see also fig. 3). The differences are generally less than the experimental errors to be expected except perhaps for $\theta = 60^0$.

Readings were also taken at $\theta = 50^0$ with channel speeds of 22.5 and 5.4 ft./sec. The theoretical values for these speeds are easily deduced from Table 6 by neglecting the small changes inside the integrals due to the slight scale effect on p_1 (see fig. 1).

The data used were

for

$$V = 22.5, \quad \theta = 50^0, \quad \upsilon = 31.5, \quad \sqrt{(Vh/r\upsilon)} = 864$$

and for

$$V = 5.4, \quad \theta = 50^0, \quad \upsilon = 7.5, \quad \sqrt{(Vh/r\upsilon)} = 423$$

From these and the values of $F_2(x)$ in Table 6 for $\theta = 50^0$ the values given in Table 6A were easily obtained. The results as shown in fig. 4 again give good agreement with experiment.

Additional experimental evidence in support of the above solution has been obtained by A. Fage at The National Physical Laboratory in connection with an investigation carried out by him on the conditions of flow in the region where the boundary layer separates from the surface.[1] Mr. Fage's remarks are given in the appendix.

The intensity of surface friction at any point on the front portion of a cylinder can be estimated by the methods of this paper. Its value is easily found to be

$$f = \mu \frac{dq}{dn} = \rho \frac{\nu^{1/2} V^{1/2}}{r^{1/2}} \frac{\sqrt{h(1-p_1)}}{F_2'(x)} \quad \text{when } n \to 0$$

showing that the skin friction is proportional to $\rho \nu^{1/2} V^{1/2}$. (cf. Lanchester's Aerodynamics §36). It is thus possible to estimate the contribution to the drag coefficient made by skin friction. Taking numerical values from theory (Table 6) from $\theta = 0^\circ$ to $\theta = 60^\circ$, and using the experimental curves (fig. 5) to calculate approximate values from $\theta = 60^\circ$ to $\theta = 90^\circ$ the total integrated skin friction drag for the front half of the cylinder was found to be

$$K_D' = 1.92 \sqrt{\nu / VD}$$

The skin friction has become small at 90° and the rear half (90° to 270°) can contribute but little so that probably a close estimate[2] to the total viscous drag is given by $K_D' = 2 \div \sqrt{VD/\nu}$. This is small compared with the total

1. The air-flow around a circular cylinder in the region where the boundary layer separates from the surface R & M. No.1179.

2. This estimate has since been verified by pressure distribution experiments round small cylinders. (See Part 6).

drag at normal values of Reynold's number but becomes important at low values.

If the thickness δ of the boundary layer is defined as the distance from the surface in which the velocity attains 95 per cent. of the outside velocity, then

$$\delta = c\sqrt{\frac{\nu r}{Vh}} \quad \text{or} \quad \delta = c\sqrt{\frac{\nu}{d\omega/ds}} \qquad \ldots \qquad \ldots \qquad (21)$$

where c is the value of $F(x)$ for $x = 0.95$ (see Table 6)

(21) can also be written

$$\frac{\delta}{r} = c\sqrt{\frac{2}{h}\frac{\nu}{VD}}$$

showing that the ratio of the thickness of the boundary layer to the radius of the cylinder is inversely proportional to Reynold's number.

Conclusion. - It has been shown that the solution obtained for the boundary layer equations holds for the flow over a cylindrical surface throughout the region where the velocity over the surface is increasing. There seems no reason to suppose that it would not hold for any smooth surface provided the same condition was fulfilled (two-dimensional flow being understood). For cylinders other than circular it is probably better to retain $d\omega/ds$ in the various expressions instead of h. Where the velocity gradient $d\omega/ds$ becomes small or negative the theory ceases to be valid as this quantity appears under the root sign. In the case of the circular cylinder the change in sign of $d\omega/ds$ is associated with a complete break down of the steady flow.

The experimental velocities in this region are shown in fig. 5. The band which was previously the boundary layer has now become (at $\theta = 90^{\circ}$) very broad being in fact the beginning of the eddy region behind the cylinder.

PART 3.

ARITHMETICAL SOLUTION FOR THE TWO-DIMENSIONAL FLOW OF AN INVISCID FLUID.

There are in existence several methods of obtaining numerical solutions to the two-dimensional flow of a perfect fluid for given boundary conditions. Part 4 of the present paper gives a method of obtaining a numerical solution for viscous steady flow. To form an introduction to the method it is proposed to give another solution of the simpler problem, illustrating it with examples bearing on the experimental work described in Part 6.

Solution of $\nabla^2 \chi = 0$

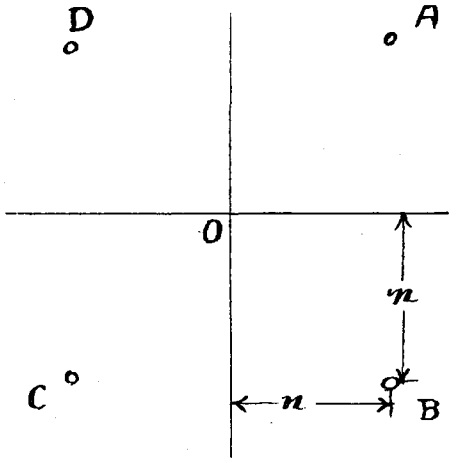

In the field of flow consider four points A,B,C, and D, placed on the corners of a small square with centre at O and sides equal to 2n. Let be the value of the stream function at O. Then the values at the corners are by Taylor's Theorem to third order terms.

$$\left.\begin{aligned}
\chi_A &= \chi + n\frac{\partial \chi}{\partial x} + n\frac{\partial \chi}{\partial y} + \frac{n^2}{2}\frac{\partial^2 \chi}{\partial x^2} + \frac{n^2}{2}\frac{\partial^2 \chi}{\partial y^2} + n^2\frac{\partial^2 \chi}{\partial x \partial y} + \frac{n^3}{6}\frac{\partial^3 \chi}{\partial x^3} + \frac{n^3}{6}\frac{\partial^3 \chi}{\partial y^3} + \frac{n^3}{2}\frac{\partial^3 \chi}{\partial x \partial y^2} + \frac{n^3}{2}\frac{\partial^3 \chi}{\partial x^2 \partial y} \\
\chi_B &= \chi + \quad - \quad + \quad + \quad - \quad + \quad - \quad + \quad - \\
\chi_C &= \chi - \quad - \quad + \quad + \quad + \quad - \quad - \quad - \quad - \\
\chi_D &= \chi - \quad + \quad + \quad + \quad - \quad - \quad + \quad - \quad +
\end{aligned}\right\} \quad (1)$$

By adding and dividing by 4, we obtain,

$$\chi = \chi_M - \frac{n^2}{2}\left(\frac{\partial^2 \chi}{\partial x^2} + \frac{\partial^2 \chi}{\partial y^2}\right) \quad \text{---------- (2)}$$

where $\chi_M = (\chi_A + \chi_B + \chi_C + \chi_D) \div 4$

So that when

$$\nabla^2 \chi = 0$$

$$\chi = \chi_M \quad \text{---------- (3)}$$

Thus, if we have approximate values of χ_A, χ_B etc.

from an assumed field, we can calculate the central value from(3)and this central value will be in general a better approximation than the corner values. Thus, we can gradually improve the solution.

Accordingly, the present method of solution is to divide the field into squares and assume values of χ for each corner. From these calculate the central values and then, using these as the corners of a new set of squares, find new values for the original corners. The process is repeated until the values recur.

Judgment must be exercised in selecting the size of square. It will be noticed that the method is correct to third order quantities but not to fourth (as may be seen by writing the next terms in Taylor's Theorem.) As the approximations get closer, the squares should be reduced in size. They are easily halved by interpolating values (using 3) in the diamond squares, that is those squares which are formed with their diagonals vertical as shown dotted in the figure annexed.

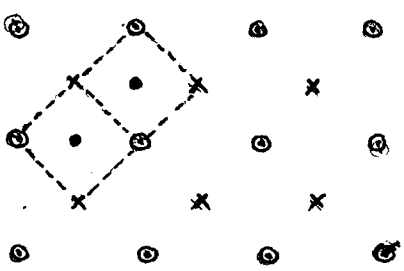

In practice a difficulty arises when the squares at the edge of the field cannot be arranged with their outer corners on the boundary; but this is easily overcome by interpolating the values (graphically or otherwise) or by breaking up the region into smaller squares.

As an illustration of the method the field chosen is that produced by the solid whose trace is two infinite parallel straight lines joined by a semicircle (see Fig.6). The nearest approach to a theoretical solution known to the author for these boundaries is that by W.M.Page,[1] the difference/

---

(1) "Some Two Dimensional Problems in Electrostatics and Hydrodynamics". Proc.Lon.Math.Soc. 1912-13. p.323.

difference being that there the lines are joined by a cycloid.

Two cases were worked:-

(a) Fluid infinite,

(b) Fluid bounded by a plane at a distance of 8 radii.

Case (a) was somewhat laborious to solve as it meant working over and over an ever increasing number of squares of increasing size until no change was produced in the neighbourhood of the semicircle. Actually the process was stopped at 80 radii. The streamlines obtained are shown for the inner part of the field in Fig.6.

The pressures round the semicircle or rather semi-cylinder are easily obtained and are shown plotted in Fig 2. The resemblance to the experimental pressures on the front half of a cylinder at high values of R is obvious.

Case (b) was much easier, having a definite boundary above. The streamlines differ but little from Fig 1. and the pressures are shown in Fig 7. Further use will be made of these fields in Part 7.

After the above work was completed Dr Hague drew the writer's attention to a paper by A.O.Muller[1] in which the above solution of $\nabla^2\psi = 0$ is discussed and ascribed to Liebmann.[2]

---

(1) "Ubereine neue methode fur Jeichnung der Feldbilder magnetischer Kraftlinien". Archiv fur Elektrotechnik, vol.xvii, pp.510, 1926.

(2) "Verfabren fur nummerischen Losung partieller Differentialgleishungen zweiter Ordnung." Sitzungs-berichte der Bayerischen Akademie der Wissenochaften,1918.

PART 4.

ARITHMETICAL SOLUTION FOR THE TWO-DIMENSIONAL STEADY FLOW OF A VISCOUS FLUID.

The general equations of two-dimensional motion of a viscous fluid are

$$\left.\begin{aligned} X - \frac{1}{\rho}\frac{\partial p}{\partial x} &= \frac{\partial u}{\partial t} - \nu\nabla^2 u + u\frac{\partial u}{\partial x} + v\frac{\partial u}{\partial y} \\ Y - \frac{1}{\rho}\frac{\partial p}{\partial y} &= \frac{\partial v}{\partial t} - \nu\nabla^2 v + u\frac{\partial v}{\partial x} + v\frac{\partial v}{\partial y} \end{aligned}\right\} \quad \text{---------} \quad (1)$$

If the motion is steady and no external forces are acting

$$\frac{\partial u}{\partial t} = \frac{\partial v}{\partial t} = X = Y = 0$$

An alternative form for these equations in which p has been eliminated is

$$\nu\nabla^2\zeta = u\frac{\partial \zeta}{\partial x} + v\frac{\partial \zeta}{\partial y} \quad \text{---------} \quad (2)$$

We also have[1] $u = -\frac{\partial \psi}{\partial x}$, $v = \frac{\partial \psi}{\partial y}$, $\nabla^2\psi = 2\zeta$ (3)

As in <u>part 3.</u>, consider a square in the field. The relation deduced there for ψ (ζ_{qn} (2)) is quite general so that we have for the values of ψ and ζ at the centre of the square

$$\psi = \psi_M - \tfrac{1}{2}n^2\nabla^2\psi \quad (4)$$

$$\zeta = \zeta_M - \tfrac{1}{2}n^2\nabla^2\zeta \quad (5)$$

Neglecting third order quantities suitable combinations of Equation 1 Part 3 give

$$\left.\begin{aligned} \partial\psi/\partial x &= (A + B - C - D) \div 4n \\ \partial\psi/\partial y &= (A + D - B - C) \div 4n \\ \partial\zeta/\partial x &= (a + b - c - d) \div 4n \\ \partial\zeta/\partial y &= (a + d - b - c) \div 4n \end{aligned}\right\} \quad \text{---------} \quad (6)$$

---

(1) In Lamb's "Hydrodynamics" $\nabla^2\psi = \zeta$, but the form given above is retained here.

where $A = \psi_A$, $a = \zeta_A$, $B = \psi_B$, $b = \zeta_B$ etc

Then from 2, 5 and 6, we get

$$\zeta = \zeta_M - \frac{\omega^2}{16\nu}\{(a-c)(B-D)+(b-d)(C-A)\} \quad \text{---- (7)}$$

and from 6 and 7

$$\psi = \psi_M - \omega^2\zeta \quad \text{.....(8)}$$

These are the expressions to be used in improving an assumed field in viscous flow as (Part 3) was used for the perfect fluid, the difference being that we must now start with assumed values of ζ as well as of ψ

In many cases the values of ψ is known along the boundaries[1]. but this is not so with the vorticity and it is necessary to use some additional method for obtaining the approximations to ζ on the surface where the fluid flows over a solid. Consider a small portion of the surface. For the moment take the axis of x along, and the axis of y normal to the surface. As a first approximation write

$$\zeta = \zeta_0 + ky \quad \text{.....(9)}$$

If y is small the normal velocity $v = \partial\psi/\partial x$ will be small. Hence approximately $\partial^2\psi/\partial x^2 = 0$ so that $2\zeta = \partial^2\psi/\partial y^2$

Hence $$\partial^2\psi/\partial y^2 = 2\zeta_0 + 2ky$$

Integrating twice and assuming that ψ is zero on the surface, we get

$$\psi = \zeta_0 y^2 + \tfrac{1}{3}ky^3 \quad \text{(10)}$$

Let ψ_1 and ψ_2 be the values of ψ when y is y_1 , and y_2 respectively. Substituting these values in 10, and eliminating k leads to

$$\zeta_0 = \frac{y_2^3\psi_1 - y_1^3\psi_2}{y_1^2y_2^2(y_2-y_1)} \quad \text{(11)}$$

This/

1. Care should be taken in applying the method where the boundaries form a right angle as the solution was based on Taylor's Theorem which will not apply to a discontinuity.

This gives the required value of the surface vorticity in terms of two values of ψ near the surface. If it is legitimate to put $k = 0$ i.e. to assume ζ constant throughout the neighbourhood, we have the simpler expression

$$\zeta_0 = \psi_1 / y_1^2 \qquad (12)$$

If on the other hand it is considered necessary to take into account the variation of ψ with x it can be done as follows:- By Taylor's Theorem put

$$\psi = ay + bx + cy^2 + dx^2 + exy + fy^3 + gx^3 + hx^2y + iy^2x$$

where $a = \partial\psi/\partial y$ etc. as in equations (1) (Part 3)

If $y = 0$ we have by differentiation

$$\partial\psi/\partial x = b + 2dx + 3gx^2$$

but $\partial\psi/\partial x = v$ and hence is zero for all values of x

$$\therefore \quad b = d = g = 0$$

similarly by differentiating with respect to y we get

$$a = e = h = 0$$

So the approximate expression for ψ near the boundary is

$$\psi = cy^2 + fy^3 + iy^2x$$

The coefficient c is the value of $\frac{1}{2}\frac{\partial^2\psi}{\partial y^2}$ when $y = 0$, but we have already seen that this is equal to ζ_0. So to determine ζ_0 take three points in the field $(x_1\ y_1)$, $(x_2\ y_2)$, and $(x_3\ y_3)$ and note the corresponding values of the stream function ψ_1 ψ_2 and ψ_3 This gives three equations to solve for c or ζ_0 Algebraically the solution is found to be

$$\zeta_0 = \frac{\frac{\psi_1}{y_1^2}(y_2x_3 - y_3x_2) + \frac{\psi_2}{y_2^2}(y_3x_1 - y_1x_3) + \frac{\psi_3}{y_3^2}(y_1x_2 - y_2x_1)}{y_1(x_2 - x_3) + y_2(x_3 - x_1) + y_3(x_1 - x_2)} \qquad (13)$$

Every time a new set of values of ψ and ζ have been found throughout the field (by 7 and 8) it is necessary to find new values of ζ_0 along the solid boundaries by 11, 12, and/or 13.

The/

The whole process must be repeated until the values of ψ and ζ recur to within what is considered a satisfactory margin throughout the field. This margin must be only a fraction (say 1/10) of the accuracy required in the solution as the quantities only approach their limit slowly. The field can now be plotted and the velocities obtained, but if pressures are required a further step is necessary. This step (which consists of integrating certain quantities along chosen lines in the field) is desirable as it can be made to give a check on the solution.

Taking the second equation of (1) we have

$$-\frac{1}{\rho}\frac{\partial p}{\partial y} = -\nu\nabla^2 v + u\frac{\partial v}{\partial x} + v\frac{\partial v}{\partial y}$$

$$\text{but} \quad \nabla^2 v = \frac{\partial^3 \psi}{\partial x^3} + \frac{\partial^3 \psi}{\partial x \partial y^2} = 2\frac{\partial \zeta}{\partial x}$$

hence

$$-\frac{1}{\rho}\frac{\partial p}{\partial y} = -2\nu\frac{\partial \zeta}{\partial x} + v\frac{\partial v}{\partial y} + u\frac{\partial u}{\partial y} + 2u\zeta \quad \ldots\ldots(14)$$

Integrating between A and B (two points on the line x = const) we get

$$p_A + \tfrac{1}{2}\rho q_A^2 = p_B + \tfrac{1}{2}\rho q_B^2 - 2\rho\nu\int_A^B \frac{\partial \zeta}{\partial x}\,dy + 2\rho\int_A^B u\zeta\,dy \quad -(15)$$

where $q^2 = u^2 + v^2$

Similarly from the first equation of (4) we get for two points on y = const.

$$p_A + \tfrac{1}{2}\rho q_A^2 = p_B + \tfrac{1}{2}\rho q_B^2 + 2\rho\nu\int_A^B \frac{\partial \zeta}{\partial y}\,dx - 2\rho\int_A^B v\zeta\,dx \quad -(16)$$

The last two terms of these expressions therefore give the change of total head between A and B. So that knowing the total head at a point C it can be found at any other point D by joining C and D by a path consisting of straight lines parallel to the x or y axis and integrating the above expressions graphically along the lines. If the path is closed a severe check is obviously obtained on the part of the field traversed by the path.

The Convergence of the Process.

In order to study the convergence of the process in one particular instance it has been applied algebraically to the case of viscous flow between parallel walls.

A portion of such a field is shown below :

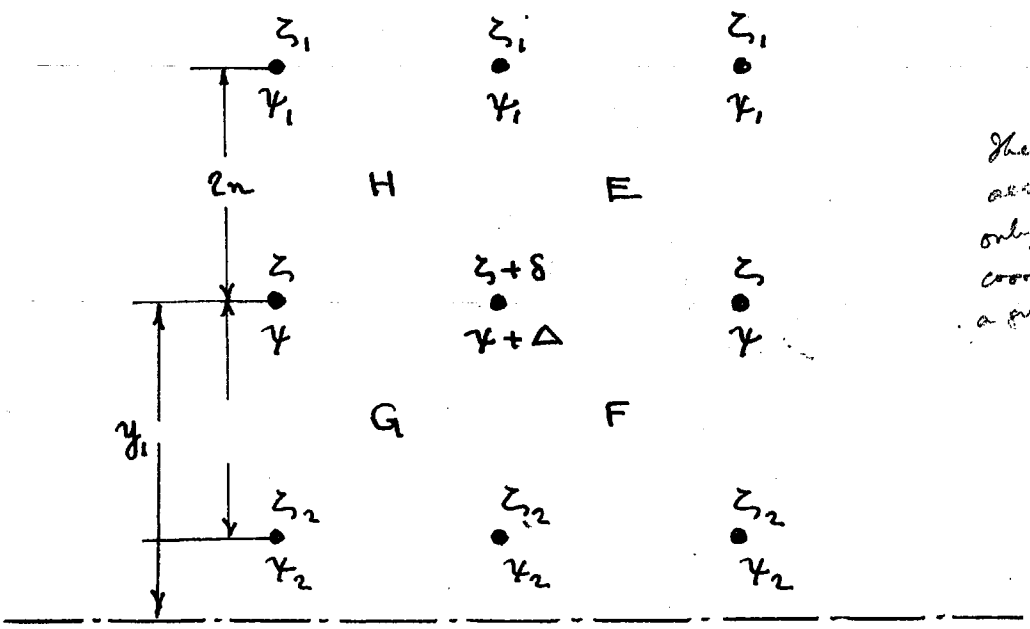

The distribution assumed is only in the y coordinate - not a general one.

The analytical solution (steady flow) is $\psi = \frac{Vy^3}{3\ell^2} - Vy$ where V = central velocity and 2ℓ = distance between the walls. x is measured along the direction of streaming and y is measured from the plane of symmetry normal to the walls. The vorticity is then $\zeta = \frac{Vy}{\ell^2}$. The true values of the various quantities in the figure in terms of the true central values ζ and ψ are

$$\zeta_1 = \frac{V}{\ell^2}(y_1 + 2n) = \zeta + \frac{2nV}{\ell^2} \quad .. \quad .. \quad .. (17)$$

$$\zeta_2 = \frac{V}{\ell^2}(y_1 - 2n) = \zeta - \frac{2nV}{\ell^2} \quad .. \quad .. \quad .. (18)$$

$$\psi_1 = \frac{V}{3\ell^2}(y_1 + 2n)^3 - V(y_1 + 2n)$$

$$= \psi + \frac{2V}{3\ell^2}(3ny_1^2 + 6n^2y_1 + 4n^3 - 3n\ell^2) \quad .. \quad .. (19)$$

$$\psi_2 = \psi - \frac{2V}{3\ell^2}(3ny_1^2 - 6n^2y_1 + 4n^3 - 3n\ell^2) \quad .. (20)$$

It is now assumed that the central values are disturbed so as to become $\zeta+\delta$, and $\psi+\Delta$. Thus we have the values as shown at the nine corner points. By four applications of (7) & (8) of the main paper the values at E,F,G and H were then obtained and from these another application gave the following new central values.

$$\zeta' = \zeta + \frac{\delta}{4} - \frac{n^2V^2}{16\nu^2\ell^2}(M^2\delta + M\Delta) \quad .. \quad .. \quad (21)$$

$$\psi' = \psi + \frac{\Delta}{4} - \frac{n^2\delta}{2} + \frac{n^4V^2}{16\nu^2\ell^4}(M^2\delta + M\Delta) \quad .. \quad (22)$$

where

$$M = \ell^2 - y_1^2 - \frac{4}{3}n^2$$

If we assume that $\Delta = 0$ then (21) becomes

$$\zeta' = \zeta + \frac{\delta}{4} - \frac{n^2V\delta}{16\nu^2\ell^4}\left(\ell^2 - y_1^2 - \frac{4}{3}n^2\right)^2 \quad .. \quad ..(23)$$

Further, take a case near the plane of symmetry so that y_1 is small. Assuming that n also is small (23) becomes

$$\zeta' = \zeta + \frac{\delta}{4} - \frac{n^2V^2}{16\nu^2}\delta$$

It is evident that if $\frac{Vn}{\nu}$ is very small the last term may be neglected and the final value $\zeta + \frac{\delta}{4}$ differs from the true value ζ by a quantity which is only one quarter of the original disturbance or error. If the last term is greater than $\frac{\delta}{4}$ and the process is repeated, the values obtained will be alternately above and below the true value but will

converge to it if $\frac{\delta}{4} - \frac{\delta}{16}\left(\frac{V_n}{\nu}\right)^2$ is algebraically greater than $-\delta$. This gives

$$\frac{1}{16}\left(\frac{V_n}{\nu}\right)^2 < 1\tfrac{1}{4} \quad \text{or} \quad \frac{V_n}{\nu} < \sqrt{20}$$

Returning to (23), the greatest possible value of y_1 is $\ell - n$. Substituting this leads to

$$\zeta' = \zeta + \frac{\delta}{4} - \frac{n^4 V^2 \delta}{16 \nu^2 \ell^4}\left(2\ell - \tfrac{7}{3} n\right)^2$$

From this the conclusion may be drawn that if n is small the criterion for convergence near the walls is :-

$$\frac{V_n}{\nu} < \sqrt{5}\left(\frac{\ell}{n}\right)$$

A detailed consideration of (22) leads to conclusions of a similar nature with regard to the criteria for convergence of γ .

The interaction of the two relations (21) and (22) may be considered by taking Δ initially zero and finding the revised values of Δ and δ after one round. These values again substituted in (21) lead to criteria so similar to those already deduced that it does not seem necessary to give the results.

The final conclusion regarding this particular type of flow is that the process is convergent provided V_n/ν is sufficiently small the value being indicated by the above relationships. The criteria given have nothing to do with the critical value of Reynolds Number associated with instability. It does not seem likely that the present method can lead to any information on instability as the $\frac{\partial}{\partial t}$ terms were omitted in its derivation, steady flow being postulated.

Part 5.

VISCOUS FLOW PAST A CIRCULAR CYLINDER AT $R = 10$

The method developed in Part 4 has been used to form the solution of the equations of steady viscous flow past a cylinder between parallel walls 8 diameters apart. To simplify the arithmetic as far as possible the following values were adopted.

Velocity of undisturbed flow = V =		6.25units/sec.
Coefficient of kinematic viscosity = ν =		6.25
Radius of Cylinder	=	5 units
Distance between walls	=	80 units
Reynold's Number = $R = VD/\nu$	=	10

Since the vorticity was assumed to be zero along the straight boundary walls the solution developed is really that past a series of cylinders at distances apart 80 units or 8 diameters. The circle of radius 5 passes through the corners of 12 squares of side unity, thus simplifying the work. With the above values we get from 7 and 8

$$\zeta = \zeta_M + \Delta\zeta = \zeta_M - 0.010 \times \{(a-c)(B-D) + (b-d)(C-A)\}$$

$$\psi = \psi_M - n^2\zeta$$

To begin the solution a field was assumed by calculating values from the expressions for the flow of an infinite inviscid fluid past a cylinder of radius 20% greater than the actual cylinder to allow for the retardation over the surface. This was corrected to suit the straight boundary by the method given in Part 3. The inner part was then "faired" to the cylinder, the surface values of ζ on the front portion being estimated from the boundary layer solution in Part 2. The assumed field was symmetrical in front and behind (i.e. about the y axis).

The/

The expressions given above were then applied to the field over and over again in conjunction with 11, 12 and 13. The field soon lost its symmetry. The process was laborious, the more so as it had to extend from about 5 diameters up stream to 8 down stream. As the work proceeded short cuts suggested themselves, such as, exterpolating the next values from the run of the figures.

Another short cut used in the solution was as follows:- Suppose we start with definite values of ζ and ψ and apply the method to find the central values. From these we get new values with which the process normally would be recommenced. In the next cycle of operations the numerical value of the second term in equation (7) would not differ greatly from its value in the first cycle. Assuming then the second term to be constant at each point formula (7) becomes $\zeta = \zeta_M - \text{CONSTANT}$.

An examination of the second cycle of operations now shows that it reduces to forming corrections to the second values of ζ by writing central values in each square which are means of the corner values of the increments obtained by the first round. The process is repeated until the corrections become small or zero when the final value of ζ at each point is obtained by adding the sum of the corrections to the second value. The ψ values can be treated in the same manner since to the same degree of approximation we can write $\psi = \psi_M - \text{CONST.}$. The full formulae 7 & 8 are then applied as before and the process repeated.

The portion of the field shown in Fig. 8 illustrates the above. To avoid confusion only the corrections to the ψ

values are shown. The method of forming these corrections is indicated on the figure. The fact that they decrease so slowly indicates that the values are still a long way from the truth. The finally adopted values at the centre of this field were $\zeta = 0.28$ and $\psi = 29.4$. The above approximate method gives results which are so close to those obtained by continuous application of the full formulae as to completely justify its employment at this stage of the solution. The sheet from which the above example was taken was one of intermediate scale between the large scale detail close to the cylinder (see Fig. 9 to main paper) and a small scale sheet extending to the outer boundary (see Table 8). To ensure continuity the fields dealt with on these sheets overlapped by several squares. The process described above was applied to each in turn working out and then in, the alterations being carried forward from one sheet and incorporated in the next.

The actual number of applications of (7) and (8) made in the whole solution was about 1600 but if short cuts like the above had not been taken possibly 5 or 10 times the number would have been required, say 10,000. As the number of points used in the whole field was about 200, it appears that a direct application of this formula, (i.e. without any attempt at extrapolation) necessitates about 50 trials per point. The solution obtained could certainly be improved, but some regions would then require the use of smaller squares which would add enormously to the work.

A portion of the work near the cylinder is shown in Fig.9. At greater distances larger squares were of course

permissible. The key given explains the figures which show the degree of approximation obtained. Near the cylinder surface the squares were afterwards reduced as in Part 3 and in places again reduced, but this work is not shown. The outer parts of the field are given in skeleton in Table 8. Figs. 10 and 11 show the streamlines and vorticity contours near the cylinder. Along the line $x = 10$ the vorticity is practically zero so that at this section the total head is that in the undisturbed stream. Hence, integrating 16 along $y = 0$, $y = 3$, $y = 4$ and $y = 5$ from this section to the surface gives pressures on the surface. The pressures behind the cylinder were got by integrating along $y = 6$ and then along $x = 0$, $x = -3$, $x = -4$, $x = -5$ from the line $y = 6$ to the surface. Several points were checked by integrating right through the vorticity region from above. The results are

θ	$p_1 = \frac{p - p_0}{\frac{1}{2}\rho V^2}$
0°	1.43
37	0.67
53	-0.4
90	-1.5
127	-1.6
143	-1.4
180	-1.3

From these the coefficient of normal pressure drag is easily deduced and found to be 0.95.

It remains to find the viscous or skin friction drag. From Lamb's Hydrodynamics we have

$$p_{xy} = \mu\left(\frac{\partial v}{\partial x} + \frac{\partial u}{\partial y}\right)$$

Taking for the moment x along the surface, this reduces to $p_{xy} = \mu \frac{\partial u}{\partial y}$ where p_{xy} is now the tangential force,

but $2\zeta_0 = \frac{\partial v}{\partial x} - \frac{\partial u}{\partial y} = \frac{\partial u}{\partial y}$ since $\frac{\partial v}{\partial x} = 0$

$$\therefore \quad p_{xy} = -2\mu\zeta_0$$

This can be integrated to give the viscous drag and expressed as a coefficient is found to be for the present example 0.74. Hence, the total drag coefficient found for a cylinder at R = 10 is 0.95 + 0.74 = say 1.7. The experimental value as found by E.F. Relf (R. & M.102) is about 1.6 which is certainly a closer agreement than was to be expected considering that the solution above has hardly been carried far enough.

Part 6.

EXPERIMENTAL DETERMINATION OF THE PRESSURES ROUND A STATIONARY CYLINDER IN AN AIR CURRENT THROUGHOUT A LARGE RANGE OF REYNOLD'S NUMBER.

Many determinations of the pressure distribution round a circular cylinder have been made in various laboratories but these have mostly been at relatively high values of Reynolds Number.

The theory of the subject has only been developed for very low scale values ($R < 10$) if we except those theories which seek to reproduce the actual conditions by placing eddies behind the cylinder in positions partly determined by theory and partly by experiment (Karman, Levy, etc.) Presumably the theory will gradually be completed for higher values of R so that it seems desirable to find experimentally the pressure distribution for as large a range as possible.

The present set of experiments cover the range between $R = 28$ and $R = 17,000$ the lower values being of less accuracy than the others. For each experiment the drag due to the normal pressure has been obtained by integration. At the lower values of R the viscous surface drag becomes relatively large as is shown by comparison of these results with the total drag determined by Relf.

A bye-product of these experiments has been a determination of the effect of the size of the hole pierced in the surface. Three sizes of cylinder were used, namely, $\frac{7}{8}$", $\frac{1}{8}$" and $\frac{1}{40}$" diameter. The first two stretched right across the channel and the last was long compared with its diameter, so that the flow was assumed two-dimensional in all cases.

At the lower velocities 2 - 5 ft/sec., a close mesh wire gauze was placed over the mouth of the channel. While

this/

this certainly helps to produce an even flow its primary object was to increase the sensitiveness of the pressure gauge to velocity changes, one side of this gauze being connected to a flush plate inside the channel and the other open to the atmosphere. The head lost in the gauze is thus included in the gauge reading so that even at 2 ft/sec. a reasonable movement is obtained. This gauge was used to enable the channel speed to be adjusted to the same value during each position of the hole in the cylinder. The actual channel speed was deduced from the observations themselves.

Special attention was directed to ensuring that the results could be referred to the true static pressure. This problem is bound up with the question of the interference of the channel walls which is discussed in Part 7. A long brass tube $\frac{1}{8}$" diameter was suspended along the channel centre line. A group of small holes were drilled in this tube at the section to be afterwards occupied by the cylinder. The pressure in these holes was then compared with that in two static plates A and B. Plate A was flush with the channel floor, the hole being directly under the cylinder position. Plate B was about 3 ft. up channel where the pressure would be unaffected by the presence of the cylinder. These comparisons were made at all speeds with the gauze on and off. The static tube was then removed and a comparison made between plate A and plate B. This was repeated with two different cylinders in position. It was found that the presence of the cylinder caused a fall of static pressure at plate A. This is due to two causes. (a) If there were no channel walls restricting the flow there would still be an increase of speed past the cylinder and hence a drop of pressure. (b) The presence of the channel walls by "compressing" the streamlines causes a further increase of velocity. In order to reduce the results approximately to the condition of

free/

free flow, it is necessary to separate these two effects. For the $\frac{7}{8}$" diameter cylinder the correction is small and the consideration of it is given in Part 7. For the smaller cylinders it is obviously quite negligible.

For the actual pressure determinations a tilting gauge was connected between plate A and the hole in the cylinder. To eliminate the effects of creep in the velocity and pressure gauges, the pressure on the front generator (which, after correction, is assumed to be $\frac{1}{2}\rho V^2$) was read after every fourth or fifth reading and the individual readings in each group of these were as far as possible distributed round the circumference. As the readings are carried right round the cylinder any constant error in θ is eliminated when means are taken.

The small cylinder (diameter $\frac{1}{40}$") presented a set of difficulties of its own. The greatest of these was the throttling effect of the necessarily small hole and passage. This was partly got over by drilling three holes in line along a generator, but even then there remained the constricted passage through the cylinder itself and slight changes of temperature caused large fluctuations in the gauge pressures. A hand held near the cup of the gauge caused a rise in pressure due to the fact that the expanded air did not get away freely. It was quite impossible to work on windy days, a flat calm being necessary. Every gust of wind outside the building caused fluctuations in pressure of the order of the total difference being measured at the lower epeeds. Opening or closing of doors in other parts of the building was particularly objectionable. When it is recalled that at 2 ft/sec. $\frac{1}{2}\rho V^2$ is equivalent to a bead of water of about 0.001 inch., the difficulties will be apparent. In fact/

fact the style of manometer used is no longer suitable. Nevertheless the results obtained at this speed are given for what they are worth. A further complication arises from the fact that the pressure on the front generator of the small cylinder at low speeds is no longer $\frac{1}{2}\rho V^2$. For this reason a small pitot tube was placed in the channel about 10 cm. above the small cylinder and the pressure in this tube measured after each group in the same way as the front generator pressure was measured for the larger cylinders.

In addition the pressure on the front generator of the small cylinder was compared with this pitot for a range of wind-speeds between 2 and 10 ft/sec. These results are given in Table 9, $H-H_0$ being the observed pressure difference between the cylinder and the pitot.

Table 10 gives the results of the pressure determination for all three cylinders. These pressures have been corrected where necessary as already indicated so that they refer to the static pressure in undisturbed free flow.

Size of Hole.

Four different sizes of hole were used in the $\frac{7}{8}$" diameter cylinder and two in the $\frac{1}{8}$" . An analysis of these results showed that for each cylinder they can be brought into substantial agreement if it is assumed that the pressure inside the cylinder is, not the pressure at the centre of the hole in the surface, but that at a point half way along the hole radius towards the front of the cylinder. In other words, if θ_0 is the angle between the front generator and the centre of the hole, then the measured pressure corresponds to $\theta = \theta_0 - \frac{1}{2}d/D$ where d = hole diameter, and D = cylinder diameter. This correction has been applied to all the results in Table 10. The plotted results for the $\frac{7}{8}$" cylinder (Fig. 12) seem to be sufficient justification for this proceeding. It is rather surprising to note how

even/

even the results obtained with a $\frac{1}{4}$" hole are brought into agreement with those from a $\frac{1}{64}$" hole. These remarks apply to the front portion of the cylinder. Behind, where the pressure gradient is small, the correction naturally makes little difference. For the short region where the pressure is rising rapidly the evidence is inconclusive.

The above results have been brought together in Figs.13 and 14 along with others from various sources. The pressure coefficient p_1 is a function of θ and R and so is shown by contours in Fig 14. The sources of information for the various parts of the diagram are given by the reference letters down the right side and are as follows.

A. Present report (Part 6) Experimental.

B. Present report (Part 5) Theoretical.

C. Present report (Part 1) Corrected.

D. Fage, Communicated. (See R & M. No.1179, T.2644.)

E. Fage, Communicated (Unpublished).

F. Fage, R. & M. No.106.

G. Taylor, R & M. No.191.

H. Parkin, R.A.S. Journal, No.204. Vol.xxxi.

I. Lamb, Hydrodynamics.

In dealing with published experiments it has been assumed (in the absence of a statement to the contrary) that the pressures have not been previously corrected for the "compression" introduced by the channel walls. This correction has been applied assuming the velocity increment to be $\frac{v_1}{V} = \frac{13}{30r+r^2}$ where r is the ratio of channel depth to cylinder diameter. (See Part 7). The resultant correction to the individual values of p_1 is $2\frac{v}{V}(1-p_1)$ approximately.

This correction becomes considerable in the case of experiments such as those of Fage with a cylinder 8"9 diameter in a 4 ft. channel which of course were not intended for the present/

present purpose but reach a higher value of R than any other known to the writer.

Coming to the other end of the scale we have Lamb's solution for low values of R . Adopting the notation and convention of this report the expression for the pressure at the cylinder surface is found to be:-

$$p_1 = \frac{1 - 2\sin^2\theta - \frac{8}{R}\sin\theta}{\frac{1}{2} - \gamma - \log \frac{R}{8}} \qquad (\gamma = 0.5772)$$

It has been assumed that this solution is valid up to $R = 0.4$ From here to $R = 2.5$ Bairstow's solution would be appropriate but it does not seem to be possible to get the pressures distribution from it without additional mathematical investigation as the authors state that they neglect a constant term,[1] which does not affect the total resistance but would presumably affect the individual pressures. As no information is available in this region the contours on Fig.14 have been dotted in by inspection and of course cannot be relied on.

---

(1) "The Resistance of a Cylinder moving in a Viscous Fluid". Bairstow, Cave and Lang. Phil.Tr.A.Vol.223,p.402.

Drag.

The drag produced by the normal pressure has been calculated from the experimental pressures given in Table 10. The results are given in the form of a coefficient $K_D' = \text{Drag} \div \rho DLV^2$ in Table 11. Fig.15 shows the values plotted on $\log_{10} R$. The total drag coefficient as determined by E.F. Relf by force measurements is also shown. The difference between the two is the skin friction drag and is shown chain dotted.

In Part 1 it is estimated that the skin friction drag is equal to $2/\sqrt{R}$ and this value is also plotted in Fig.15 showing a reasonable agreement with the above. The values obtained by the arithmetical solution of the fundamental equations in Part 5 are also shown and used to produce the curves.

PART 7.

EFFECT OF THE CHANNEL WALLS ON THE FLOW PAST A CYLINDER.

The presence of parallel channel walls above and below a horizontal cylinder by preventing the expansion or bulge of the stream lines increases the mean velocity past the cylinder. An estimate of this increase has been made in R. & M No.1018 by considering the flow of an inviscid fluid past a rotating cylinder. If τ is the ratio of channel height to cylinder diameter then the mean increase in velocity is there estimated to be about $100/\tau^2$%. This value seems to be too low for a stationary cylinder. This is probably due to the eddying region behind the cylinder preventing the streamlines from closing for some distance. It is evident that this will produce a larger "bulge" at the cylinder. This is shown by a field obtained in Part 3. for the flow past the solid shown in Fig.6. The bulge of the streamlines at various distances across the section of this field through the centre of the semi-circular arc is shown in Fig.16. When two parallel boundaries were placed at distances of 8 radii from the axis and the solution repeated the increment in velocity at various points across this section was found to be about 7% agreeing with that given in Fig.16. This figure also shows the bulge given by the expression obtained by Levy for the flow past a cylinder with a vortex pair behind it.

To obtain further experimental information the decrement in pressure on the channel wall exactly below the centre of the cylinder due to the presence of the latter was measured with the following results.

Cyl.Dia. in	r	$\Delta P/\frac{1}{2}\rho V^2$ Press.Decrement. %	v_3/V Vel.Increment. %	From Field in Fig.6. v_2/V %	v_1/V %	$v_3/V = (v_1+v_2)/V$ %
0.875	30	3	1.5	0.7	1.1	1.8
3.15	8·2	16	8	1.0	6·0	7·0

This velocity increment may be divided into two parts v_1 and v_2 arising from different causes. The first v_1 is the increase in velocity which would have existed at this point had there been no channel walls at all and the second v_2 is that produced by the compression of the flow produced by the walls. The last three columns give the values computed from the field which is shown in Fig.1.&6 In plotting these values in Fig.16 it has been assumed that $v_1 = v_2$ so that the plotted value is $\frac{1}{2} v_3/V$

When the pressure distribution has been measured on a large cylinder in a small channel and the true drag coefficient for the cylinder at this R is known, we can deduce a value for the correction to the mean velocity. Such a case is that given in Part 1. [illegible].Parkins in Toronto has also carried out a series of experiments on channel wall interference for cylinders of various lengths etc. His results for the cylinder spanning the channel are also shown in Fig.16.

After considering the somewhat inconsistent evidence available it was decided to adopt the following provisional value for the correction

$$\frac{v_1}{V} = \frac{13}{30r + r^2} \qquad \text{for } r > 4.5$$

For a cylindrical body of any cross section provided the dimension in the direction of the flow is small compared to the height of the channel v_1 is nearly equal to v_2 This can be seen by replacing the channel walls by images of the body. The effect of the nearest image on one side will

be/

be to give an additional velocity increment v_2 and at the same time a similar increment is being produced on the other side. So that the average increment given by the channel walls is of the same magnitude as that existing at the position of the channel walls if these were removed. Thus either of these increments is half the total as obtained in the channel by the above method of measuring the pressure increment on the wall opposite the section. For a body like an aerofoil which has a small wake, this should give a fairly reliable method of measuring the compression correction provided the body spans the channel. For a body with a section long in the direction of flow (such as that in Fig. 6) v_1 will be greater than v_2.

+++++
+++
+

PART 8.

THE PRESSURES ROUND A CYLINDER ROTATING IN AN AIR CURRENT.

The difficulty of measuring the pressure at a point on the surface of a rotating cylinder is considerable[1] and the results cannot be regarded as having a high degree of accuracy. To get the information required, it is necessary to have some means of opening a small valve in the surface of the cylinder for a small portion of every revolution, when the hole comes round a definite position relative to the direction of the undisturbed airflow. Thus, the pressure of the air inside the cylinder is made approximately equal to the pressure on the surface at the part where the hole is open. This pressure can be measured by being transferred through the cylinder spindle to a pressure gauge.

The first type of valve tried was unsuitable. It consisted of a small leather pad operating like a flute stop on the inner surface of the cylinder. It was found that this produced an alteration of pressure (positive or negative, depending on a variety of factors) inside the cylinder by acting as a small pump. It was impossible to allow for this as it was very erratic.

Apparatus. - The arrangement finally adopted is shown in Figs. 17 and 18.

1. It might have been better to have used a small static tube placed near the cylinder as is described in Part 10, but towards the end of the cylinder there would have been the difficulty of being certain that the tube was along the air direction.

A small steel plunger (p) $\frac{5}{32}$ in. diameter works in a brass cylinder (Fig.18). A hole drilled through both is opened and closed by the movement of the plunger.

The plunger is moved by a lever on a spindle which passes through the end of the pressure chamber. At this point a cam (m) projecting above the surface of the rotating cylinder comes into contact with a fixed stop, thus opening the hole. A spring (S) is used to close the hole when the cam leaves the stop. Difficulty was experienced in keeping the bearing air tight where the small spindle passes through the end of the airtight section. This was overcome very simply by adopting a suggestion made by Mr. Ping, the foreman mechanic in the laboratories. The bearing was tapped and the spindle threaded and screwed through it. As the spindle only rotates about 20°, the small axial movement produced is not sufficient to affect the measured pressure. The whole unit can be mounted anywhere along the rotating cylinder and so various sections can be explored (Fig.17).

The pressure is transferred through the main spindle and a mercury seal to the Chattock gauge, the other side of which was connected to a hole in a plate on the inside of the channel. A correction was afterwards applied for the difference between the pressure at this plate and the true static pressure of the air approaching the cylinder. This difference was subsequently determined by placing a static tube at several positions just ahead of the cylinder. The small pressure produced at these points by the cylinder

was calculated by the usual formula for the flow of a perfect fluid past a cylinder, and applied as a correction to the measured difference between the plate pressure and the static tube pressure.

Fig. 17 shows the arrangement of the cylinder in the channel. The gap at the lower end was about 4 mm. That at the top was slightly greater, but this can only affect slightly the results as no pressure measurements were made above mid-channel. To support the stop in an effective manner a rod was introduced as shown on the side of the cylinder where the pressure was being measured. As it was thought that changing this rod to the other side might affect the flow a dummy rod was kept in position as shown and changed over when the support rod was changed.

Measurements of angle were in all cases made to the point at which the cam made contact with the stop as this point was definitely known. Obviously the valve will not close when the cam leaves the stop, but the point at which it does close will depend on the speed of the cylinder, the strength of the spring, etc. Further, even if the point of closing was determined, it is not certain that the pressure inside the cylinder will settle down to the pressure at this point. It may tend to come to an average over the arc throughout which the valve is open. These considerations indicated that it would probably be advisable to determine the "lag" (that is, the angle between the point of contact and the point at which the pressure was measured) from the observations themselves, by

comparing the resultant integrated pressure over the whole surface with the resultant previously measured on the balance (R. & M. 1018).[1.]

As this involved a considerable amount of experimental work, it was decided to keep the cylinder speed the same in all experiments so that one determination of the angle of "lag" would suffice. The speed chosen was 1,400 r/m. This involved varying the channel speed from 19.2 to 4.8 ft./sec. to get a range of values of v/V from 1 to 4. The stop, which consisted of a hardened steel pin, was placed so as to open the valve at the required position, and its distance from the cylinder adjusted so that when the cylinder was rotated slowly by hand the angle of turn ($\Delta\theta$) throughout which the cam was in contact with the stop was about 5°. The actual $\Delta\theta$ was recorded in each case and a mean taken for each experiment. The angle (θ_1) throughout which the cylinder was turned to bring the hole from the up-wind generator of the cylinder to the position when the cam first touched the stop was measured. The cylinder was then rotated at 1,400 r/m. and the channel velocity brought to the required value.

Simultaneous readings were taken of the pressure and the channel speed. The channel flow was then stopped and the pressure again read with the cylinder rotating at the same speed as before. The difference between the two readings was divided by $\frac{1}{2}\rho V^2$ where V is the actual

1. Experiments on the air forces on rotating cylinders. By A. Thom.

measured channel speed.

The above procedure was adopted to eliminate the centrifugal pressure produced in the column of air from the cylinder centre to the surface and the slight pumping action which an initial experiment had demonstrated was still present even with the plunger type of valve. This pumping was probably caused by a slight lack of symmetry in the passages to and from the plunger.

The above method, however, introduces another source of error because with a perfect valve the measured pressure should be increased (numerically) by the centrifugal pressure integrated throughout the radius of the cylinder. But more than this is contained in the correction. The pressure measured in still air includes the centrifugal pressure due to any rotation imparted to the air by the cylinder. Hence the result is higher by the amount of the pressure produced by the rotation of the external air. An experiment carried out in still air with the stop open gave the following results :-

TABLE 12.

n revs./min.	p Pressure lbs./ft.	$\frac{p}{n^2} \times 10^7$
600	0.088	2.45
680	0.120	2.59
960	0.230	2.49
1,040	0.277	2.56
1,200	0.370	2.56
1,300	0.443	2.54
1,400	0.493	2.51
1,480	0.558	2.54
1,550	0.595	2.46
	Mean - - -	2.52

The centrifugal pressure integrated throughout the radius r is $p = 2\pi^2 r^2 n^2 \rho \div 3600$.

Since $r = 4$ cm., and $\rho = 0.00234$, $p/n^2 = 2.21 \times 10^{-7}$, whereas the mean from the above Table is $= 2.52 \times 10^{-7}$.

The experimental value corresponds to a radius of 4.26 cm., and indicates that a layer of air at least 0.26 cm. thick is in motion outside the cylinder.

The calculated pressure due to $r = 4$ cm. at 1,400 r./m. is $= 0.434$ lb./ft.^{2}, leaving 0.059 for the pressure due to the motion of the air.

A rough experiment on the velocity close to the cylinder rotating in still air at 1,400 r./m. was carried out with a small pitot and static tube about 0.9 mm. diameter. The results are shown in Fig. 23. It will be seen that the velocity at distances greater than 2 cm. from the surface is too small to measure, being probably less than 1 ft./sec. (See also Part 9)

The centrifugal pressure due to this annulus of moving air was estimated from Fig. 23 by plotting v^2/r and integrating, and found to be about 0.03 lb./ft.^{2}, which is as near to the measured value (0.059) obtained above as can be expected considering that an error of 2 per cent. in the cylinder speed would affect this figure by 0.017.

The total effect on the measured pressures (the latter being pressure with wind on minus pressure with wind off) is that the result is too high by an amount 0.059 lb./ft.^{2}, that is $2p/\rho V^2$ is high by an amount $0.059 \div \frac{1}{2}\rho V^2 \fallingdotseq 50/V^2$.

This somewhat uncertain correction has not been made for a reason to be explained later.

Exploration of Pressure over the whole Surface at $v/V = 2.$ - With a wind speed of 9.6 ft./sec., the pressure was measured as described above at about 90 points over the lower half of the cylinder. These points lay on four sections distant from the lower end 29.5, 16.2, 9.7 and 1.2 cm. The results are given in Table 13, and are shown on Fig. 19 with the correction for lag applied. This correction was obtained as follows :-

The total force along two axes ($\theta_1 = 90^\circ$ and $\theta_1 = 180^\circ$) was obtained by integrating $p' \cos\theta_1$ and $p' \sin\theta_1$ graphically.

The results are shown in Table 14 where k_L is the force coefficient on the cylinder in a direction $\theta_1 = 90^\circ$ and k_D is the force coefficient in a direction $\theta_1 = 180^\circ$.

These are not the lift and drag coefficients but are force coefficients referring to axes inclined to the lift-drag axis at an angle equal to the lag. Mean values for the cylinder as a whole were obtained by plotting k_L and k_D on the span and integrating. These are given in the last line of the Table. The final resultant for the whole cylinder is 1.84 inclined at an angle $\phi_1 = 90^\circ.5$.

The resultant as measured on the balance (R. & M. No. 1018) was 2.06 inclined at 104°, so that the mean correction for lag is $104^\circ.0 - 90^\circ.5 = 13^\circ.5$. The valve is thus seen to have been open for an arc of at least 13°. If the pressure read is the average over the open arc, then the valve was presumably open for twice this angle. This would also have the effect of flattening the peaks in the pressure curve and since the largest peak produces lift the measured lift

would be low. Any leakage or rebound of the valve would have a similar effect, so that the low value of the resultant force obtained is partially explained.

The value obtained for the above mean angle of lag is probably correct within $\pm 2^{\circ}$, which is sufficiently close when it is considered that the lag probably varies slightly from point to point due to a variety of causes, among which may be mentioned :-

(a) Variations in the setting of the stop.
(b) Differences in the stiffness of the stop supports at different positions.

These, by altering the impact of the blow delivered to the cam, would alter the time of closing. The mean lag for each section was estimated from the above value by assuming it to be proportional to the mean arc of contact $\Delta\theta$ (see page 48) for the section. Values so obtained are shown in Table 14, where they are used to obtain the lift and drag at the various sections (cols. 10 and 11) from $k_L = K_R \sin\phi$ and $K_D = -K_R \cos\phi$. These are shown plotted on Fig. 24. It will be seen that the distribution of lift and drag along the span is not uniform except possibly for a short distance in the centre. The lift would appear to drop to zero at the end of the cylinder. That this drop is not altogether the result of a fall in velocity towards the end is shown by the comparatively normal value of the pressure at the front stagnation point on the end section (about $0.8 \times \frac{1}{2}\rho V^2$), indicating a fall in velocity of only about 10 per cent.

From the curve showing the distribution of lift along the span it is possible to calculate the approximate distribution of induced drag. Thus, if x is measured along the span and ω is the down velocity produced by the trailing vortices at a position x' we have

$$d\omega = \frac{aV}{2\pi} \cdot \frac{\partial K_L}{\partial x} \cdot \frac{dx}{x'-x} \qquad (1)$$

where a = radius of the cylinder. $\frac{\partial K_L}{\partial x}$ can be determined approximately at all points along the span from Fig. 24 and the value of ω for any point determined by a graphical integration.

The only difficulty of the operation is that $d\omega$ becomes infinite when $x = x'$. As an example of the method adopted to overcome this difficulty, the calculation for the velocity at section 2 where $x' = 16.2$ will be considered in detail. Fig. 25 shows $\frac{2\pi}{aV} d\omega$ plotted on x for this section. To avoid the region where the curve tends to infinity, two points A and B were chosen at equal distances from the ordinate at $x = x'$. The area under A B is taken as being approximately equal to the area under the part of the curve between A and B for the following reason.

Throughout the small region considered $\frac{\partial K_L}{\partial x}$ is continuous and may be written with sufficient accuracy

$$\frac{\partial K_L}{\partial x} = m + n\bar{X} + q\bar{X}^2 \qquad (2)$$

Where $\bar{X} = x' - x$, and m, n, and q are constants.

From $\bar{X} = -e$ to $\bar{X} = +e$, where e is the distance of A and B from the ordinate at $x = x'$, the contribution to ω of this part becomes $\omega_1 = \frac{aV}{2\pi} \int_{-e}^{+e} (m/\bar{x} + n + q\bar{X})\, d\bar{x}$ which reduces to

$$\omega_1 = \frac{aV}{2\pi} 2ne$$

The ordinates at A and B are respectively

$$\frac{aV}{2\pi}\left(-\frac{m}{e} + n - qe\right) \quad \text{and} \quad \frac{aV}{2\pi}\left(\frac{m}{e} + n + qe\right)$$

so that the area under the line A B is also $\frac{aV}{2\pi} 2ne$. The curve can thus be integrated by planimeter. The resulting values of the induced drag obtained in this manner are given in Table 14 and illustrated in Fig. 24.

The above method of calculating the induced drag neglects the presence of the channel walls. A method of allowing for the walls at the end of the cylinder was indicated by Mr. C.N.H. Lock.

Suppose that every trailing vortex in the channel is one of an infinite series of straight vortices equally spaced at distances apart ℓ , where ℓ is the distance between the channel walls. Since the lift distribution curve is symmetrical every vortex towards one end of the cylinder is accompanied by one of equal strength symmetrically placed towards the other end. Evidently the resulting double series gives the effect of the end walls. The velocity produced at any point by a single series is given by Lamb ("Hydrodynamics," Art.156 (4)), so that the total effect at any point is easily obtained by a graphical

integration, as previously described.

The expression previously given for $d\omega$ in (1) now becomes

$$d\omega = \frac{aV}{2b} \frac{\partial K_L}{\partial x} \cot \frac{\pi(x'-x)}{b} dx \quad .. \quad .. \quad (3)$$

This expression was integrated graphically along the length of the cylinder for various values of x', using values of $\partial K_L/\partial x$ from Fig. 24. The resulting values of ω were then used to calculate the induced drag for the various sections. These values are given in Table 14 and Fig. 24 along with those previously obtained by neglecting the walls entirely.

The total induced drag for elliptic lift distribution as calculated by the usual expression is :- $4a K_L^2/\pi$ (span)^2 = 0.26. It will be seen that while the value obtained neglecting the walls (0.28) is near this, that obtained by allowing for the end walls is very much lower (0.08).

The profile drag (the difference between the observed drag and the induced drag) is higher towards the ends than at the centre. This may be due to (1) experimental errors, (2) faulty method of calculating the induced drag, or (3) an actual higher profile drag due to a greater eddying near the walls.

Determination of Pressure round the centre Section at Various Values of v/V. - The second series of experiments consisted of determining the pressure round the centre section at various values of v/V.

As a change in cylinder speed would involve a

redetermination of the angle of lag, it was decided to keep the cylinder speed the same as in the previous experiments (1,400 r./m.) and to use different wind speeds.

The speeds adopted were: 19.2, 6.4 and 4.8 ft./sec. To complete the series, the pressure round the stationery cylinder was obtained by rotating the cylinder 10^0 or 20^0 at a time and measuring the pressure at speeds of 12.5 and 24 ft./sec. Thus, with the experiment already described, pressure curves have been obtained at the following values of v/V:- 0, 1, 2, 3 and 4.

The experiments at the lower wind speeds (i.e., v/V = 3 and 4) are naturally less accurate than the others, as the pressures are low at these speeds and the errors due to pumping in the valve, etc., are relatively large.

An estimate of the limits within which the errors should lie has been made and is given in Table 13 along with the results corrected for lag. The pressure curves obtained are plotted on Fig. 20. The lift and drag obtained from these curves by integrating $p' \cos\theta$ and $p' \sin\theta$ are given in Table 4, together with an estimate of the errors.

In the case of $v/V = 2$ an estimate has already been made of the induced drag k_d. Assuming that at other values of v/V the lift distribution curve retains the same shape the induced drag will be proportional to K_L^2. On this assumption columns 9 and 10 of Table 15 have been computed and are plotted in Fig. 22. The negative profile drag found at v/V = 3 and 4 is not necessarily a violation of the law of the conservation of energy, since work has

to be done rotating the cylinder. In view, however, of the difficulties of the experiment and of the somewhat uncertain assumptions, it would be unwise to place much confidence in these results.

With each experimental curve has been plotted a theoretical curve giving the same lift. These show the pressure which would obtain in a perfect fluid having a circulation corresponding to the lift integrated from the observed pressure curve and have been calculated from

$$\frac{2p}{\rho V^2} = 1 - (2 \sin\theta + K_L/\pi)^2.$$

The observed pressure curves for the various values of v/V have been collected in Fig. 21. Examination of the curves shows several interesting features. There is first of all the fact that the curves all attain about the same maximum, namely, $\frac{1}{2}\rho V^2$. This is more remarkable than at first appears because the correction to the pressures mentioned on page 50 has not been made. The numerical values of this correction are as follows :-

v/V	0	1	2	3	4
Cor. to $\frac{2p}{\rho V^2}$	0	-0.14	-0.54	-1.2	-2.2

With this correction applied, the curves would no longer have a common maximum of $\frac{1}{2}\rho V^2$, but the maximum would vary. The conclusion to be drawn would seem to be that the rotating cylinder is surrounded by a layer of air

which clings to the surface and, remaining the same whether there is a general external translational velocity or not, takes no direct part in this external circulation. Apparently, therefore, the external circulation produced in the air flowing past is different from and additional to the annulus of moving air measured and shown in Fig. 23. The curves in Figs. 19 and 20 as they stand are really the pressures round the surface, not of the cylinder but of the annulus above mentioned, produced by placing the rotating cylinder in a current of air. That this is so will be seen when it is recalled that the values tabulated and plotted are the difference between the pressures measured with the channel running and with it stopped.

It will be noticed from Fig. 20 that in the experimental curves the maximum pressure occurs earlier than in the theoretical, especially at the higher values of v/V. The discrepancy is made greater by a correction for induced downflow as a downflow will make such phenomena occur later, unless the downflow angle is negative. In fact, the local conditions are such as would accompany a larger circulation than that used in plotting the theoretical curves. The same tendency is apparent when we examine the value of the minimum pressure except in the case of $v/V = 1$. So that generally the conditions over the front half of the cylinder correspond with a higher circulation than that given by integrating the lift forces.

The sharp rise in pressure on the centre section at $v/V = 2$, about 200°, is interesting (Fig. 19). It will

be seen that it occurs at the position in which the theoretical curve is a maximum, that is where the line separating the flow over the top of the cylinder and the under flow would be expected to meet the cylinder. Experiments by the writer[1] on the flow past a cylinder at $v/V = 2$, show that this line probably meets the cylinder in this region and further show[2] that it divides the wake into two regions, one of positive and the other of negative vorticity. Apparently, turbulence tends to equalise the pressure from about 140° to 190° and again from 210° to 280°; but these two regions are at different pressures corresponding to the two halves of the wake. At other values of v/V the separation is not visible, but the tendency towards a constant pressure is apparent.

All the curves show a sudden rise in pressure at about 100°. This is merely the usual breakdown which tends to occur with diverging streamlines, in this instance probably allowing a tongue of high pressure from the rear to intrude under the high velocity air above the cylinder.

1. Institute of Engineers and Shipbuilders in Scotland, 1924-25.

2. Ph.D. Thesis (Unpublished).

PART 9.

EXPERIMENTS ON THE BOUNDARY LAYER OF A CYLINDER ROTATING IN STILL AIR.

The apparatus used in this experiment was that prepared to investigate the boundary layer on a rotating cylinder in an air current (Part 10) and hence the cylinder used (4½ inches diameter) was mounted in the 2 ft. wind channel. Measurements close to the surface could not be made at the higher rotational speeds due to vibration troubles. A preliminary experiment gave the values shown in Table 16. These were obtained by a Pitot and static tube mounted 8 mm. apart so as to be the same distance (n) from the surface and to be approximately parallel to the tangent. The Pitot tube was of glass 0.63 mm. outside diameter and the static tube was aluminium tube flattened till the minor axis of the section (placed normal to the surface) was about 0.5 mm.

The results are shown plotted in Fig. 26. It will be noticed that the velocities at corresponding distances are relatively lower at the higher rotational speeds. In other words the boundary layer is thicker at low speeds.

The weakness in the above method of measurement lies in the method of obtaining the static pressure. In measurements of velocity in the boundary layer on a stationary surface it appears to be justifiable to assume the static pressure constant along the normal. As the

surface is approached the velocity falls so that even if the curvature is appreciable the centrifugal pressure remains small. When dealing with the surface layer on a rotating cylinder the static pressure gradient along the normal due to centrifugal force may require consideration since the velocities near the surface are high. Thus the exact position of the static tube may be important and probably it should be curved so as to be parallel to the surface.

To get over these difficulties and to get an idea of the magnitude of the changes in pressure due to centrifugal force it was decided to measure the total head only and to calculate the static pressure. This pressure was assumed to be below atmospheric pressure by the centrifugal pressure of the circulating air outside the point considered and so (reckoning atmospheric pressure zero) at radius r_1 it is given by

$$p = -\rho \int_{r_1}^{\infty} \frac{v^2}{r}\, dr \qquad \ldots \qquad \ldots \qquad (1)$$

This expression contains v the quantity sought thus introducing a difficulty which can be circumvented either by (a) a step by step integration or (b) taking an assumed velocity distribution to calculate the static pressure and revising the calculation when the velocity has been obtained. Method (b) was used outside 5 mm. from the surface. From 5 mm. inwards the following step by step method was used :- At radius r_1 let the total head be H_1 lbs/ft^2 and the pressure be p_1. At radius $r_2 = r_1 - \delta r$ let these quantities be H_2 and $p_2 = p_1 - \delta p$. Then by

Bernoulli's equation we have

$$v_2^2 = \frac{2}{\rho}(H_2 - p_2) \quad .. \quad .. \quad .. \quad (2)$$

and from the centrifugal effect

$$\delta p \doteq \rho\left(\frac{v_1^2}{r_1} + \frac{v_2^2}{r_2}\right)\frac{\delta r}{2} \quad .. \quad .. \quad (3)$$

Hence

$$v_2^2 = \frac{2}{\rho}\left\{H_2 - p_1 + \frac{\rho}{2}\left(\frac{v_1^2}{r_1} + \frac{v_2^2}{r_2}\right)\delta r\right\}$$

$$= \frac{2}{\rho}(H_2 - p_1) + \left(\frac{v_1^2}{r_1} + \frac{v_2^2}{r_2}\right)\delta r$$

or

$$v_2^2\left(1 - \frac{\delta r}{r_2}\right) = \frac{2}{\rho}(H_2 - p_1) + \frac{v_1^2}{r_1}\delta r \quad .. \quad (4)$$

Thus if the velocity and pressure are known at any section and the distribution of total head has been measured the velocity at a section just inside is found from (4) and the pressure from (2). These give the information necessary for the next step.

Table 17 shows the results of total head measurements made with a small glass tube (diameter = 0.36 mm.) the rotational speed of the cylinder being 820 r/m. A graphical integration of (1) using the velocity measurements in Table 16 gave the pressure at n = 5 mm. as being

= - 0.0089 lbs./ft.^{2} The results of the step by step calculation from n = 5 mm. to the surface are given in Table 18. It is evident that the pressure gradient though small is appreciable. The velocities are dotted on to

Fig. 26 along with those found using the somewhat crude Pitot and static tubes.

A knowledge of the torque necessary to rotate the cylinder would enable the eddy viscosity to be found from the velocity gradient. The cylinder used in the present experiment being too heavy for the balance used previously for torque experiments this could not be obtained directly. In R. & M. No.1018, the writer gave the results of some torque experiments on cylinders and spheres. Using the formula and values given there the torque required to rotate the cylinder of the present experiment at 820 r/m is about 5.4×10^{-4} ft. lbs. per ft. length of cylinder. Evidently

$$Q = \text{torque} = \bar{\mu}\, 2\pi \ell r^2 \frac{dq}{dr}$$

where

$\bar{\mu}$ = coefficient of eddy viscosity

ℓ = length of cylinder.

Taking dq/dr from a plot of the values found in Table 18 the following values of $\bar{\mu}$ were obtained

(mm.)	.1	.2	.4	.7	1.0	1.5	2	3	4
$\bar{\mu} \times 10^6$ gs/ft.sec.	0.47	0.38	0.79	1.9	3.3	4.7	7.4	12	27

These values are plotted in Fig. 27 A. The accepted value of the coefficient of viscosity for air at 15° C is $\mu = 0.378 \times 10^{-6}$ slugs ft./sec. Thus, close to the cylinder $\bar{\mu}$ is approximately equal to μ showing that turbulence is probably absent. From n = 0.4 mm. outwards

it appears that the turbulence increases steadily for an indefinite distance.

PART 10.

EXPERIMENTS ON THE BOUNDARY LAYER OF A CYLINDER ROTATING IN AN AIR CURRENT.

As yet there is no satisfactory theory giving the lift experienced by a rotating cylinder in an air stream. There seems, however, to be general agreement that the circulation is affected largely by the eddies generated on the surface. It was accordingly decided to explore the surface layer. The cylinder used was of brass $4\frac{1}{2}$ inches diameter. The channel speed throughout was kept at about 8 ft./sec. and the rotational speed at 820 r/m giving a ratio

$$\frac{\text{Surface Speed}}{\text{Wind Speed}} = 2$$

The low rotational speed was adopted to avoid vibration troubles. To obtain uniformity with previous experiments the above ratio was chosen, and this fixed the channel speed.

The method adopted was to measure the total head and the static pressure separately, i.e. at different times. The Pitot tube was of glass 0.45 mm. × 0.36 mm. external measurements at the end. The total head was compared with the pressure in a hole in the channel wall some distance up-wind. The pressure in this hole was afterwards compared with the pressure on the front generator of the cylinder (when stationary) and the total heads recorded in Table 19, and plotted in Figs. 28, 29 and 30, are referred to this

front generator pressure (H_0). The same remarks apply to the static pressure so that the recorded pressure would be zero at a point of zero velocity if there were no loss of head.

The apparatus used was identical with that employed for the investigation of the boundary layer on a stationary cylinder described in Part 1. and the Pitot tube corrections discussed there apply also to the present experiment. The corrections for the tube used are shown in Fig. 28A from which it is seen that at high and low velocities the correction is negligible. These values were deduced from Table 1, Part 1.

Measurements of total head and static pressure were made along lines normal to the surface at $\theta = 0^\circ$, 20°, 40°, 60°, 80°, 90°, 100°, 120°, 160°, 200°, 240°, 280°, and 320° where θ is measured from the up-wind direction. On the sections at $\theta = 240^\circ$, 280°, and 320° at a short distance from the surface the velocity changes sign being no longer in the same direction as the velocity of the cylinder surface. This necessitated exploring these sections with the Pitot tube in both directions. The results for the tube facing the reversed velocity are given in Table 20 and will be found plotted with the others in Figs. 28, 29 and 30. At the point on the sections where the two directions give the same pressure the static pressure should also have an identical value, unless the reversal of the tube causes a change in the flow. The agreement is as good as can be expected at $\theta = 280^\circ$, and $\theta = 320^\circ$, while

while at $\theta = 240^{\circ}$ exploration with the tube in its normal position, has not been carried far enough.

With the above exception no attempt has been made to make the tube face the air direction beyond placing it parallel with the tangent to the surface and this should be kept in mind when examining the curves of velocity obtained.

A preliminary estimate of the velocity having been made at each point on every section, the corrections to the total head were obtained from Fig. 28A (see Table 19). The corrected values are shown in Figs. 28, 29 and 30, along with the static pressure. The finally adopted velocities are given in Table 22 and are shown plotted in Fig. 31. It is seen that in most cases the velocity tends to approach the circumferential velocity of the cylinder as the surface is approached. Fig. 32 shows contours of constant velocity throughout the region explored the figure being distorted by enlarging the boundary layer in order to show the latter more clearly. In a previous paper the writer showed contours of velocity round a rotating cylinder at the same ratio of circumferential speed to wind speed namely 2, but in that case the apparatus used could not be brought nearer the surface then about 0.7 radius. Fig. 33 has been constructed by combining the results of the two experiments. There is still an annular region not covered by either experiment. The contours have been dotted through this region. A few isolated readings indicated that these dotted contours are approximately correct but further experiment is required to complete this region.

The velocity curves in Fig. 31 were integrated and the integral curves used to plot the streamlines shown in Fig. 35.

Equation 14, Part 4, can be rewritten

$$2\rho u\zeta = -\frac{\partial}{\partial y}(p+\tfrac{1}{2}\rho v^2+\tfrac{1}{2}\rho u^2) + 2\mu\frac{\partial\zeta}{\partial x}$$

$$= -\frac{\partial H}{\partial y} + 2\mu\frac{\partial\zeta}{\partial x} \quad \ldots\ldots (1)$$

In the present experiment, taking x along the surface and taking the normal value of μ for air, $2\mu\frac{\partial\zeta}{\partial x}$ was found to be negligible compared to $\frac{\partial H}{\partial y}$ so that if the flow close to the surface can be represented by (1) the vorticity is given by $-\frac{1}{2\rho u}\frac{\partial H}{\partial y}$. The numerical results obtained by this expression are given in Table 23 and shown as contours in Fig. 34 the sign adopted being shown on the latter diagram. In Part 9 it appears that for a cylinder rotating in still air the effective coefficient of viscosity increases rapidly with the distance from the surface, so that it is possible that in the present case the last term in (1) may become appreciable. For this reason the results obtained for the vorticity are not above suspicion.

It is interesting to compare the static pressure close to the surface as obtained by the small static tube with that obtained in Part 8 by other means. This comparison is shown in Fig. 36. Unfortunately different cylinder diameters were used in the two experiments. The results obtained in Part 8 show the large influence of the end walls. This influence will of course depend on the

~~T.2553~~

FIG. 1.

THE BOUNDARY LAYER ON THE FRONT PORTION OF A CYLINDER.

Pressure distribution round stationary cylinder.

Cylinder diameter = 4·5 inches.

—●— Wind speed = 12·3 ft/sec.

--×-- " " = 36 ft/sec.

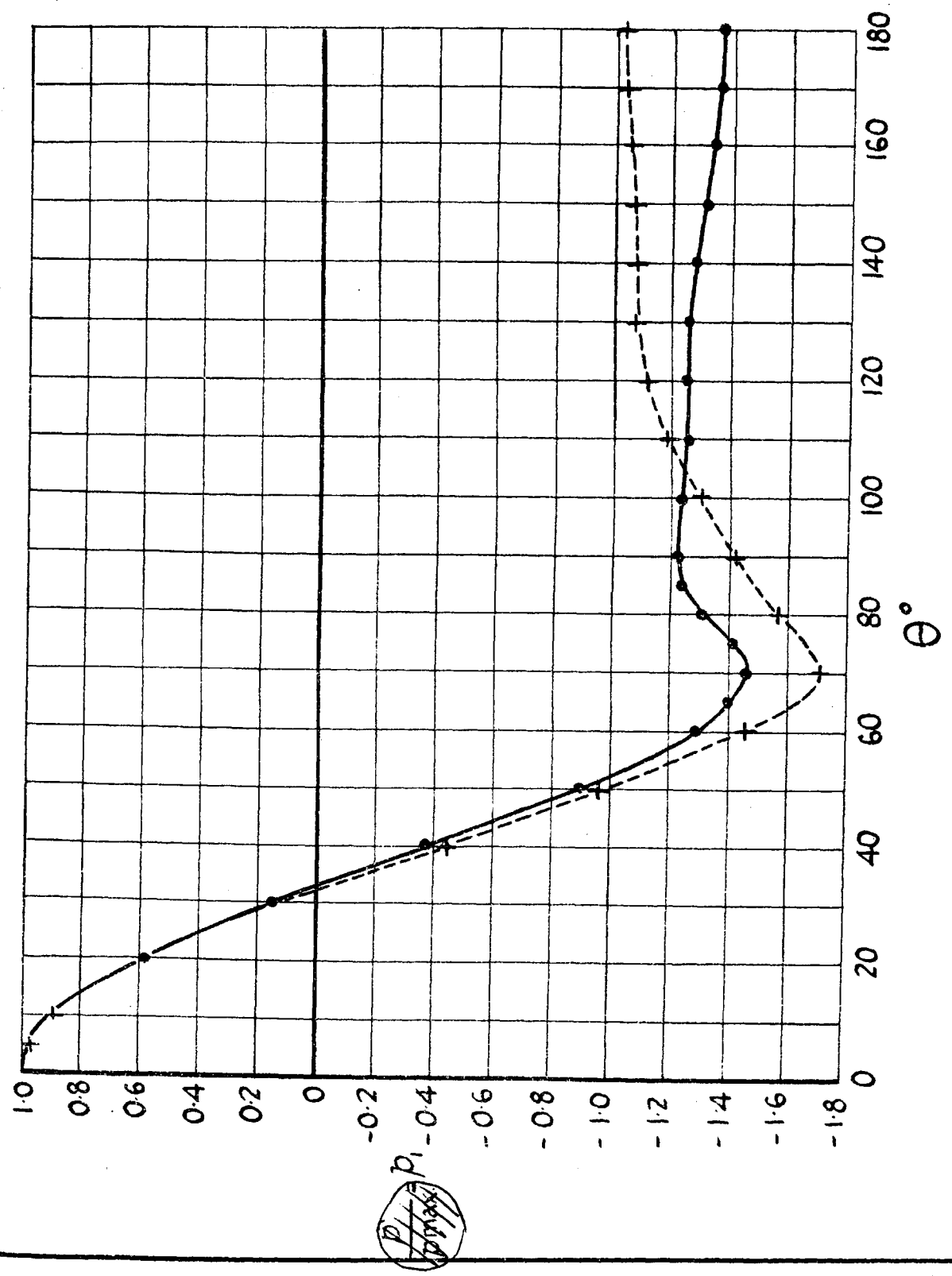

~~F.2553.~~

FIG. 2.

THE BOUNDARY LAYER ON THE FRONT PORTION OF A CYLINDER.

Wind Speed = 12·3 ft/sec.

Cylinder Dia 4·5 inches.

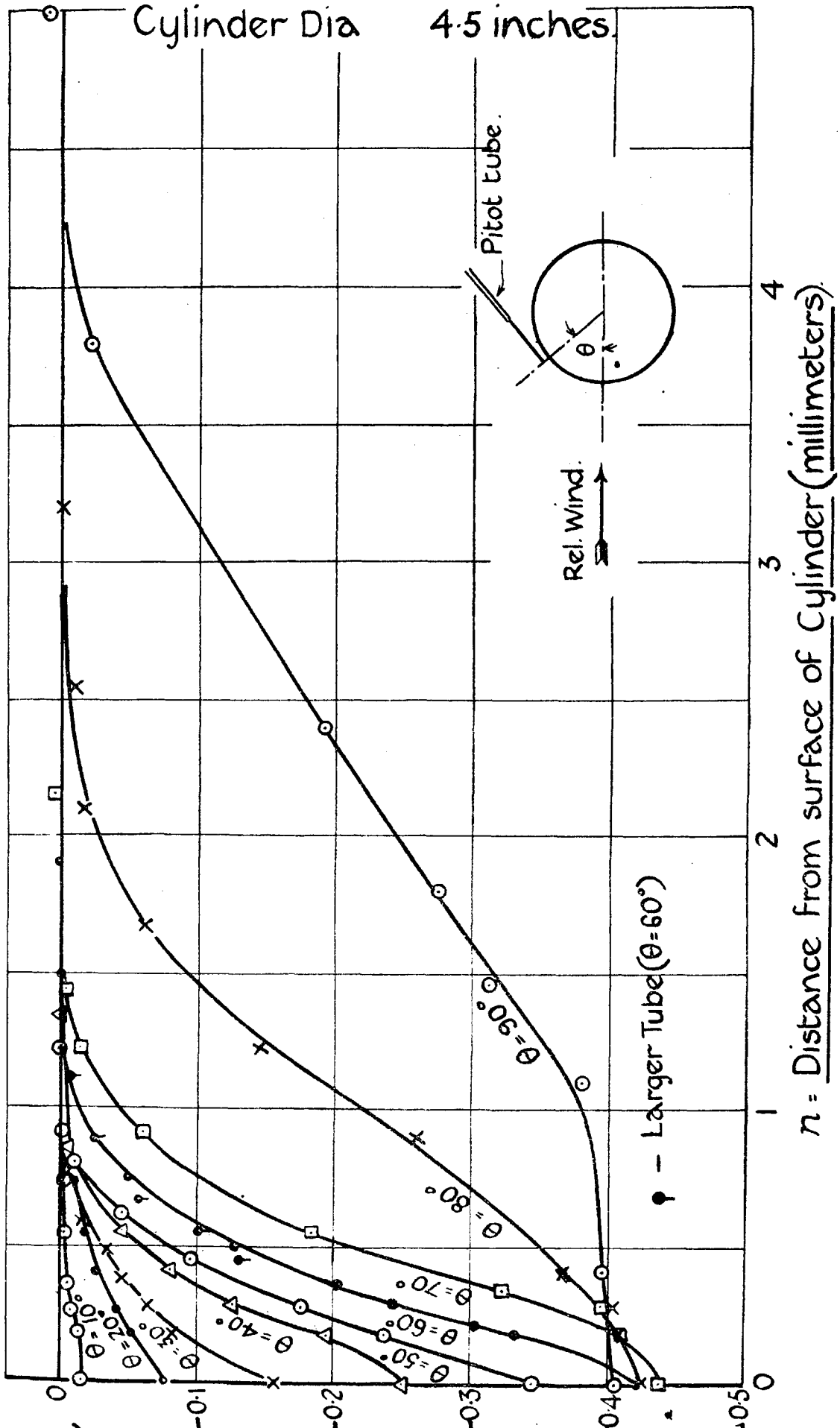

~~F.2553.~~

FIG. 3.

THE BOUNDARY LAYER ON THE FRONT PORTION OF A CYLINDER.

Comparison of various solutions and experiments.

+ θ = 10° Experiment
• θ = 20° "
□ θ = 30° "
⊙ θ = 40° "
× θ = 50° "
△ θ = 60° "
↖ θ = 10° Mechanical Solution.
——— 1st Approx (all angles)
- - - - θ = 10° 2nd Approx.
—·—·— θ = 60° " "

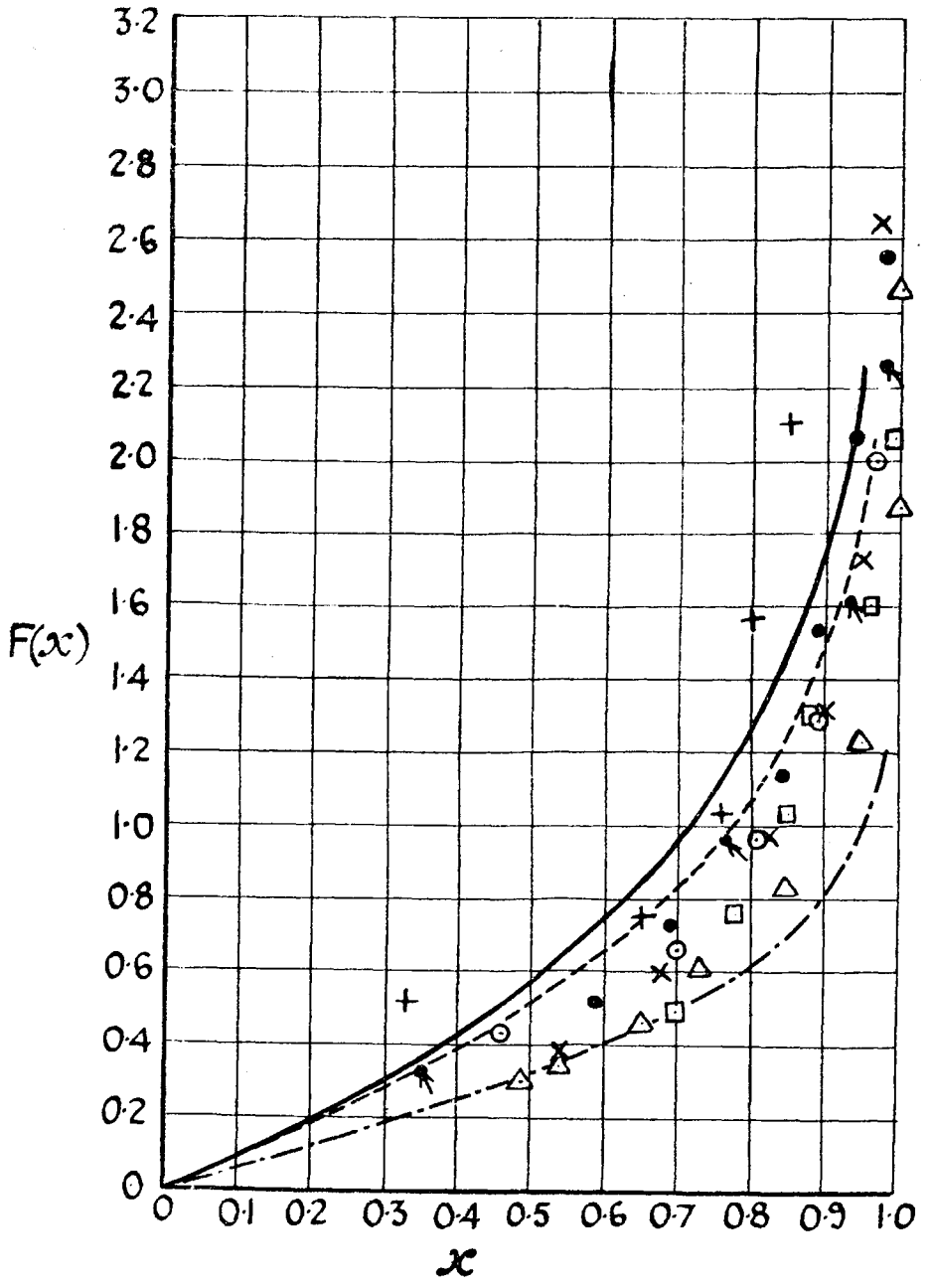

~~T.255~~

FIG. 4.

THE BOUNDARY LAYER ON THE FRONT PORTION OF A CYLINDER.

Comparison of observed and calculated velocities.

⊙ Experimental value. —●— Calculated values.

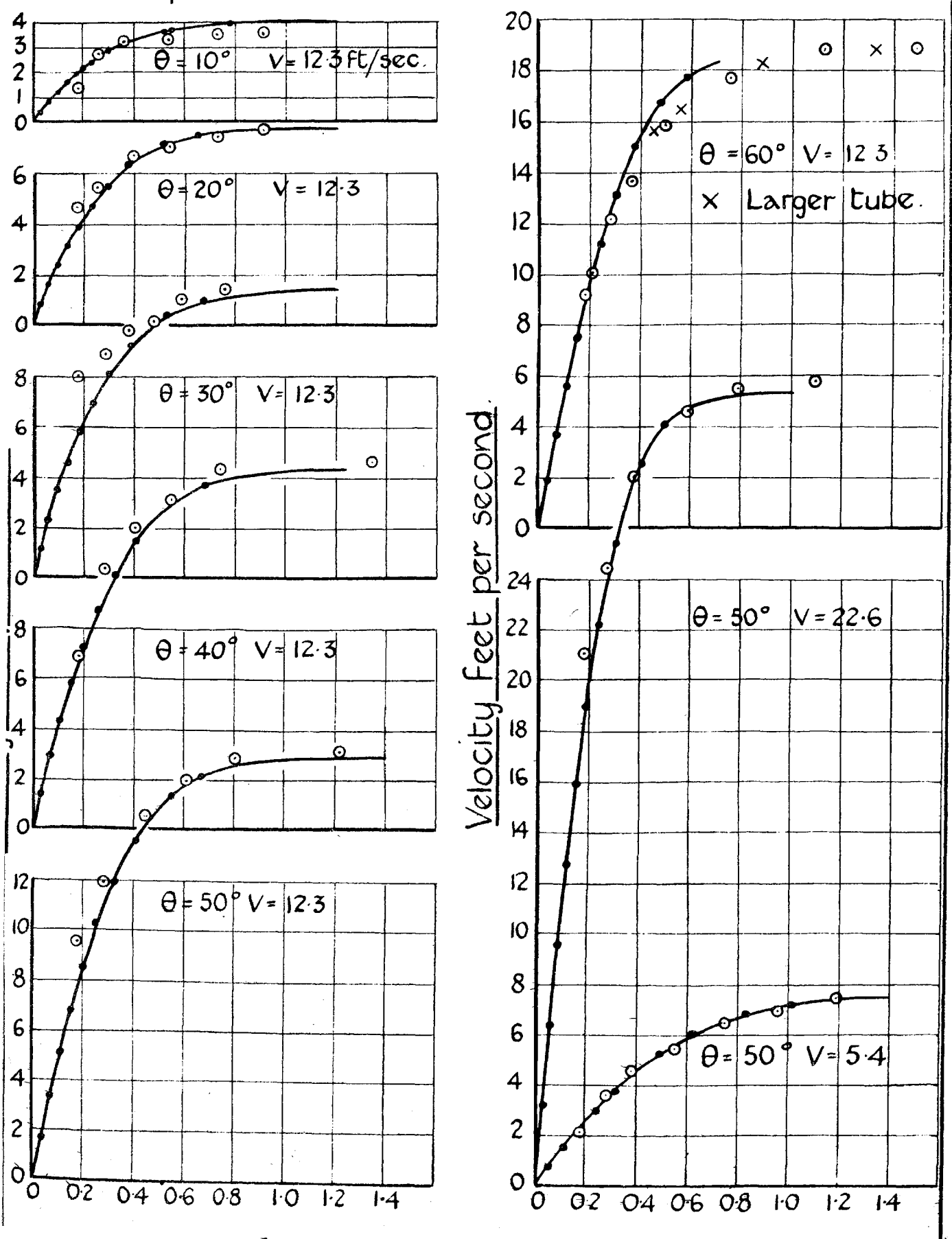

~~T. 2553.~~

FIG. 5.

THE BOUNDARY LAYER ON THE FRONT PORTION OF A CYLINDER.

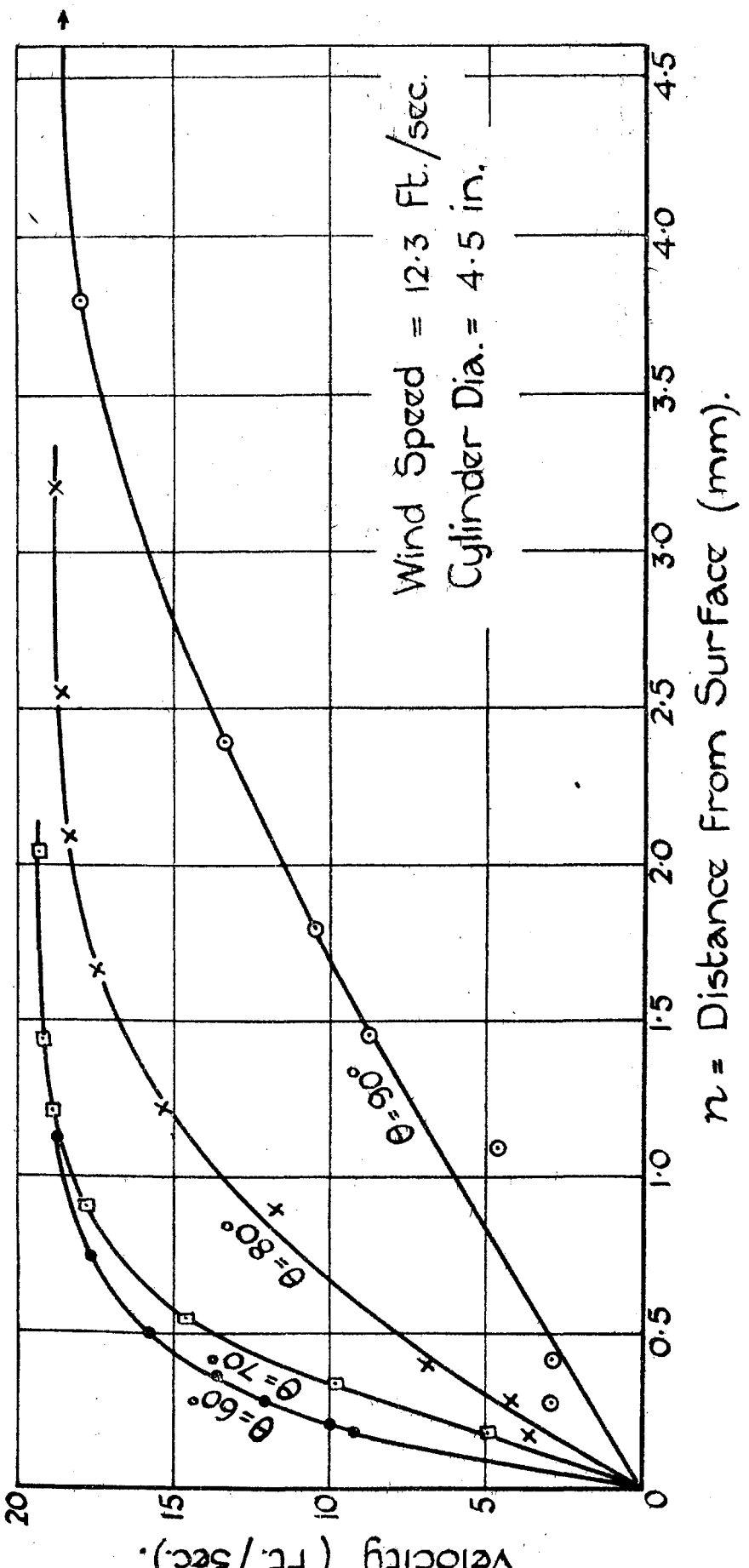

~~1.2.30.~~

FIG. 6

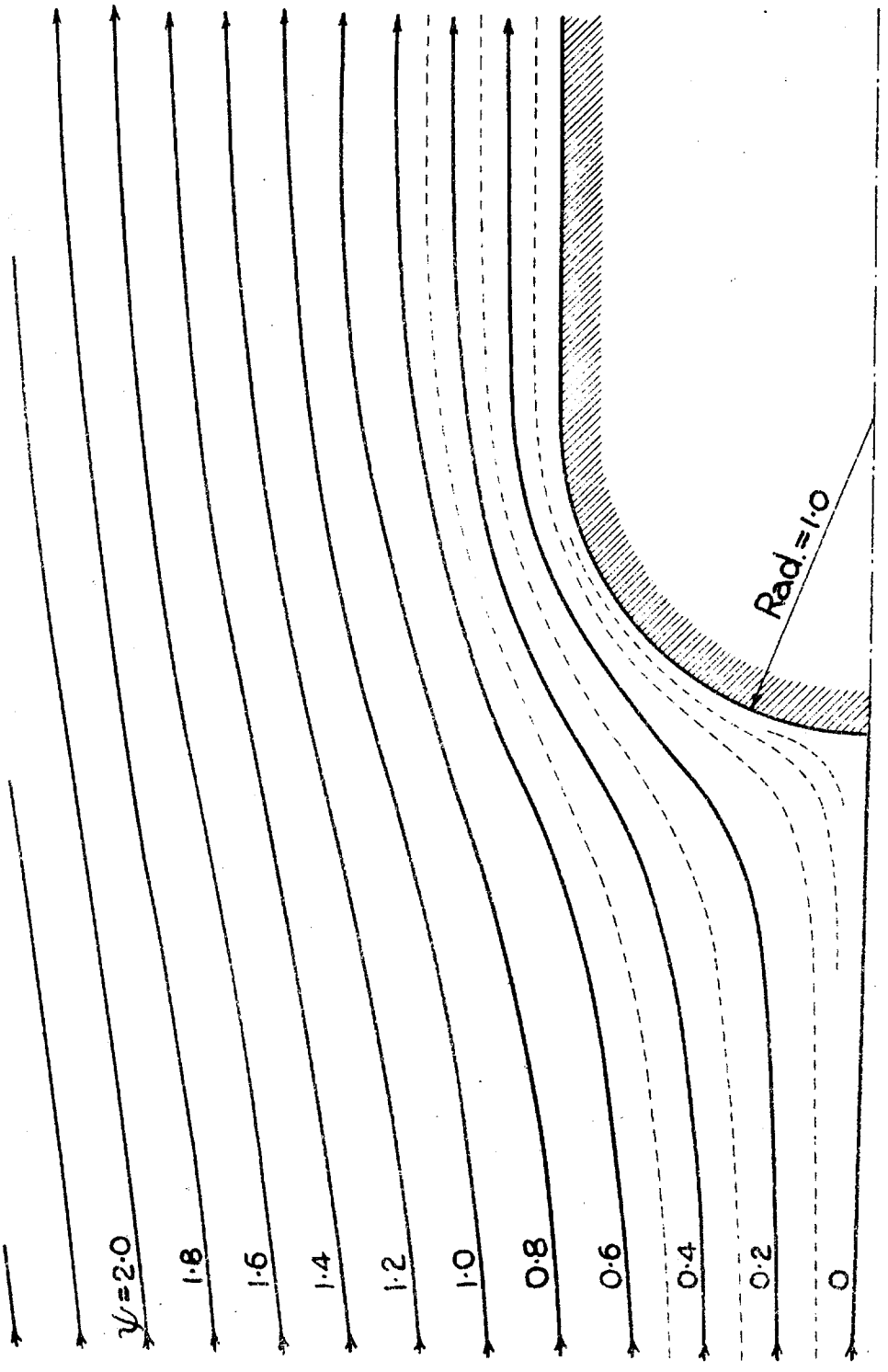

T. 2680
FIG. 7.

Pressures as obtained by Theory for Perfect Fluid.

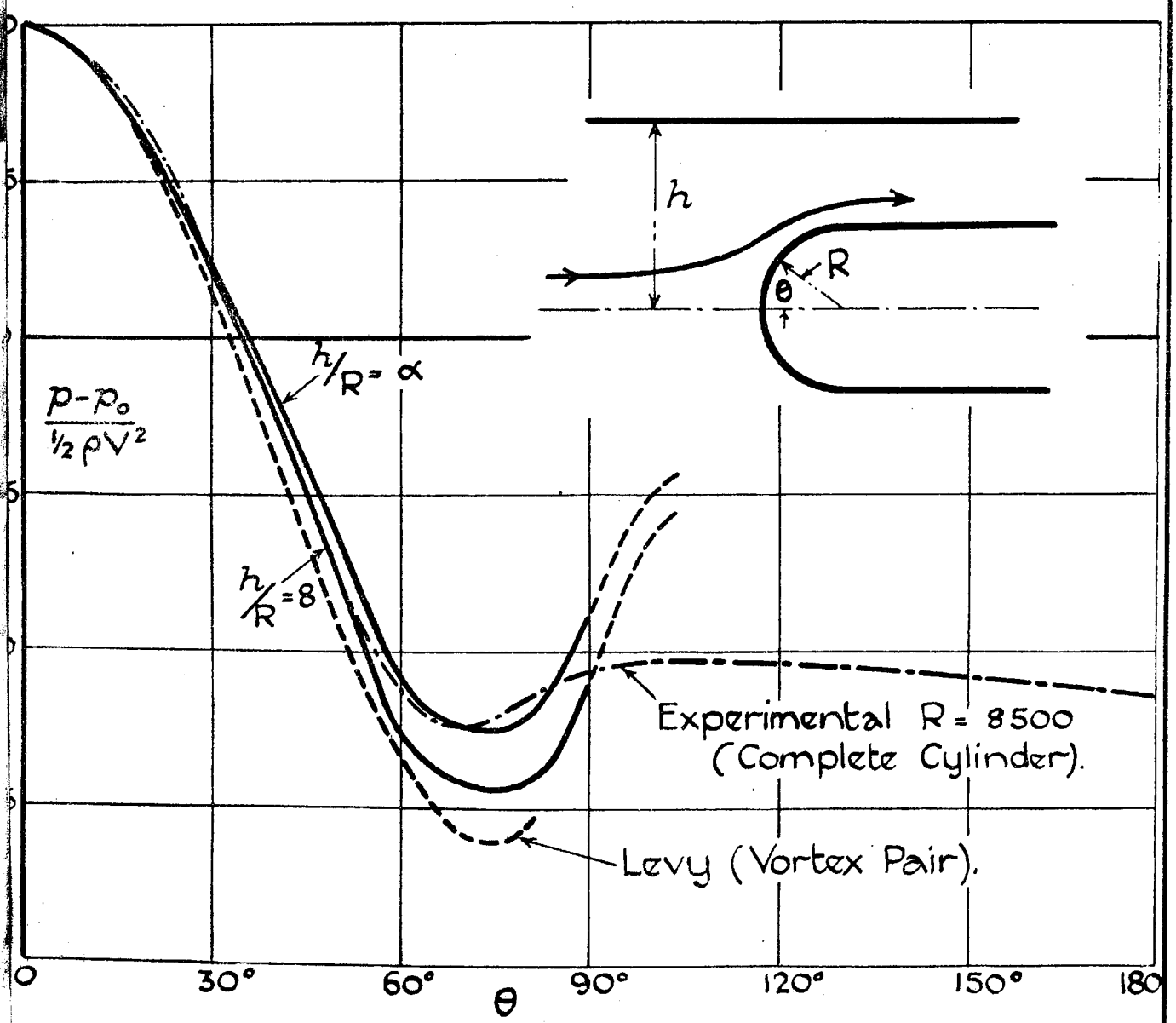

Fig 8

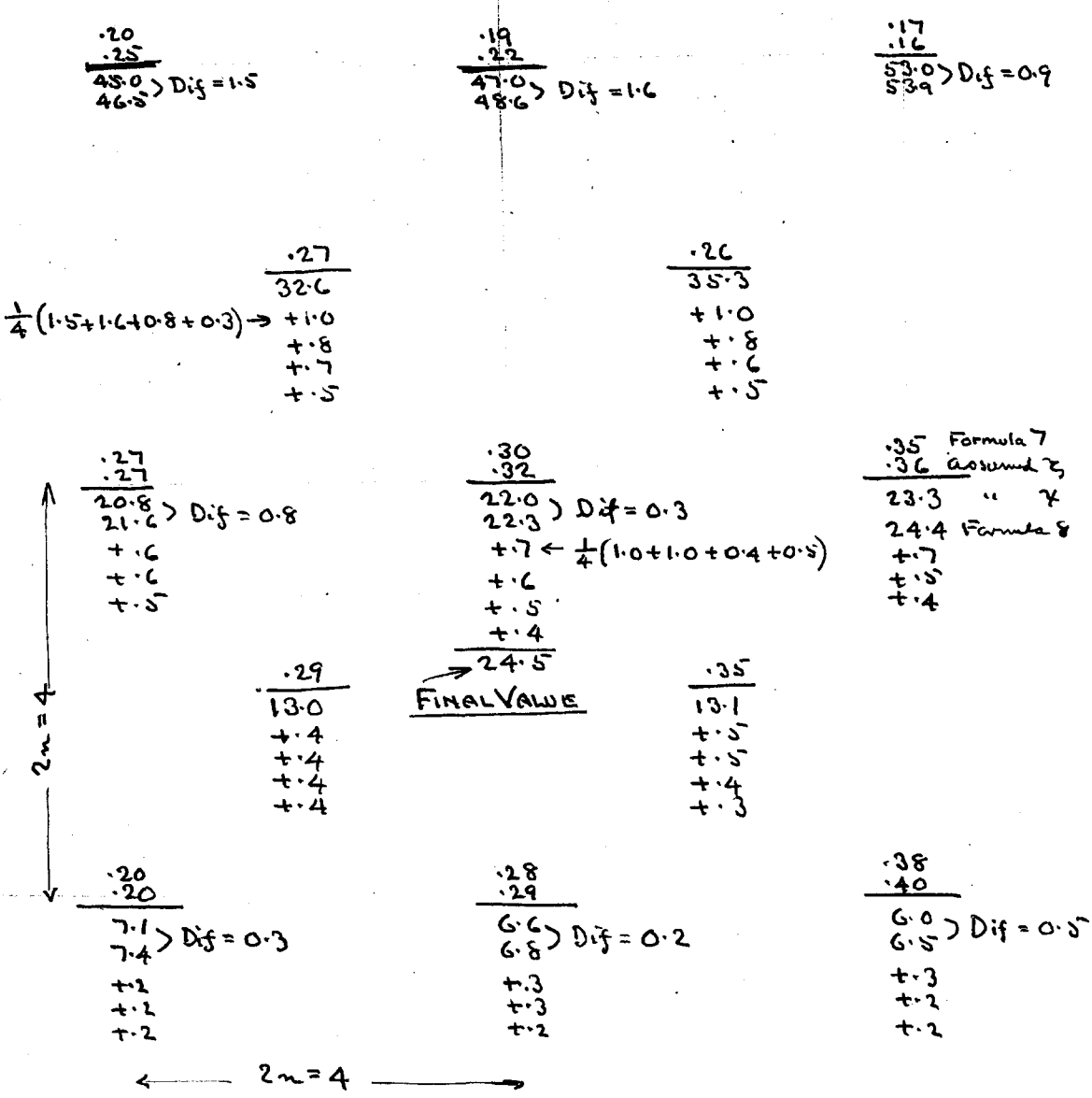

SPECIMEN FIELD BEHIND CYLINDER

Coordinates of centre of above field are $x = -13$, $y = +12$. Values written immediately above and below the short lines are values of ζ and η respectively being taken from previous sheet in the case of the 9 main corners.

Final Values in the Numerical Solution of the Viscous Flow past a Cylinder.

Inner Part of Field.

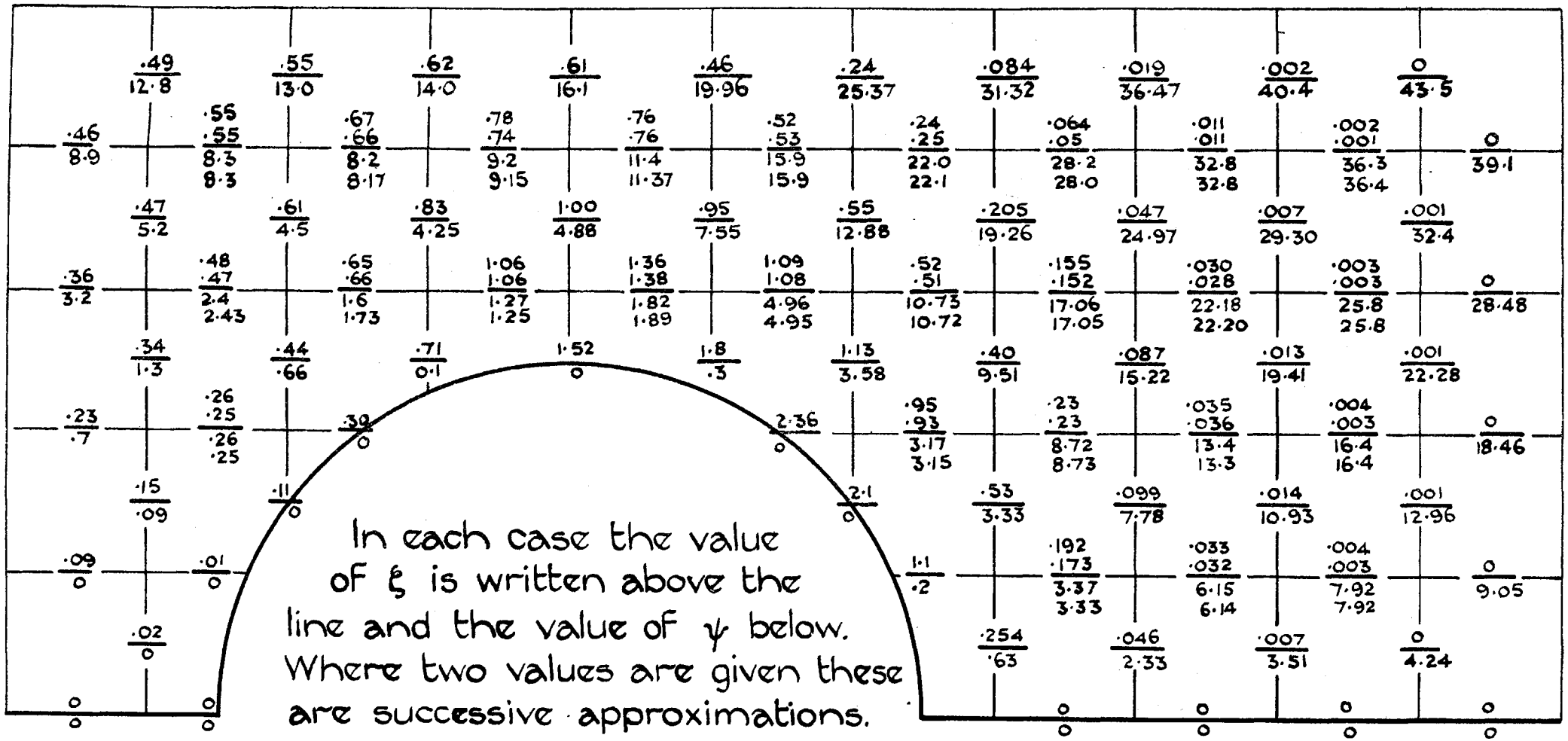

FIG. 9.

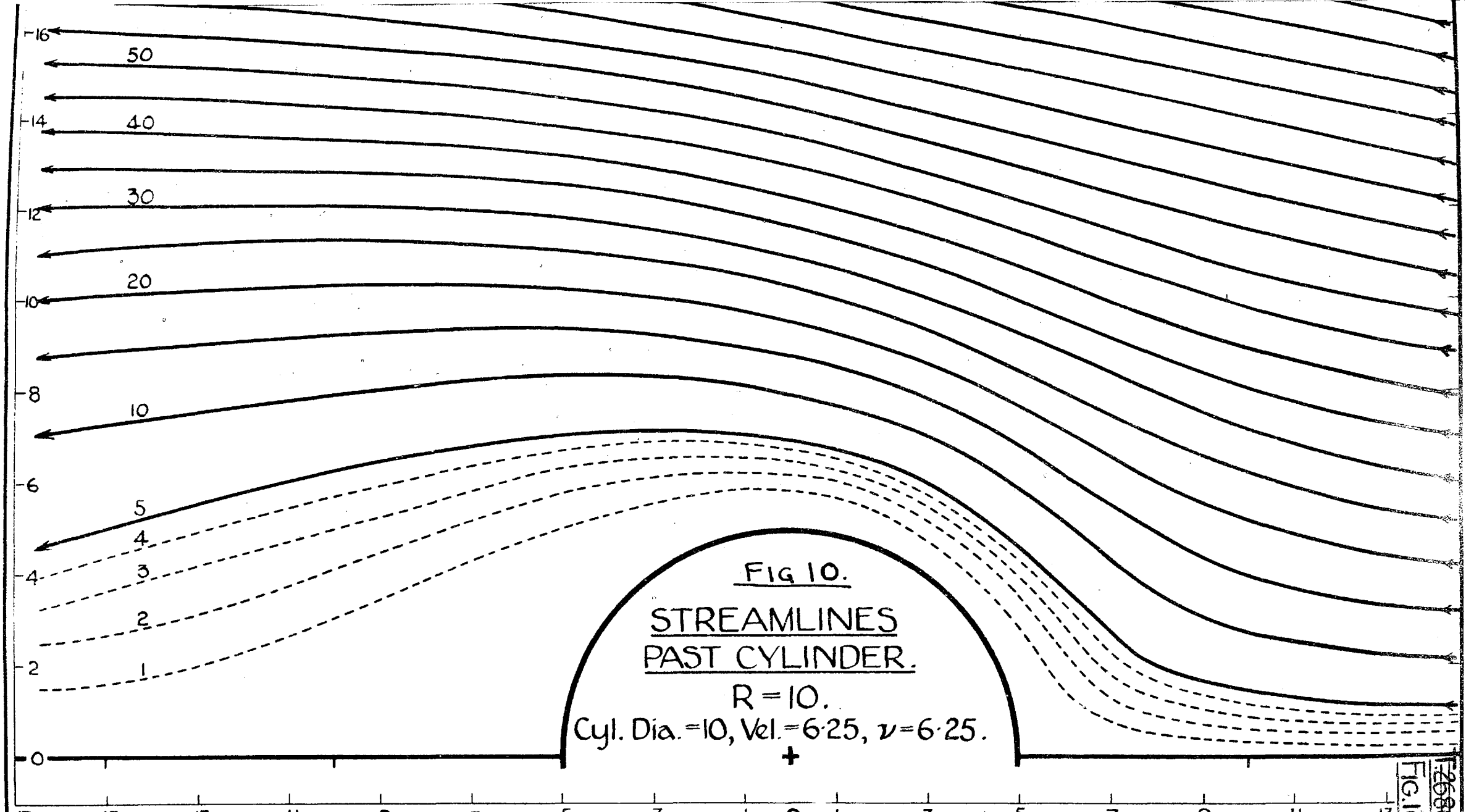

FIG 10.

STREAMLINES PAST CYLINDER.

R = 10.

Cyl. Dia. = 10, Vel. = 6·25, ν = 6·25.

T.2688
FIG. 10

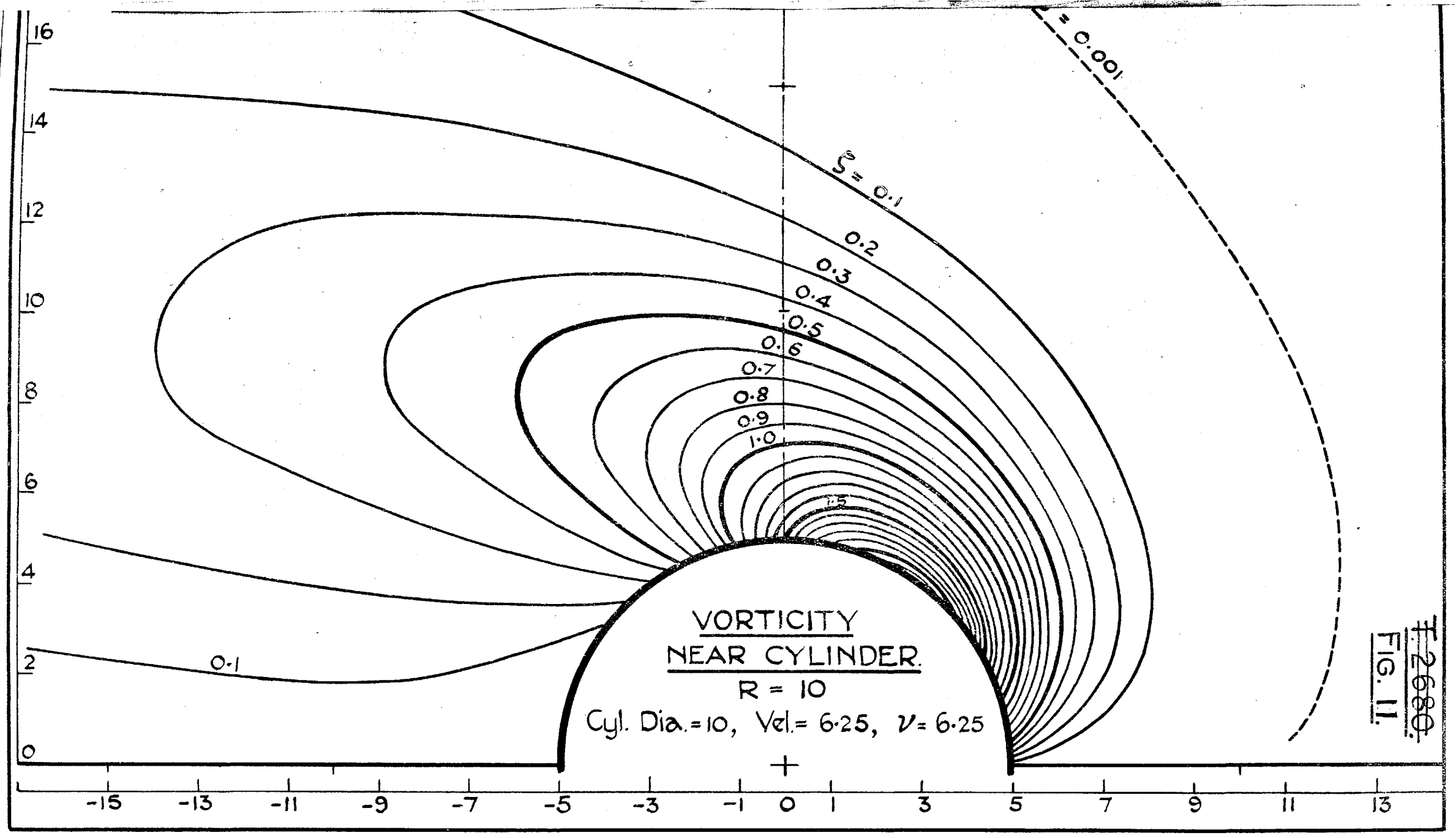
ζ = 0.001
ζ = 0.1
0.2
0.3
0.4
0.5
0.6
0.7
0.8
0.9
1.0
1.5
0.1
VORTICITY
NEAR CYLINDER.
R = 10
Cyl. Dia. = 10, Vel. = 6·25, ν = 6·25
16
14
12
10
8
6
4
2
0
-15
-13
-11
-9
-7
-5
-3
-1
0
1
3
5
7
9
11
13

FIG. 11.

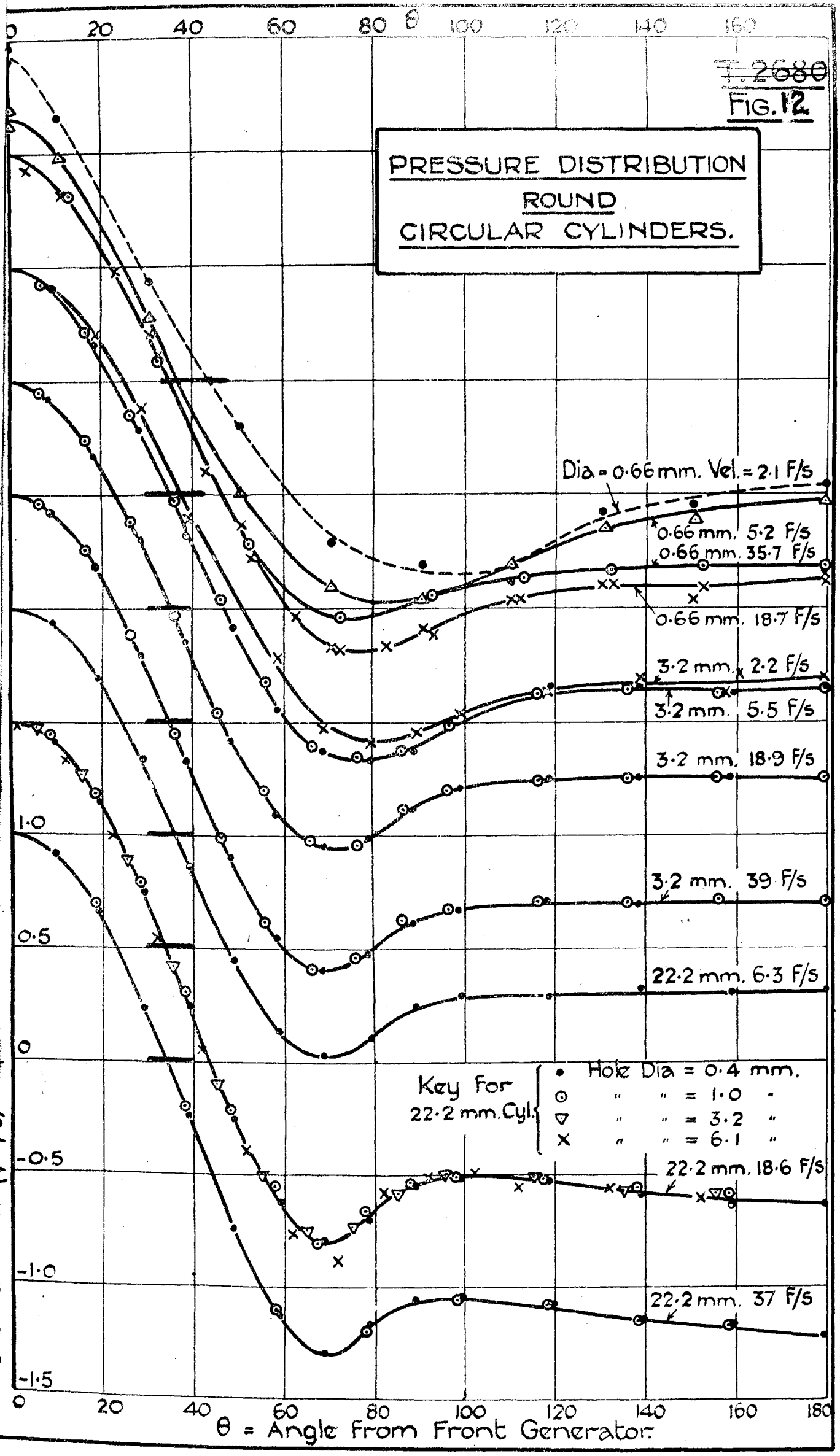
θ
0
20
40
60
80
100
120
140
160
180
T.2680
FIG. 12
PRESSURE DISTRIBUTION
ROUND
CIRCULAR CYLINDERS.
Dia = 0·66 mm. Vel. = 2·1 F/s
0·66 mm. 5·2 F/s
0·66 mm. 35·7 F/s
0·66 mm. 18·7 F/s
3·2 mm. 2·2 F/s
3·2 mm. 5·5 F/s
3·2 mm. 18·9 F/s
3·2 mm. 39 F/s
22·2 mm. 6·3 F/s
22·2 mm. 18·6 F/s
22·2 mm. 37 F/s
Key For 22·2 mm. Cyl.
• Hole Dia = 0·4 mm.
⊙ " " = 1·0 "
▽ " " = 3·2 "
× " " = 6·1 "
1·0
0·5
0
-0·5
-1·0
-1·5
θ = Angle From Front Generator

~~T. 2680.~~

FIG. 13.

VARIATION OF PRESSURE WITH R, AT $\theta = 80^\circ$ & $\theta = 160^\circ$.

+ — R. & M. Nº 1176.
⊙ — Present Report (Expt.).
△ — " " (Theory).
● — Fage.
▲ — " (Large Cylinder).
× — Taylor. R. & M. Nº 191.
⊡ — Parkins.

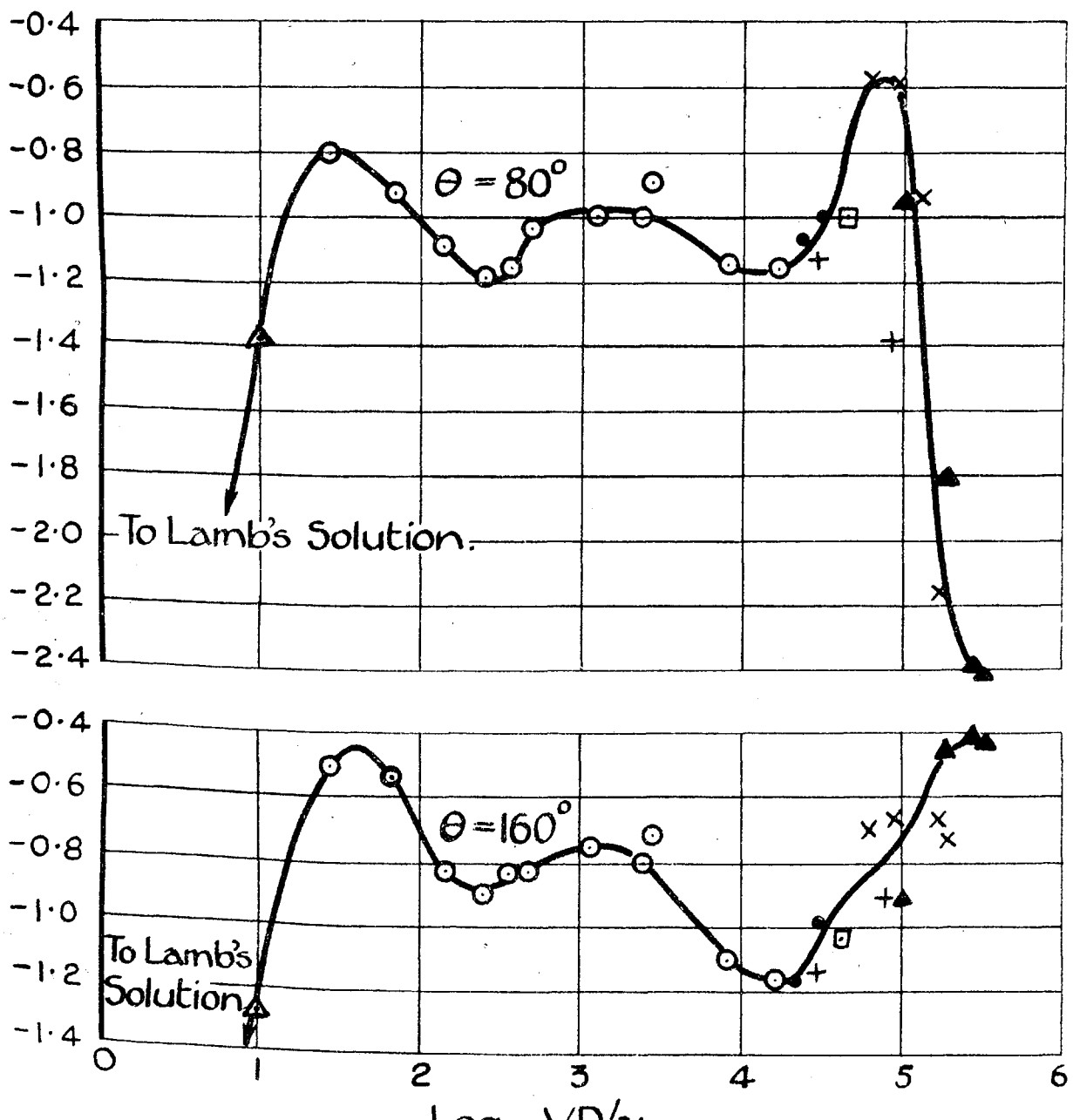

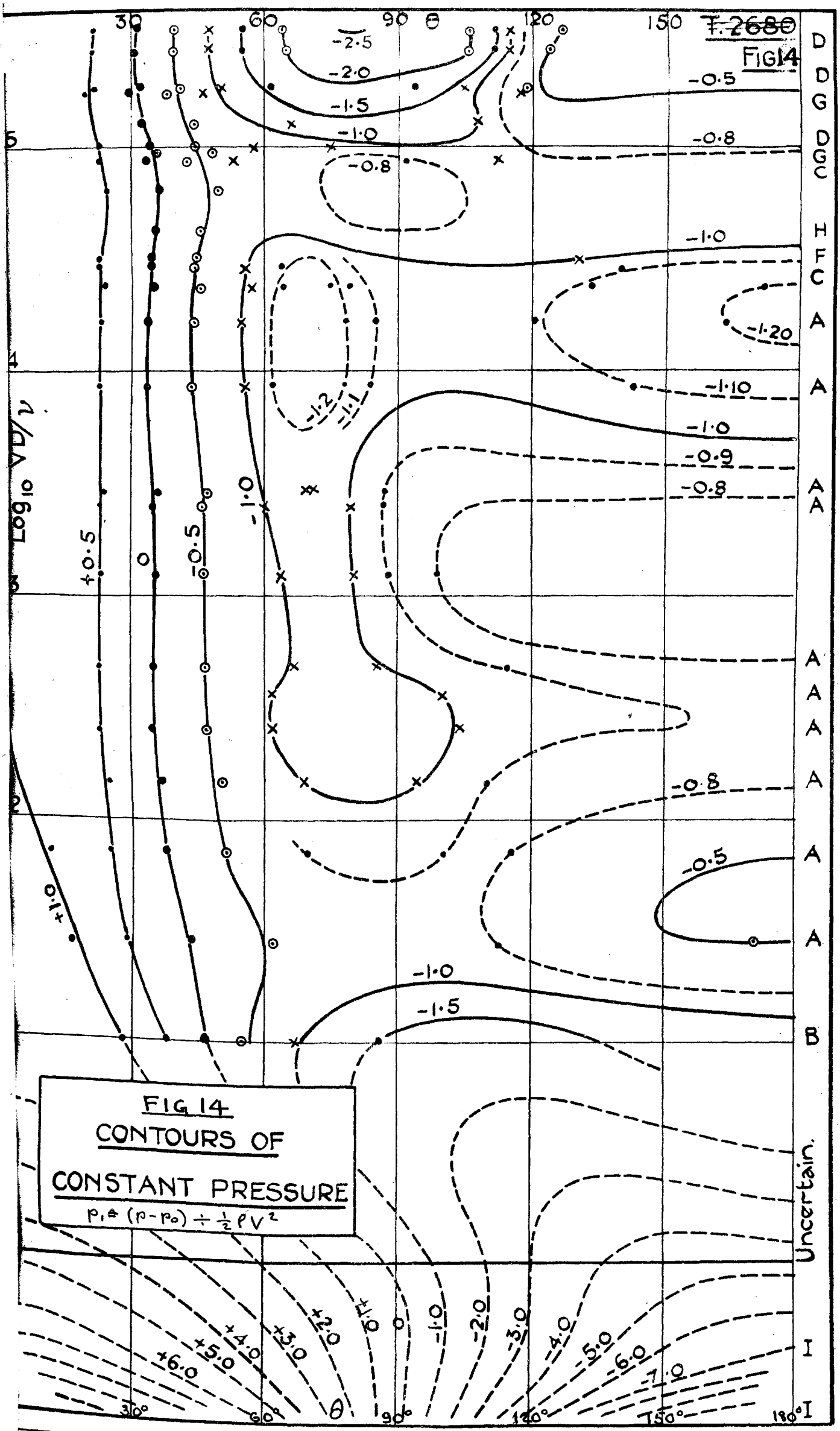

FIG 14
CONTOURS OF
CONSTANT PRESSURE
$p_1 \triangleq (p - p_0) \div \frac{1}{2}\rho V^2$

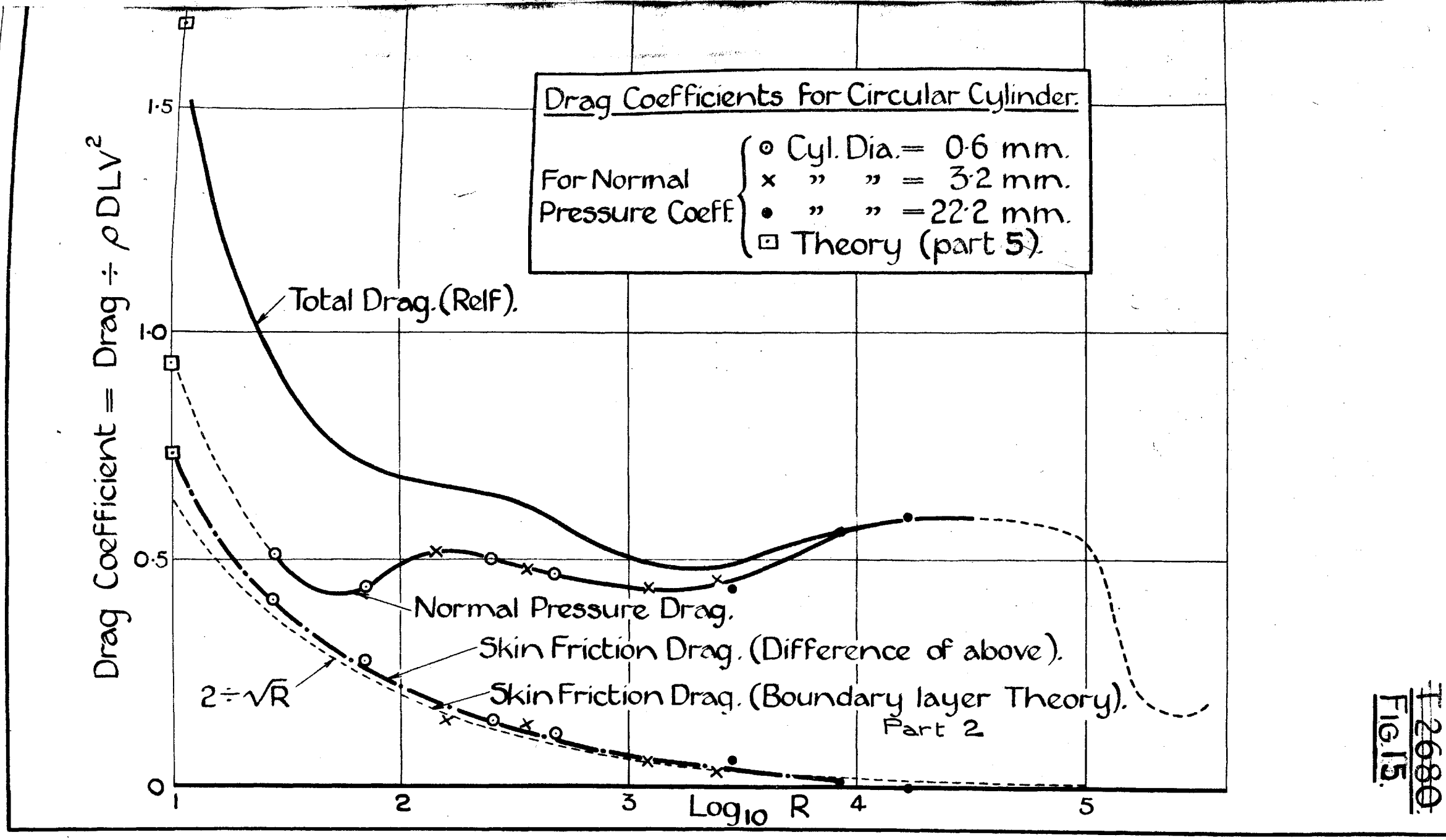
Drag Coefficients for Circular Cylinder.
For Normal Pressure Coeff.
⊙ Cyl. Dia. = 0·6 mm.
× " " = 3·2 mm.
• " " = 22·2 mm.
⊡ Theory (part 5).
Drag Coefficient = Drag ÷ ρDLV²
1·5
1·0
0·5
0
1
2
3
4
5
Log10 R
Total Drag. (Relf).
Normal Pressure Drag.
Skin Friction Drag. (Difference of above).
Skin Friction Drag. (Boundary layer Theory).
Part 2
2÷√R

R. 2680.
FIG. 15.

~~T.2680.~~
FIG. 16.

EFFECT OF CHANNEL WALLS.

⊙----- Wall Pressure Experiments.
⊡—— Parkins.
•—— Pressure Distribution R.&M. Nº 1176.

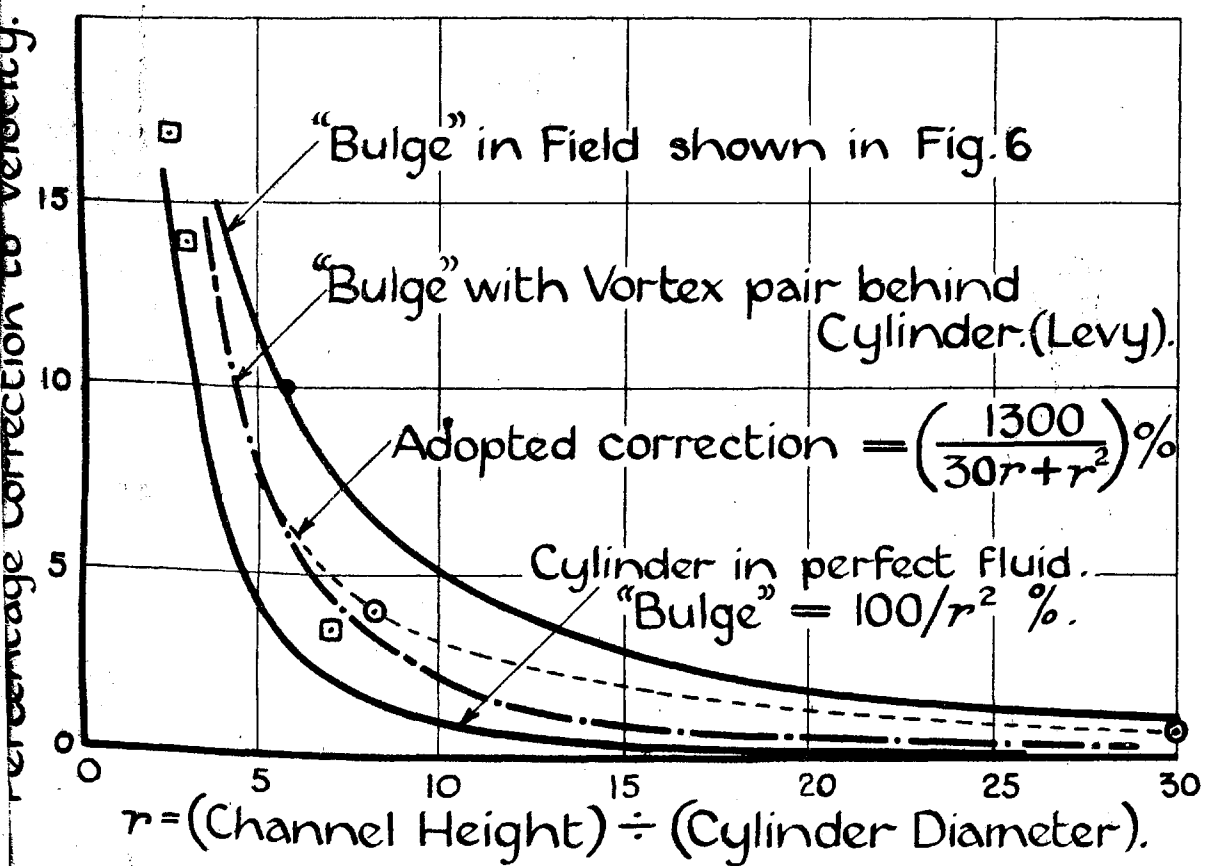

Fig 17

ARRANGEMENT OF CYLINDER IN CHANNEL.

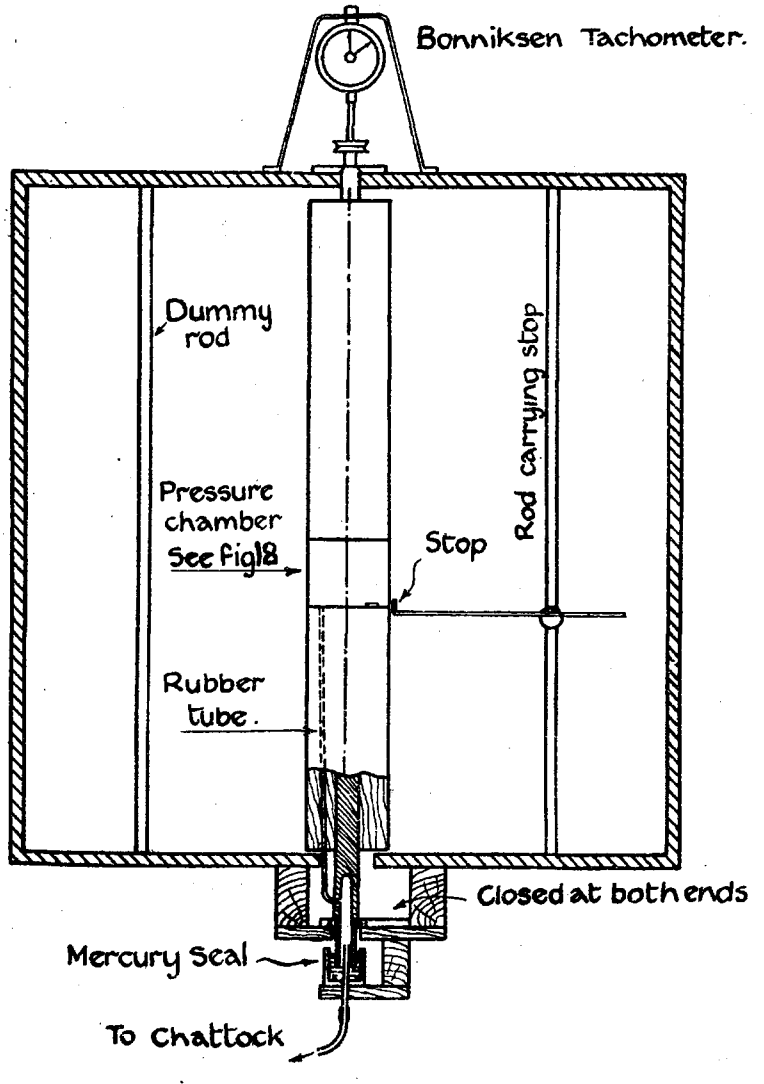

FIG 18

AIR TIGHT SECTION OF CYLINDER.

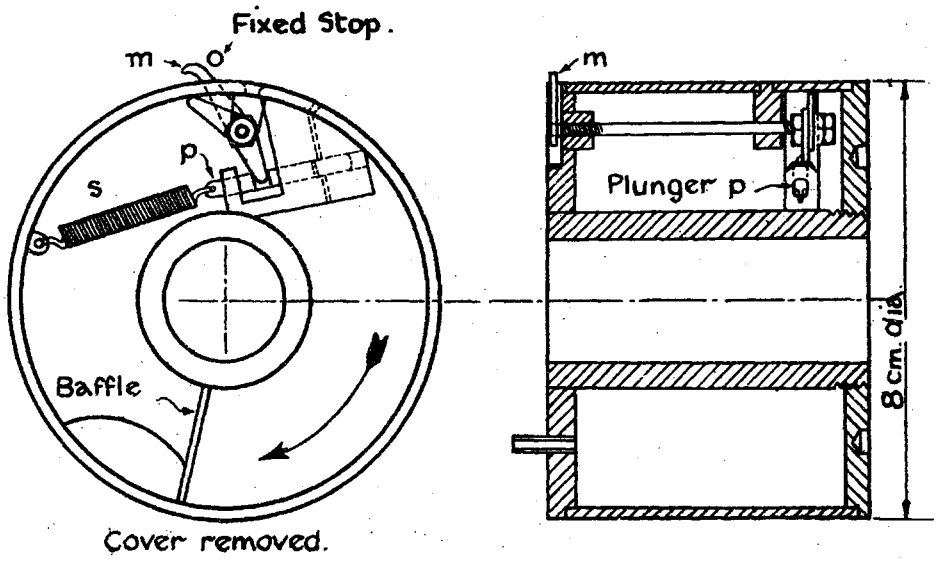

Fig 19

PRESSURE ROUND VARIOUS SECTIONS OF A ROTATING CYLINDER, 8CM. DIAM., 61·7CM. LONG.

Wind Speed = 9·6 ft/sec., Circumferential Speed of Cylinder = 19·2 ft/sec.

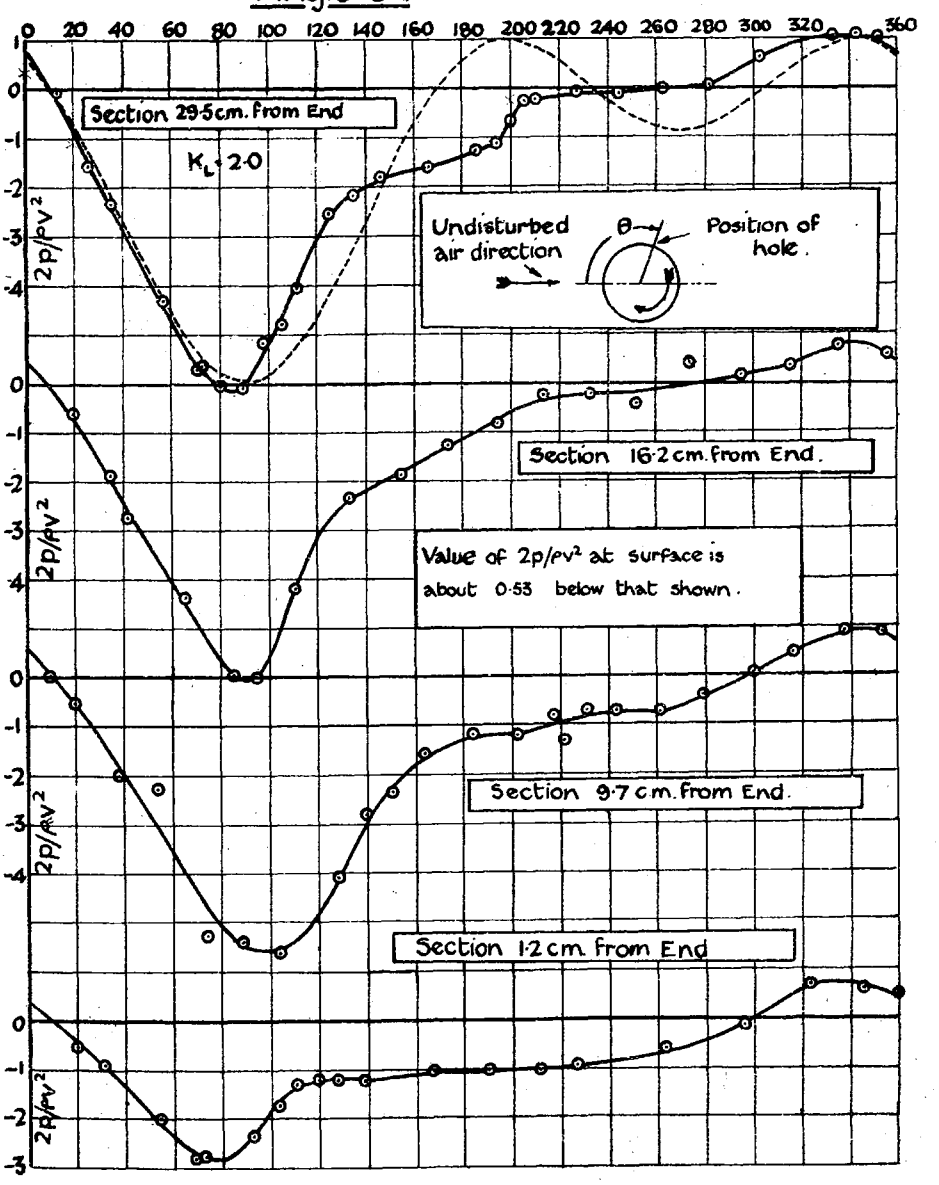

PRESSURE ROUND CENTRE SECTION AT VARIOUS VALUES OF v/V

Angle θ

FIG. 20

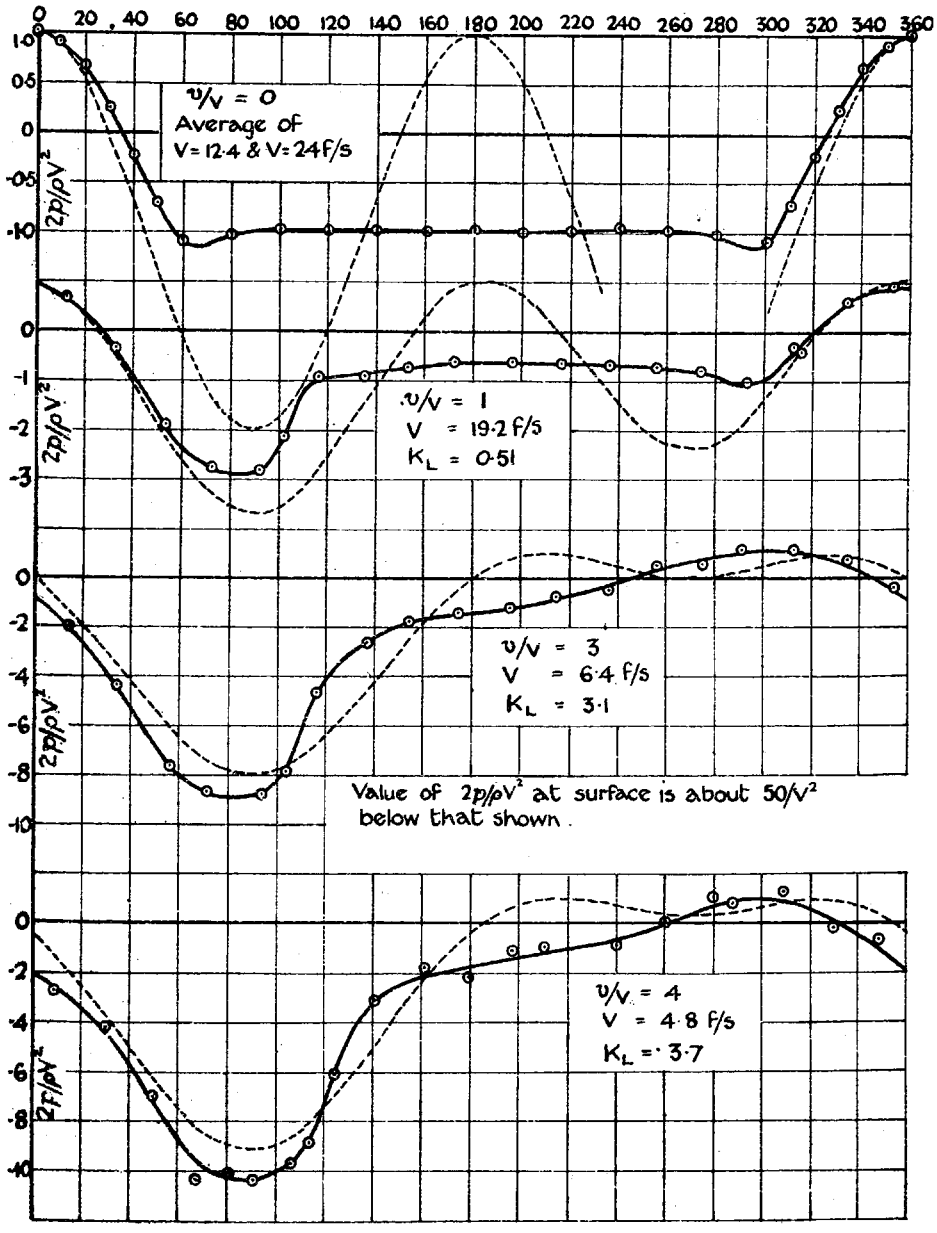

Fig 21

Pressure Distribution round the Centre of a Rotating Cylinder at Various Values of v/V

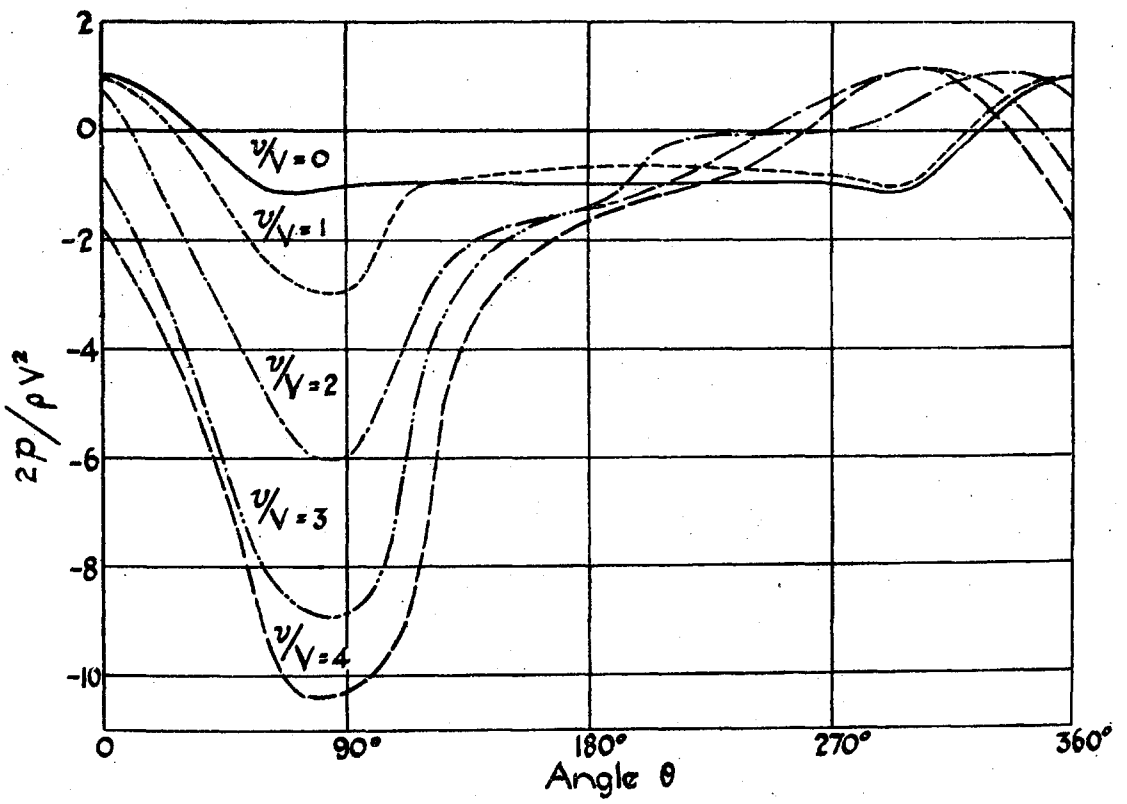

Figs 22 & 23

LIFT AND DRAG COEFFICIENT DEDUCED FROM PRESSURE CURVES.

FIG. 22

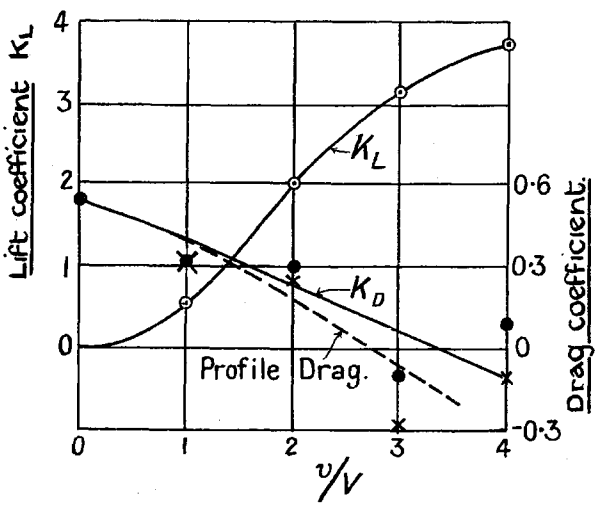

⊙ Lift coefficient
● Drag "
× Profile Drag. coefficient.

FIG. 23

Air velocities near the surface of a cylinder rotating in still air.

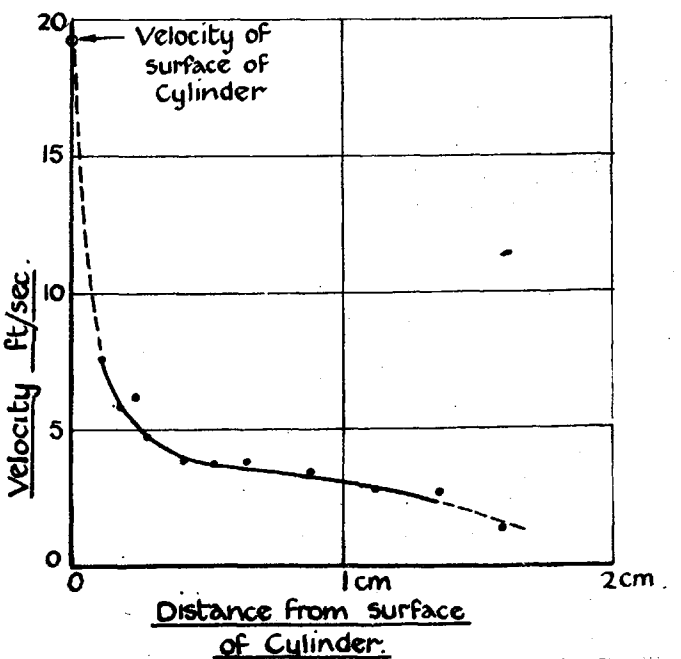

P.1180 A

Malby & Sons, Photo-Litho

FIG 24

Distribution of Lift and Drag along Cylinder.

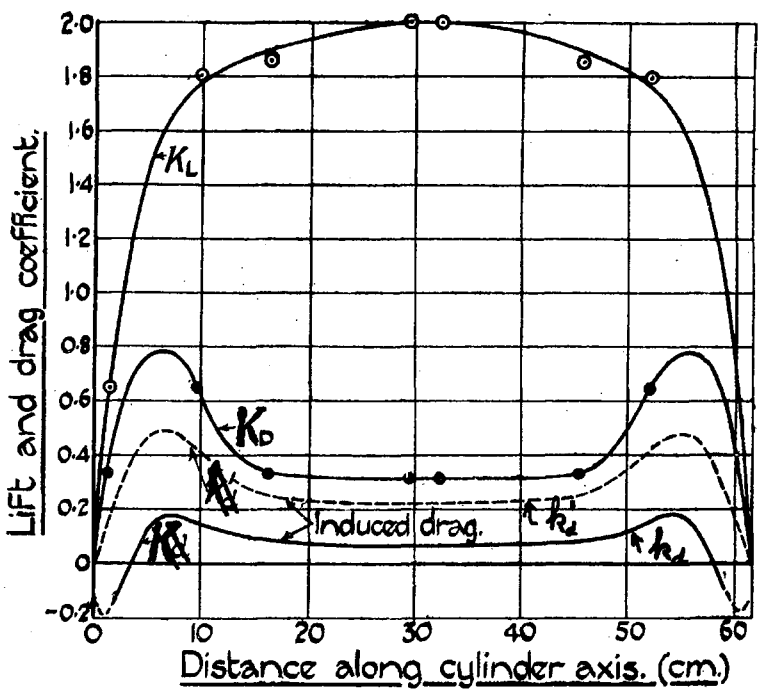

FIG 25

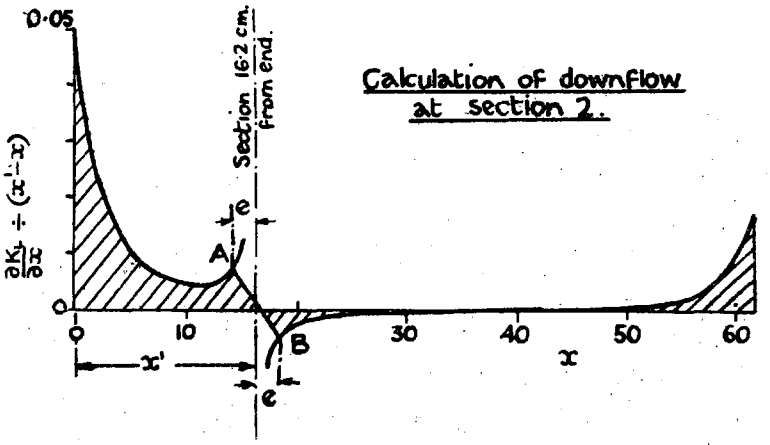

Calculation of downflow at section 2.

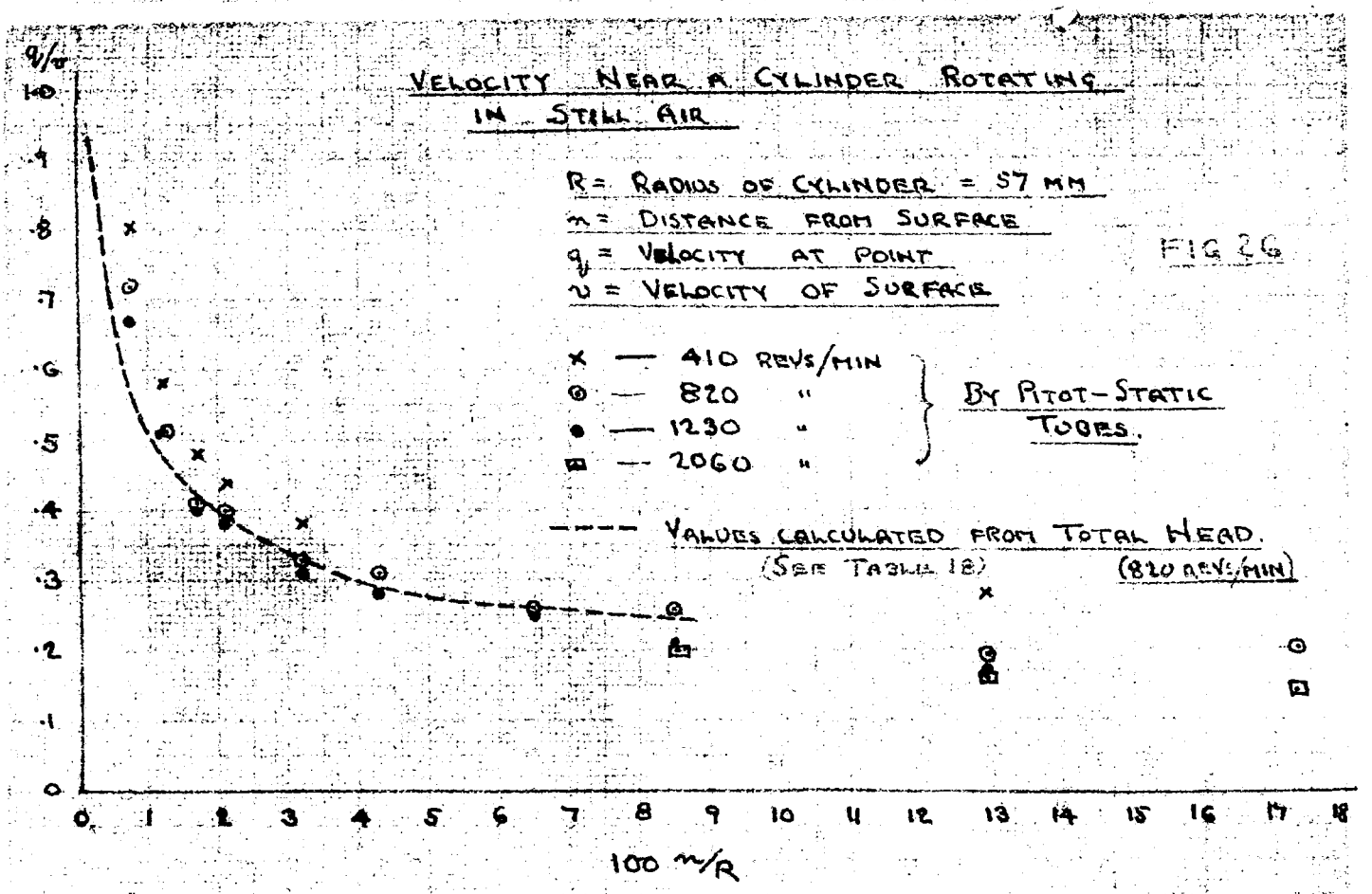

VELOCITY NEAR A CYLINDER ROTATING IN STILL AIR

R = RADIUS OF CYLINDER = 57 MM
m = DISTANCE FROM SURFACE
q_y = VELOCITY AT POINT
v = VELOCITY OF SURFACE

× — 410 REVS/MIN
⊙ — 820 "
● — 1230 "
⊡ — 2060 "
} BY PITOT-STATIC TUBES.

---- VALUES CALCULATED FROM TOTAL HEAD. (SEE TABLE 18) (820 REVS/MIN)

FIG 26

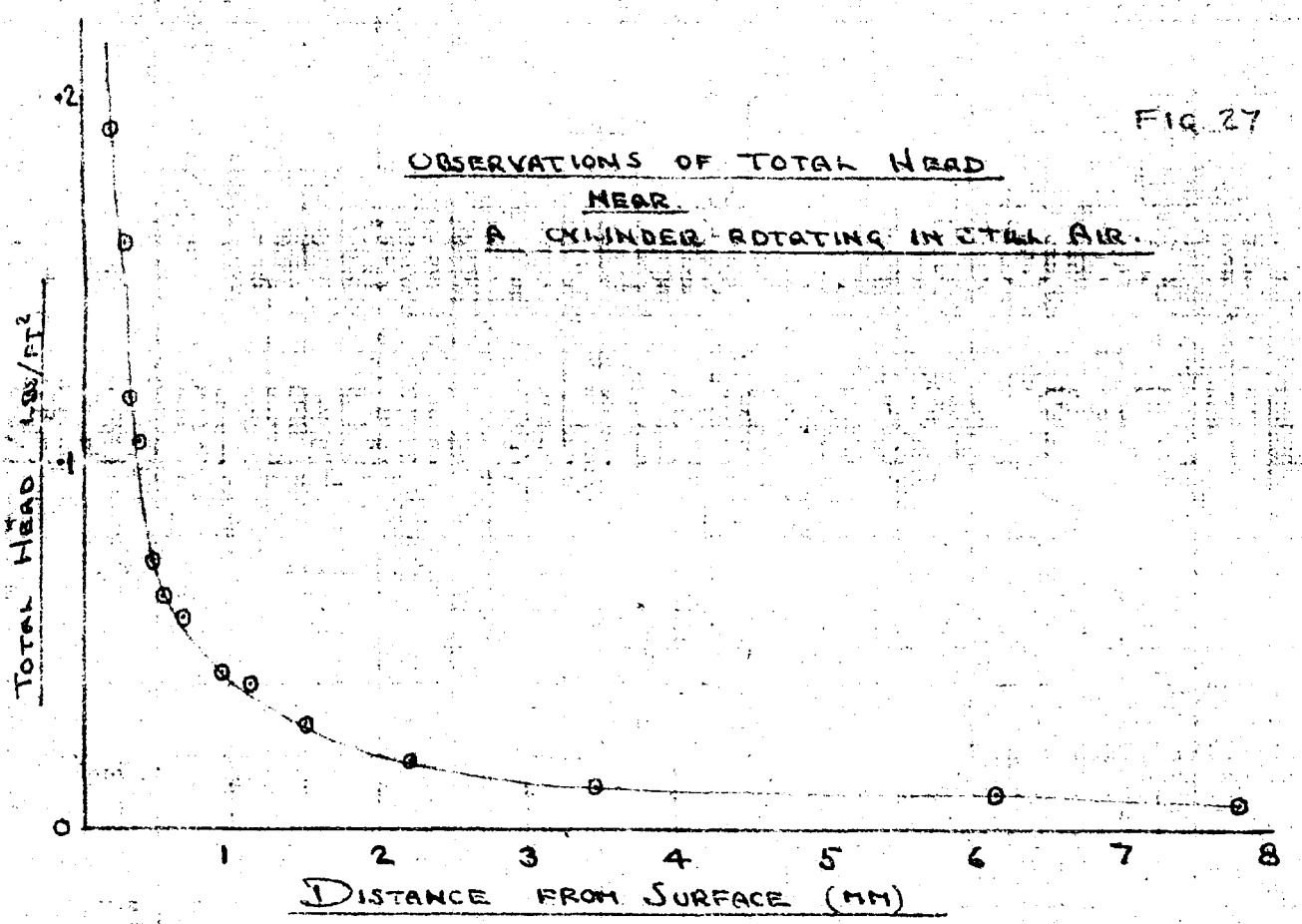

FIG 27

OBSERVATIONS OF TOTAL HEAD NEAR A CYLINDER ROTATING IN STILL AIR.

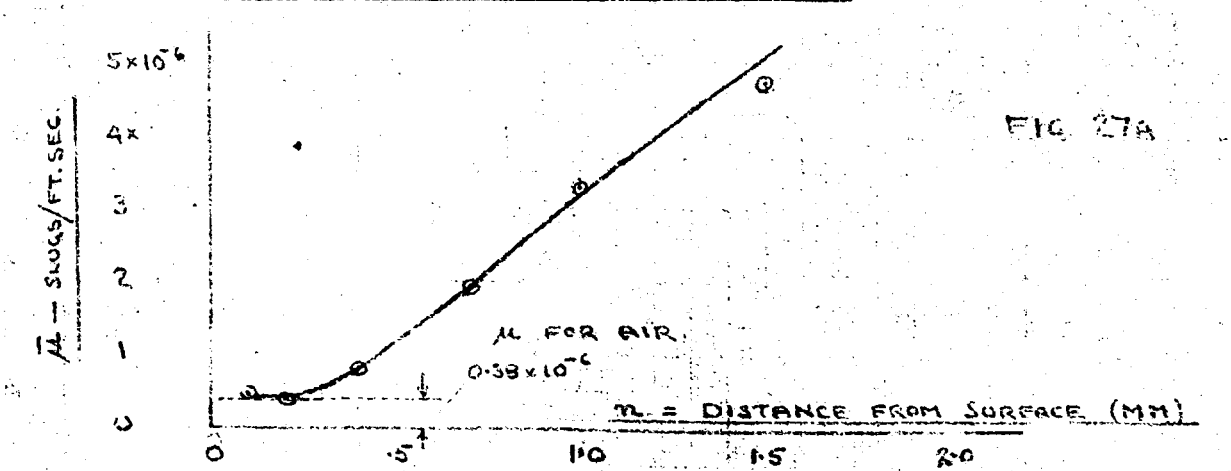

FIG 27A

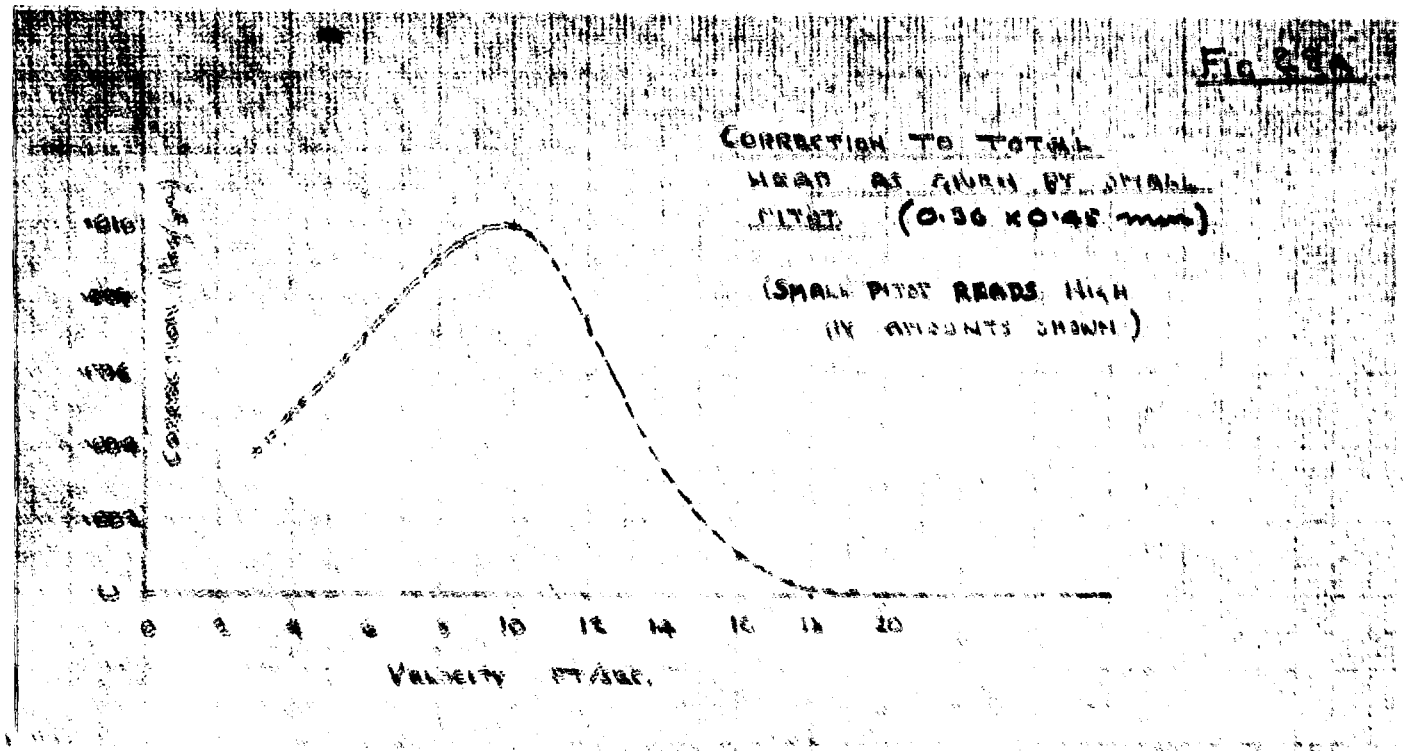
Fig 2.8a
CORRECTION TO TOTAL
HEAD AS GIVEN BY SMALL
PITOT (0.36 x 0.45 mm)
(SMALL PITOT READS HIGH
IN AMOUNTS SHOWN)
CORRECTION
0
2
4
6
8
10
12
14
16
18
20
VELOCITY FT/SEC.

TOTAL HEAD AND STATIC PRESSURE NEAR A CYLINDER ROTATING IN AN AIR STREAM

Fig 28

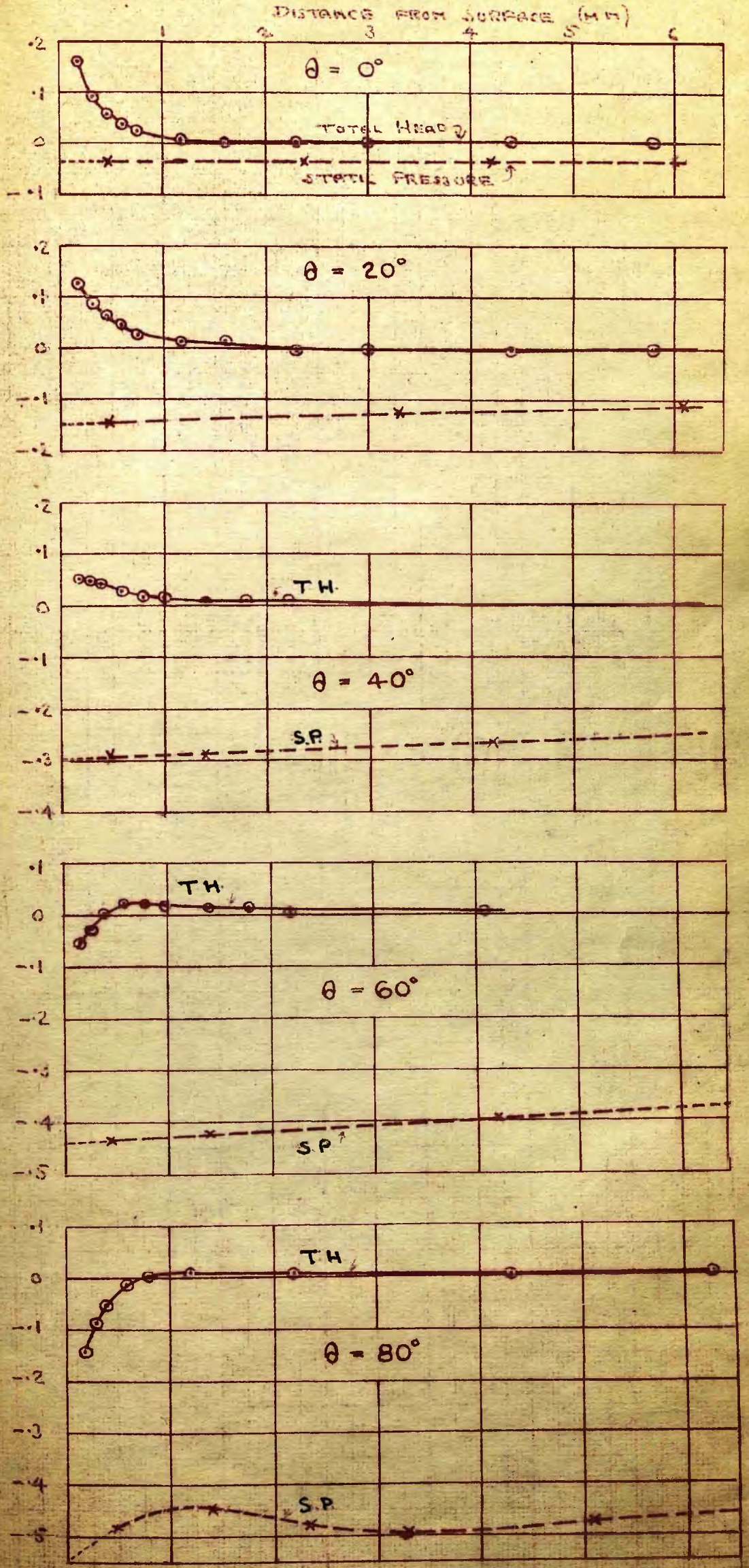

TOTAL HEAD AND STATIC PRESSURE NEAR A CYLINDER ROTATING IN AN AIR STREAM

Fig 29

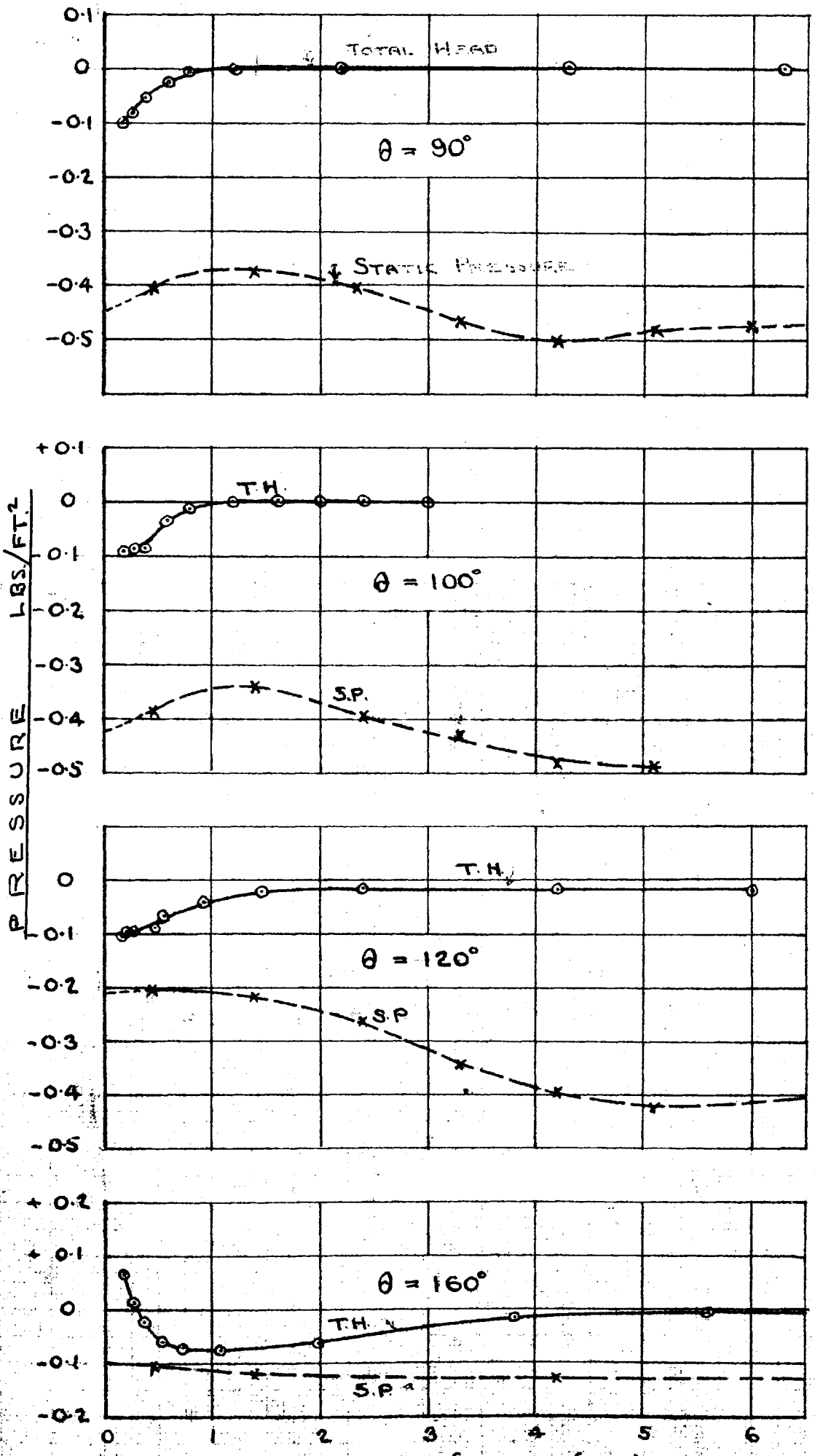

PITOT HEAD AND STATIC PRESSURE NEAR A CYLINDER ROTATING IN AN AIR STREAM

Fig 30

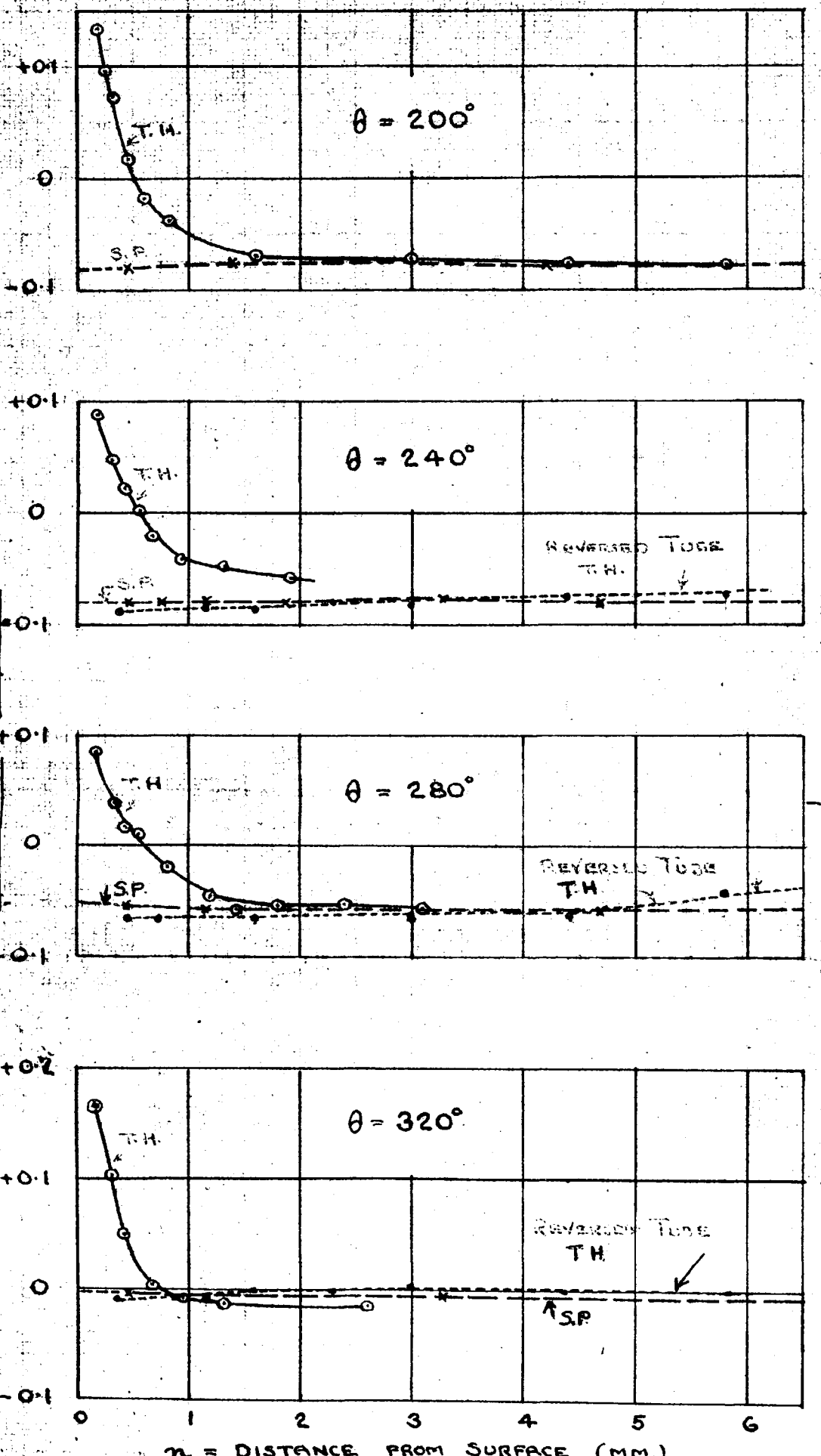

Velocity near a cylinder rotating in an air stream

Channel vel = 8 ft/sec
Surface vel. = 16 ft/sec.

Cylinder Dia. = 4½ in.
= 114 mm

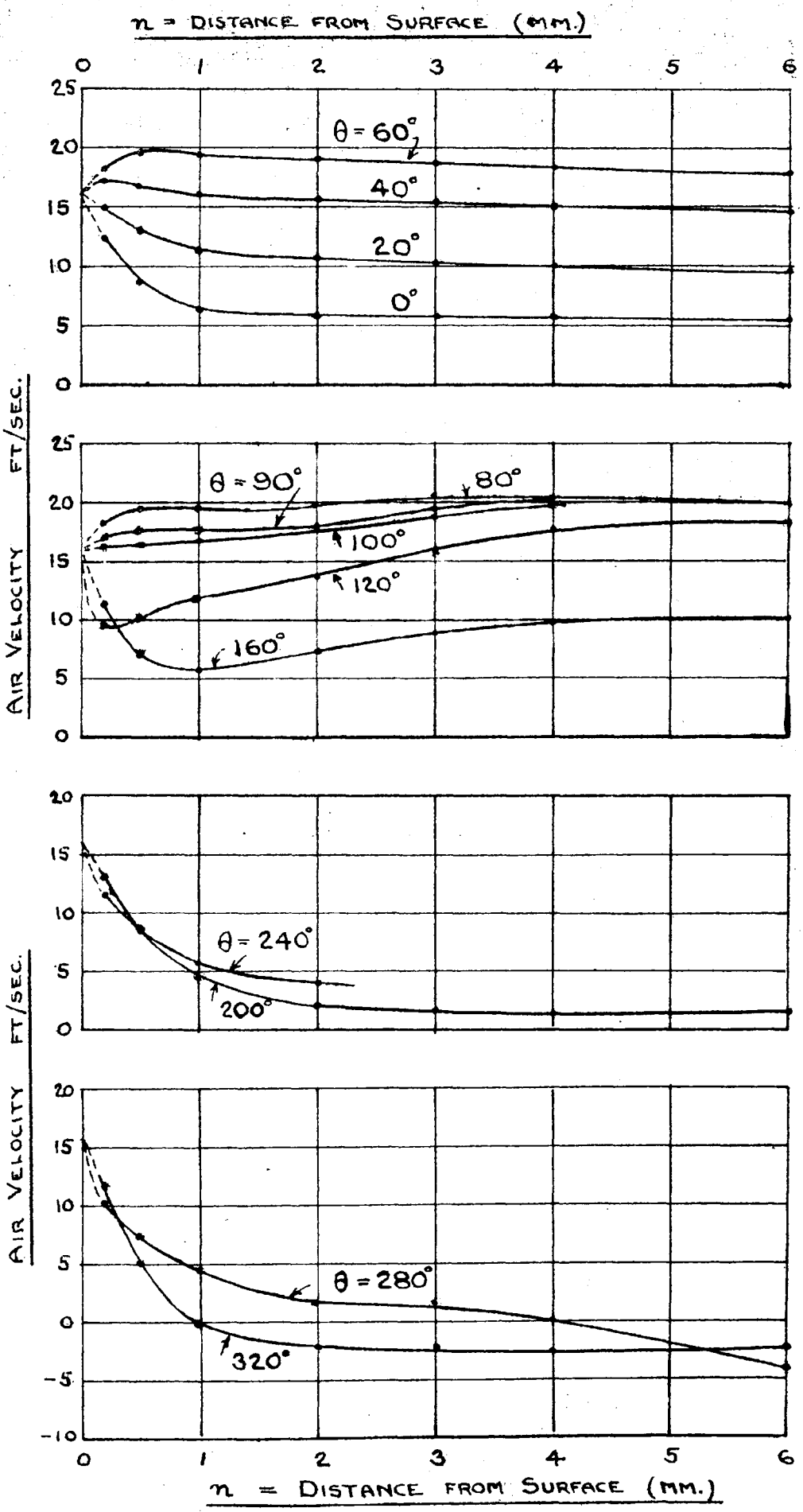

VELOCITY CONTOURS CLOSE TO ROTATING CYLINDER IN AN AIR STREAM.

FIG 32.

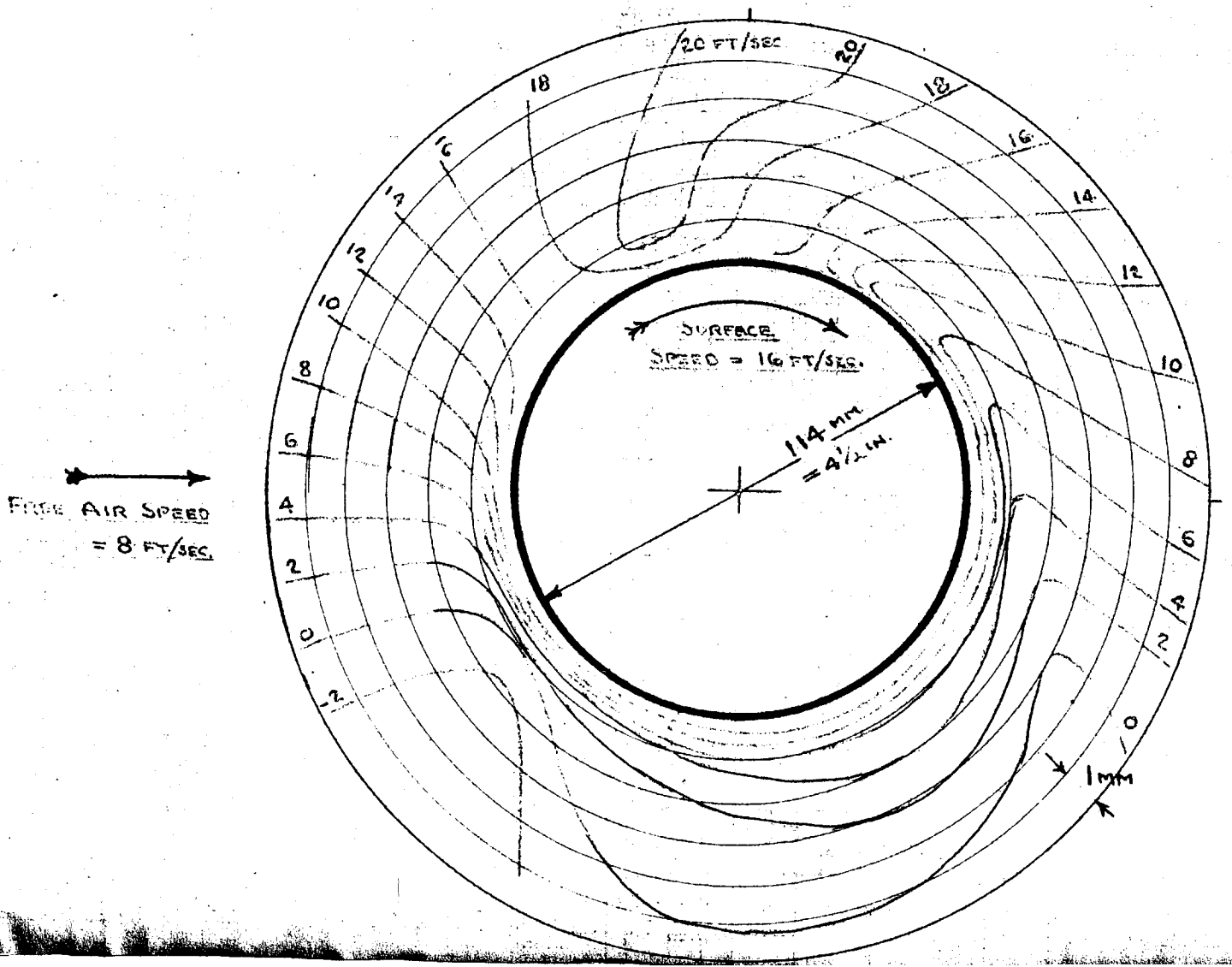

SKETCH SHOWING DISTRIBUTION OF VELOCITY IN THE NEIGHBOURHOOD OF A CYLINDER ROTATING IN AN AIR STREAM.

VELOCITY OF AIR STREAM = 1·0 , CIRCUMFERENTIAL SPEED OF CYLINDER = 2·0

Fig 33

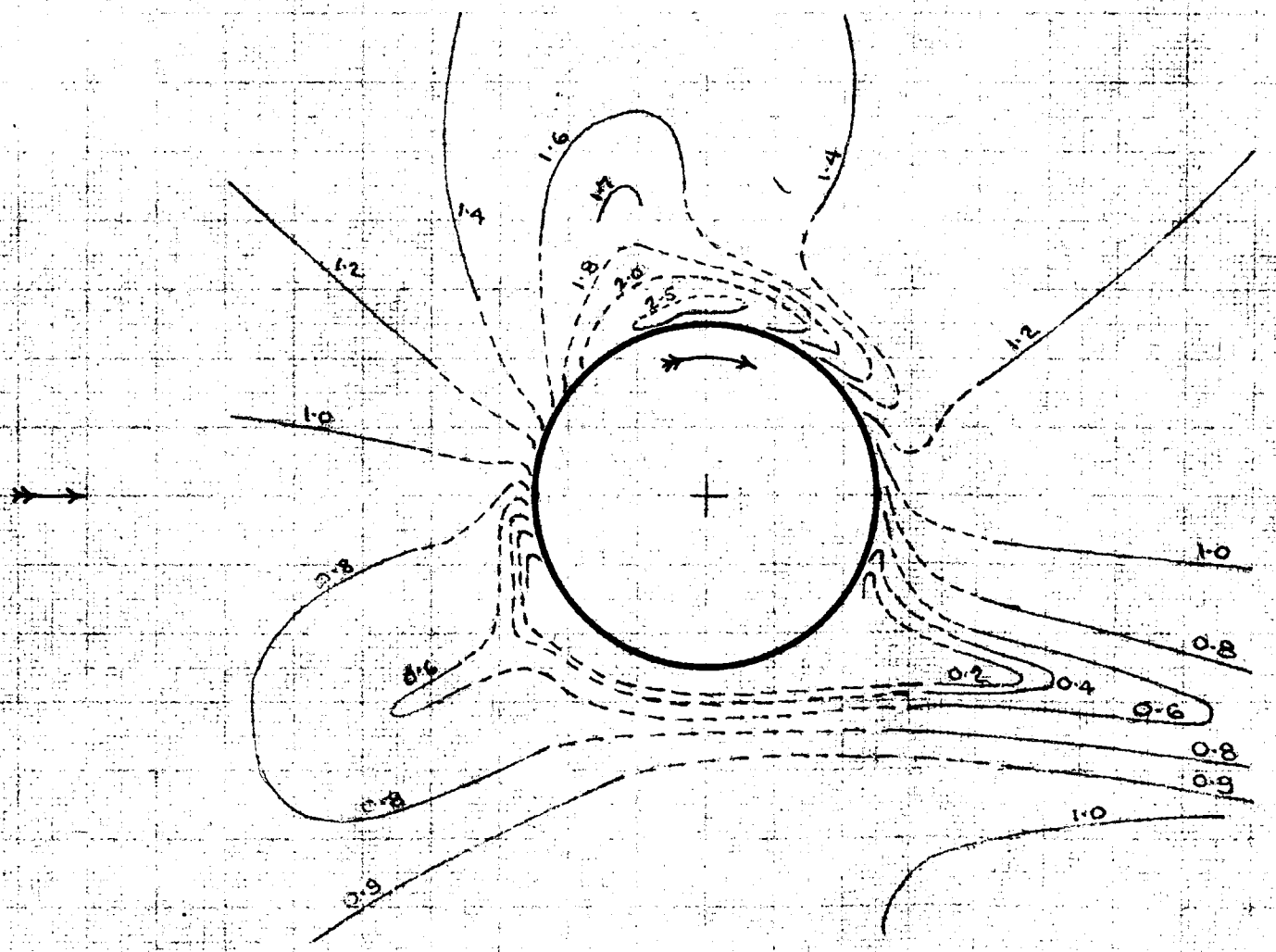

VORTICITY CONTOURS NEAR CYLINDER ROTATING IN AN AIR STREAM.

Fig 34

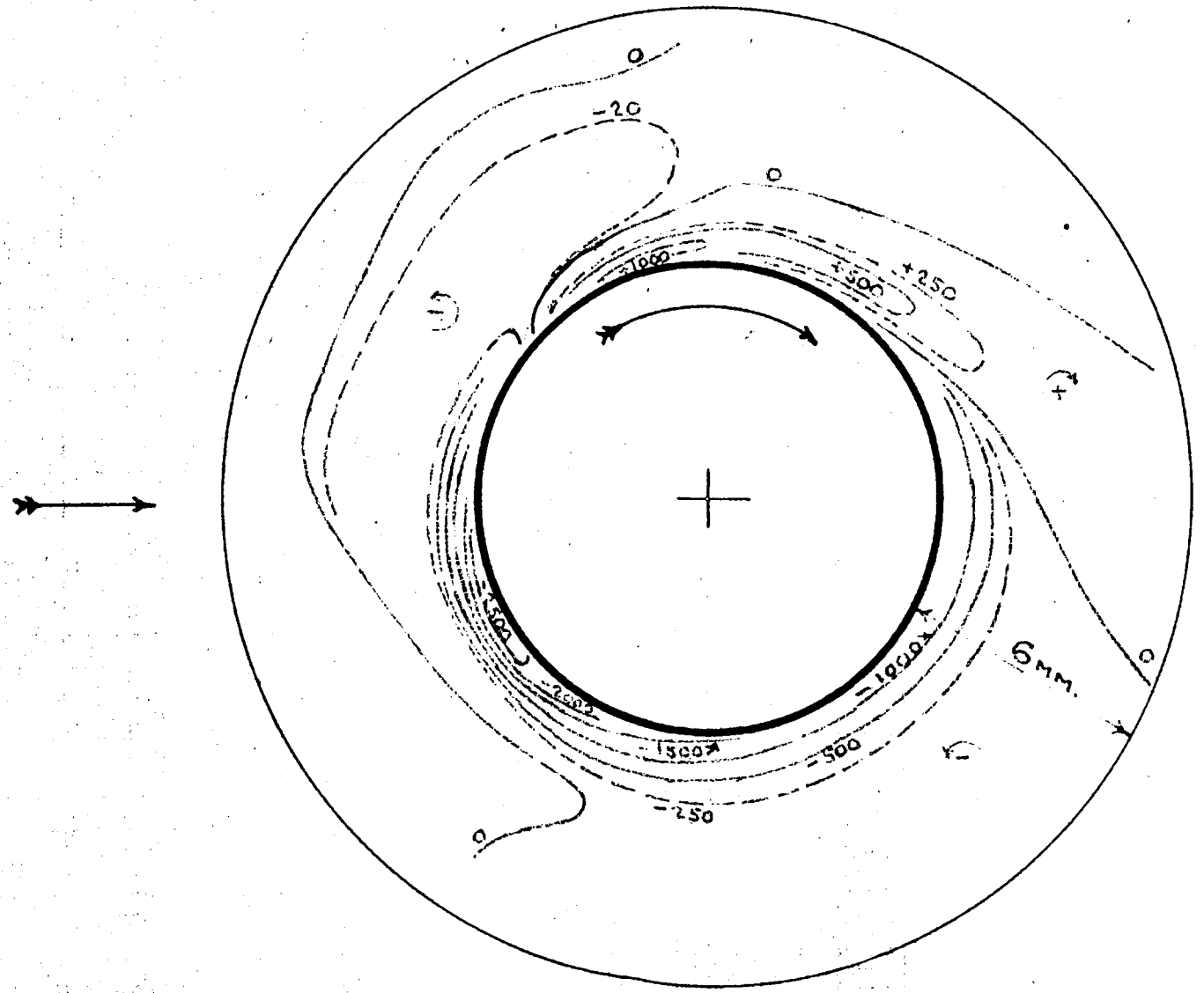

APPROXIMATE STREAMLINES CLOSE TO CYLINDER ROTATING IN AN AIR STREAM

FIG 35

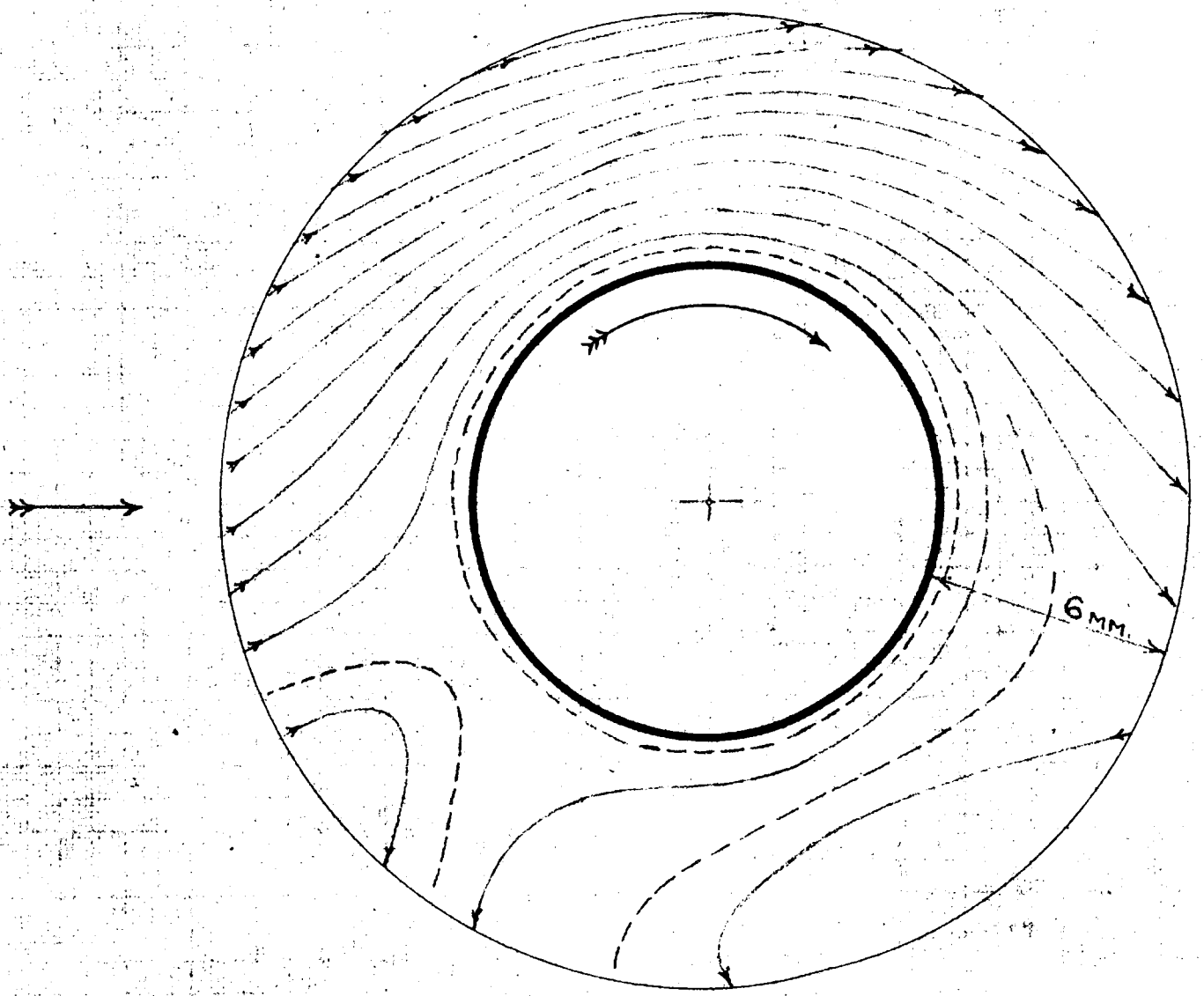

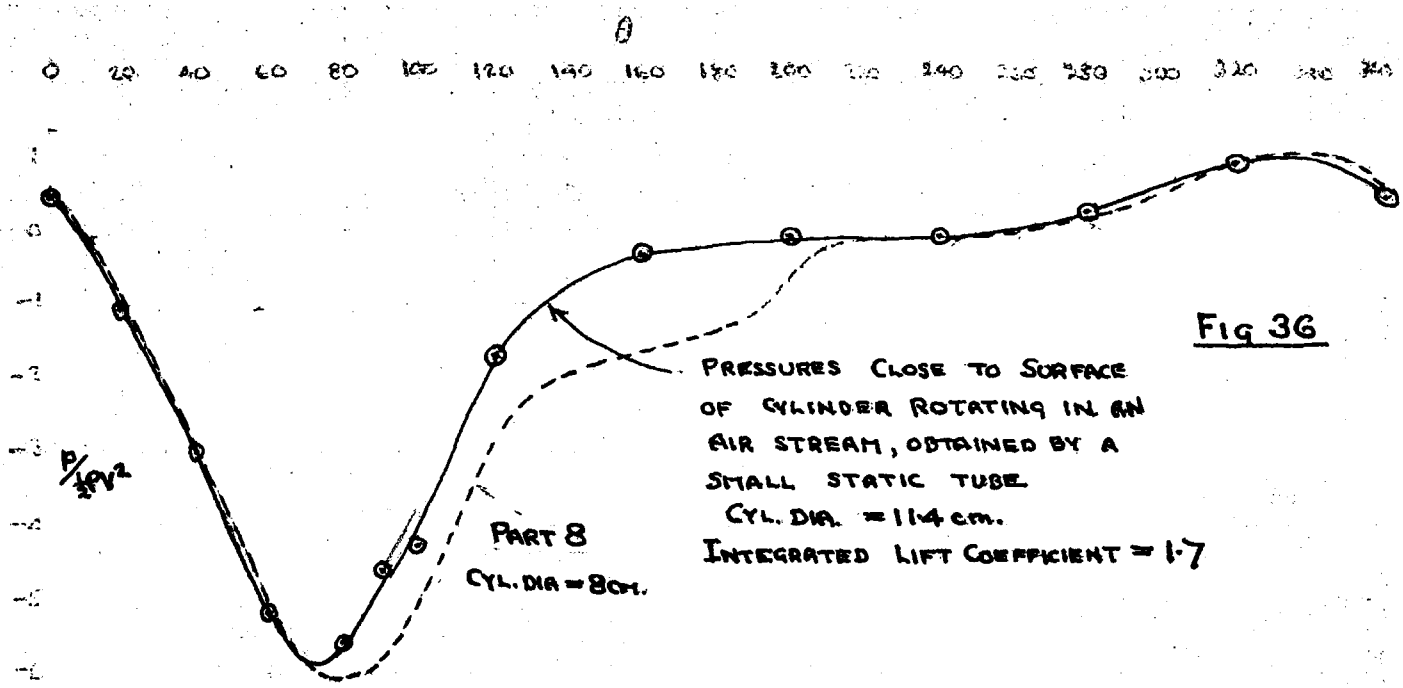
θ
0 20 40 60 80 100 120 140 160 180 200 220 240 260 280 300 320 340 360
P/½ρV²
PART 8
CYL. DIA = 8CM.
PRESSURES CLOSE TO SURFACE OF CYLINDER ROTATING IN AN AIR STREAM, OBTAINED BY A SMALL STATIC TUBE.
CYL. DIA. = 11·4 cm.
INTEGRATED LIFT COEFFICIENT = 1·7

Fig 36

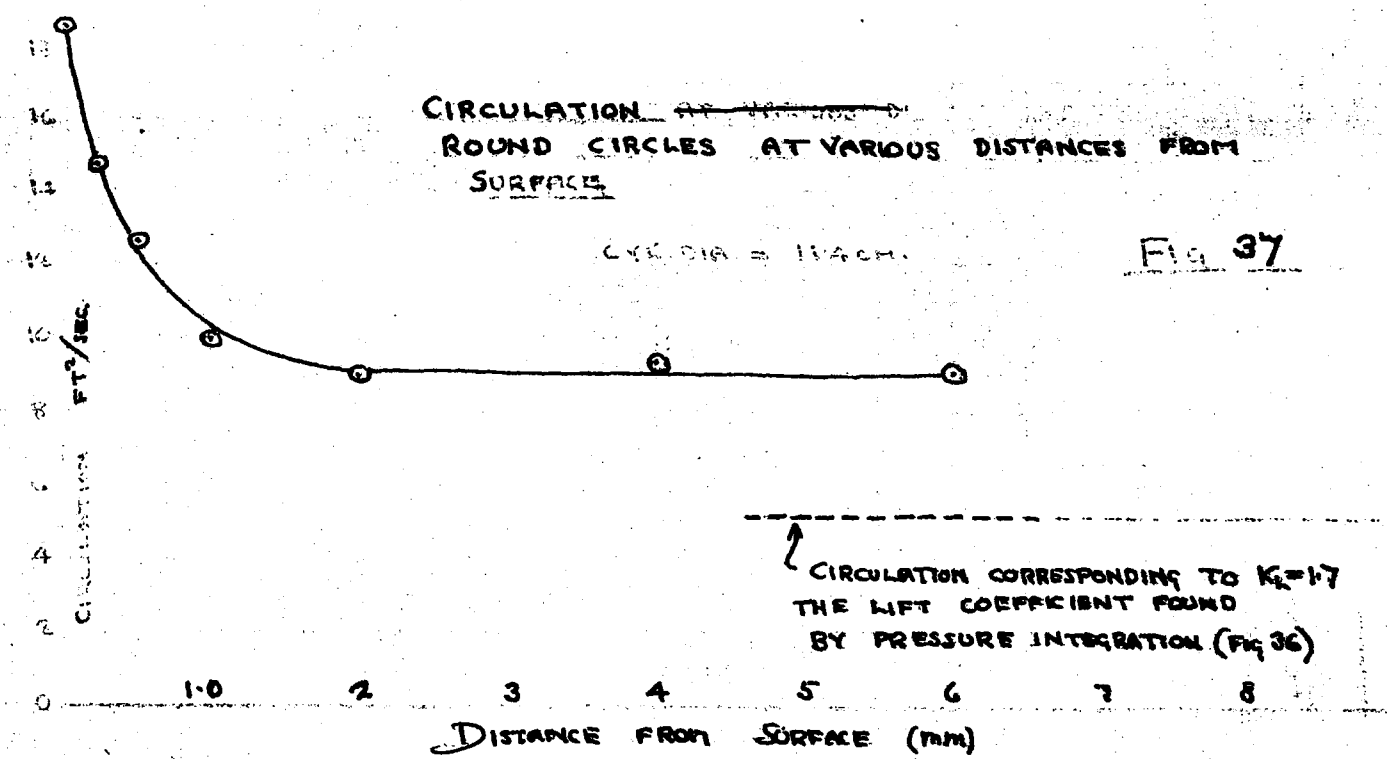
CIRCULATION ROUND CIRCLES AT VARIOUS DISTANCES FROM SURFACE
CYL. DIA = 11·4 cm.
CIRCULATION FT²/SEC.
CIRCULATION CORRESPONDING TO K_L=1·7 THE LIFT COEFFICIENT FOUND BY PRESSURE INTEGRATION (Fig 36)
1·0 2 3 4 5 6 7 8
DISTANCE FROM SURFACE (mm)

Fig 37

Table 2.

Pressure Distribution round Cylinder.

θ	$p_1 = \frac{p - p_0}{(p - p_0)_{max.}}$	
	VD = 4.6 ft²/sec	VD = 13.6 ft²/sec.
0	1.00	1.00
5	0.98	0.97
10	0.91	0.89
20	0.58	0.60
30	+0.15	+0.13
40	-0.37	-0.44
50	-0.90	-0.96
60	-1.30	-1.45
65	-1.40	
70	-1.46	-1.71
75	-1.42	
80	-1.31	-1.57
85	-1.24	
90	-1.22	-1.41
100	-1.23	-1.30
110	-1.25	-1.18
120	-1.24	-1.11
130	-1.25	-1.07
140	-1.27	-1.07
150	-1.30	-1.06
160	-1.33	-1.05
170	-1.36	-1.03
180	-1.34	-1.02
K_D =	0.64	0.49

For Table 1 See Page 5

TABLE 3.

Total Head near the Surface of a Cylinder in an Air Stream.

V = 12·3 θ = 10° d = 0·4			V = 12·3 θ = 20° d = 0·4			V = 12·3 θ = 30° d = 0·4 — 0·6			V = 12·3 θ = 40° d = 0·4 — 0·6		
n	H — H_0	*q*	*n*	H — H_0	*q*	*n*	H — H_0	*q*	*n*	H — H_0	*q*
0	—0·016	0	0	—0·077	0	0	—0·158	0	0	—0·250	0
0·18	—0·014	1·3	0·18	—0·052	4·6	0·18	—0·082	8·0	0·18	—0·195	6·8
0·26	—0·008	2·6	0·26	—0·042	5·4	0·28	—0·064	8·9	0·28	—0·125	10·3
0·36	—0·005	3·0	0·40	—0·026	6·6	0·38	—0·044	9·8	0·41	—0·079	12·0
0·54	—0·004	3·2	0·54	—0·019	7·0	0·48	—0·036	10·1	0·55	—0·045	13·1
0·73	—0·002	3·4	0·73	—0·012	7·4	0·59	—0·015	11·0	0·84	—0·007	14·3
0·91	—0·002	3·4	0·91	—0·006	7·7	0·76	—0·004	11·4	1·34	+0·002	14·6

V = 12·3 θ = 50° d = 0·4 — 0·6			V = 12·3 θ = 60° d = 0·4 — 0·6			V = 12·3 θ = 60° d = 0·9			V = 12·3 θ = 70° d = 0·4 — 0·6		
n	H — H_0	*q*	*n*	H — H_0	*q*	*n*	H — H_0	*q*	*n*	H — H_0	*q*
0	—0·345	0	0	—0·422	0	0·45	—0·131	15·6	0	—0·438	0
0·18	—0·237	9·5	0·18	—0·322	9·2	0·56	—0·101	16·4	0·18	—0·409	4·9
0·28	—0·177	11·9	0·21	—0·303	10·0	0·67	—0·058	17·5	0·34	—0·323	9·8
0·45	—0·095	14·5	0·28	—0·243	12·1	0·89	—0·023	18·3	0·35	—0·184	14·6
0·61	—0·044	15·9	0·37	—0·022	13·6	1·11	—0·010	18·6	0·91	—0·060	17·8
0·80	—0·009	16·8	0·50	—0·127	15·8	1·33	—0·001	18·8	1·22	—0·014	18·9
1·22	+0·001	17·1	0·75	—0·050	17·7	For comparison with values by smaller tube.			1·44	—0·002	19·2
			1·13	—0·004	18·8				2·15	+0·004	19·3

V = 12·3 θ = 80° d = 0·4 — 0·6			V = 12·3 θ = 90° d = 0·58			V = 22·6 θ = 50° d = 0·4			V = 5·4 θ = 50° d = 0·4		
n	H — H_0	*q*	*n*	H — H_0	*q*	*n*	H — H_0	*q*	*n*	H — H_0	*q*
0	—0·424	0	0	—0·405	0	0	—1·20	0	0	—0·064	0
0·18	—0·409	3·6	0·28	—0·395	2·9	0·18	—0·678	21·0	0·18	—0·059	2·1
0·28	—0·403	4·2	0·41	—0·396	2·8	0·28	—0·490	24·4	0·28	—0·050	3·5
0·40	—0·367	6·9	1·10	—0·380	4·6	0·38	—0·273	28·0	0·38	—0·040	4·5
0·90	—0·259	11·8	1·46	—0·313	8·8	0·59	—0·094	30·6	0·55	—0·029	5·4
1·22	—0·144	15·3	1·80	—0·275	10·5	0·79	—0·022	31·5	0·75	—0·015	6·4
1·67	—0·061	17·5	2·4	—0·192	13·4	1·20	0	31·8	0·96	—0·007	6·8
2·10	—0·016	18·5	3·8	—0·021	18·0				1·20	—0·001	7·3
2·55	—0·010	18·7	5·0	+0·005	18·6						
3·2	—0·002	18·8									

V = Channel speed (ft./sec.).
θ = Angle from front generator.
d = External diameter of pitot tube (mm.).
n = Distance of centre of tube from surface (mm.).
H — H_0 = Pilot head less head on front gemerator (lbs. ft.).
q = Deduced velocity at tube (ft./sec.).

All measurements of head have been corrected for the scale effect shown in Table 1.

TABLE 4.

Mechanical Solution of Boundary Layer Equations for Flow past a Cylinder, Radius = Unity.
Channel Velocity = 100 units/sec. Reynolds Number = VD/ν = 28,000

Outside Vel. = v		0	6·35	13·05	19·54	26·02	32·45	38·84	45·2	51·5	57·8	63·9	$k_2 w$ at $\theta = 20°$
$k_2 w$ at $\theta = 0°$	n												
—0·105	0·020	0		13·0		25·9		38·7		51·3		63·7	—0·093
—0·091	0·018		6·49		19·45		32·28		44·96		57·45		—0·080
—0·078	0·016	0		12·9 12·93		25·8 25·80		38·4 38·52		51·0 51·06		63·3 63·38	—0·069
—0·065	0·014		6·41		19·19		31·89		44·41		56·74		—0·058
—0·052	0·012	0		12·6 12·60		25·1 25·14		37·5 37·54		49·7 49·74		61·6 61·72	—0·048
—0·041	0·010		6·08		18·22		30·26		42·14		53·8		—0·037
—0·029	0·008	0		11·3 11·38		22·6 22·68		33·8 33·85		44·8 44·85		55·6 55·63	—0·027
—0·019	0·006		5·00		14·98		24·90		34·64		44·2		—0·017
—0·009..	0·004	0		7·8 7·83		15·6 15·64		23·3 23·28		30·8 30·81		38·3 38·14	—0·008
—0·004	0·002		2·30		6·86		11·39		15·81		20·15		—0·004
0	0	0		0		0		0		0		0	0
$k_2 w$ at	n ↑ / θ →	0	2°	4°	6°	8°	10°	12°	14°	16°	18°	20°	↑ $k_2 w$ at
$\theta = 0$	k_3 →	0	0·35	0·69	1·03	1·36	1·69	2·01	2·32	2·62	2·91	3·18	$\theta = 20°$

Table 5.

Summary of Data for Calculating Boundary Layer Velocities.

V = Channel velocity = 12.3 ft./sec.
r = Cylinder Radius = 0.1875 ft.
ν = 0.00016 ft.^{2}/sec.

θ	p_1	$\frac{dp_1}{d\theta}$	$\sqrt{1 - p_1}$	$h = \frac{1}{2\sqrt{1 - p_1}} \frac{dp_1}{d\theta}$	$\frac{3}{2} \frac{\sqrt{1 - p_1}}{h^2} \frac{dh}{d\theta}$	$\sqrt{\frac{Vh}{r\nu}}$
10	0.89	-1.20	0.32'	1.84	-0.045	869
20	0.59	-2.25	0.64	1.75	-0.38	845
30	0.13	-2.98	0.93	1.60	-0.66	810
40	-0.38	-3.10	1.17	1.33	-1.71	736
50	-0.90	-2.70	1.38	1.00	-4.35	640
60	-1.30	-1.85	1.52	0.60	-16.5	496

Explanation of Table 6.

1st approx.

$$F'_1(x) = 1 \div \sqrt{\frac{2}{3}(x^3 - 3x + 2)}$$

$$F_1(x) = \sqrt{2} \log \frac{\sqrt{3} - \sqrt{x + 2}}{\sqrt{1 - x}\,(\sqrt{3} - \sqrt{2})}$$

2nd approx.

$$\varphi(x) = \frac{1}{F'_1(x)} \int x\, F'_1(x)dx, \quad M = 3 \int_{x=x}^{x=1} \varphi(x)dx$$

$$f(x) = x \frac{F_1(x)}{F_1'(x)} \quad N = -\frac{3}{2} \frac{\sqrt{1-p_1}}{h^2} \frac{dh}{d\theta} \int_{x=x}^{x=1} f(x)dx$$

$$F_2'(x) = 1 \div \sqrt{\frac{2}{3}(x^3 - 3x + 2 + M + N)} \quad F_2(x) = \int F_2'(x)\,dx$$

$$n = \sqrt{\frac{\nu r}{V h}} F_2(x) \qquad q = x\,\upsilon \qquad \upsilon = V\sqrt{1 - p_1}$$

~~Table 6.~~

TABLE 6.

Calculation of Boundary Layer Velocities for V = 12·3 *ft./sec.*

θ	$x =$		0	0·1	0·2	0·3	0·4	0·5	0·6	0·7	0·8	0·9	0·95
All values.	$F'_1(x)$	=	0·866	0·939	1·032	1·154	1·316	1·55	1·90	2·48	3·66	7·18	14·23
	$F_1(x)$	=	0	0·088	0·188	0·296	0·420	0·565	1·735	0·952	1·250	1·75	2·25
	$\int -x F'(x)\,dx$	=	0	0·0045	0·0192	0·046	0·090	0·155	0·248	0·390	0·613	1·04	1·51
	$\varphi(x)$	=	0	0·005	0·019	0·040	0·072	0·100	0·143	0·157	0·193	0·173	0·128
	M	=	0·26	0·26	0·26	0·25	0·24	0·213	0·174	0·078	0·021	0·101	0·001
	$f(x)$	=	0	0·0094	0·036	0·077	0·128	0·182	0·232	0·269	0·273	0·219	0·150
	$\int_x^{1·0} f(x)\,dx$	=	0·145	0·144	0·142	0·136	0·126	0·111	0·090	0·065	0·038	0·013	0·004
	$x^3 - 3x + 2$	=	2·00	1·701	1·408	1·120	0·864	0·626	0·416	0·244	0·112	0·029	0·001
10°	N	=	0·007	0·007	0·006	0·006	0·006	0·005	0·004	0·003	0·002	0·001	0
	$x^3 - 3x + 2 + M + N$	=	2·26	1·97	1·68	1·39	1·16	0·844	0·594	0·376	0·192	0·051	0·017
	$F_2'(x)$	=	0·81	0·87	0·95	1·04	1·14	1·33	1·59	2·00	2·80	5·4	9·4
	$F_2(x)$	=	0	0·084	0·175	0·274	0·383	0·51	0·65	0·83	1·07	1·48	1·84
	n (mm.)	=	0	0·03	0·06	0·10	0·14	0·18	0·23	0·29	0·38	0·52	0·66
	q (ft./sec)	=	0	0·4	0·8	1·2	1·6	2·0	2·4	2·8	3·2	3·6	3·8
20°	N	=	0·06	0·05	0·05	0·05	0·05	0·04	0·03	0·02	0·014	0·005	0·001
	$x^3 - 3x + 2 + M + N$	=	2·32	2·01	1·72	1·43	1·15	0·88	0·62	0·39	0·204	0·055	0·018
	$F'_2(x)$	=	0·81	0·86	0·94	1·03	1·14	1·31	1·56	1·97	2·71	5·2	9·1
	$F_2(x)$	=	0	0·083	0·17	0·27	0·38	0·50	0·64	0·82	1·05	1·44	1·79
	n (mm.)	=	0	0·03	0·06	0·10	0·14	0·18	0·23	0·30	0·38	0·52	0·65
	q (ft./sec.)	=	0	0·8	1·6	2·4	3·1	3·9	4·7	5·5	6·3	7·1	7·5
30°	N	=	0·09	0·09	0·09	0·09	0·08	0·07	0·06	0·04	0·02	0·01	0
	$x^3 - 3x + 2 + M + N$	=	2·35	2·05	1·76	1·47	1·18	0·91	0·65	0·41	0·21	0·06	0·017
	$F'_2(x)$	=	0·80	0·85	0·92	1·01	1·13	1·29	1·52	1·91	2·68	5·0	9·4
	$F_2(x)$	=	0	0·082	0·17	0·27	0·37	0·50	0·64	0·81	1·04	1·41	1·78
	n (mm.)	=	0	0·03	0·06	0·10	0·14	0·19	0·24	0·30	0·39	0·53	0·67
	q (ft./sec.)	=	0	1·2	2·3	3·5	4·6	5·8	6·9	8·1	9·2	10·4	10·9
40°	N	=	0·25	0·25	0·24	0·23	0·22	0·19	0·15	0·11	0·065	0·022	0·007
	$x^3 - 3x + 2 + M + N$	=	2·51	2·21	1·91	1·61	1·32	1·03	0·74	0·48	0·255	0·072	0·024
	$F'_2(x)$	=	0·77	0·82	0·89	0·97	1·07	1·21	1·43	1·77	2·44	4·6	7·9
	$F_2(x)$	=	0	0·080	0·165	0·268	0·370	0·48	0·616	0·776	0·99	0·34	1·65
	n (mm.)	=	0	0·03	0·07	0·11	0·15	0·20	0·25	0·32	0·41	0·55	0·68
	q (ft./Sec.)	=	0	1·4	2·9	4·3	5·8	7·2	8·6	10·1	11·5	13·0	13·7
50°	N	=	0·63	0·63	0·62	0·59	0·55	0·482	0·392	0·283	0·165	0·058	0·018
	$x^3 - 3x + 2 + M + N$	=	2·89	2·59	2·29	1·97	1·65	1·32	0·982	0·656	0·355	0·108	0·035
	$F'_2(x)$	=	0·72	0·76	0·81	0·88	0·95	1·06	1·24	1·51	2·06	3·72	6·54
	$F_2(x)$	=	0	0·074	0·152	0·236	0·328	0·429	0·544	0·681	0·86	1·15	1·40
	n (mm.)	=	0	0·035	0·072	0·112	0·156	0·204	0·259	0·32	0·41	0·56	0·67
	q (ft./sec.)	=	0	1·7	3·4	5·1	6·8	8·5	10·2	11·9	13·6	15·3	16·1
60°	N	=	2·40	2·39	2·34	2·25	2·08	1·82	1·49	1·07	0·626	0·219	0·066
	$x^3 - 3x + 2 + M + N$	=	4·66	4·35	4·01	3·62	3·18	2·66	2·08	1·44	0·816	0·269	0·083
	$F'_2(x)$	=	0·57	0·59	0·61	0·64	0·69	0·75	0·85	1·02	1·36	2·37	4·25
	$F_2(x)$	=	0	0·058	0·118	0·181	0·247	0·319	0·399	0·493	0·611	0·798	0·964
	n (mm).	=	0	0·036	0·072	0·111	0·152	0·196	0·245	0·303	0·376	0·490	0·593
	q (ft./sec.)	=	0	1·87	3·74	5·6	7·5	9·4	11·2	13·1	15·0	16·8	17·8

Table 7

Calculated Values for Channel Speeds of 22.5 and 5.4 ft./sec.

$\theta = 50°$

V	x =	0	0.1	0.2	0.3	0.4	0.5	0.6	0.7	0.8	0.9	0.95
22.5	n (mm.)	0	0.026	0.054	0.083	0.115	0.151	0.192	0.240	0.303	0.405	0.495
	q (ft./sec.)	0	5.2	6.3	9.5	12.7	15.9	19.0	22.2	25.4	28.5	30.1
5.4	n (mm.)	0	0.053	0.11	0.17	0.24	0.31	0.39	0.49	0.62	0.83	1.01
	q (ft./sec.)	0	0.75	1.50	2.25	3.0	3.75	4.5	5.2	6.0	6.7	7.1

Table 7

Table 8.

Skeleton Solution for Viscous Flow Past a Cylinder.

Upper figures are values of ζ
Lower figures are values of ψ

y ↓ / x →	-41	-33	-25	-17	-9	-1	+7	+15	+23	+31	+ ∞
40	0 250	0 250	0 250	0 250	0 250	0 250	0 250	0 250	0 250	0 250	0 250
32	0.01 184	0 183	0 183	0 184	0 187	0 189.9	0 193.1	0 194.8	0 198.0	0 199.0	0 200
24	0.06 120	0.08 117	0.05 116	0.03 117	0 122	0 129.6	0 136.1	0 142.0	0 146.3	0 148.3	0 150
16	0.12 65	0.14 60	0.16 56	0.19 54.6	0.15 58.4	0.02 67.5	0 79.7	0 89.6	0 95.4	0 99.0	0 100
8	0.13 26	0.14 21.5	0.18 16.6	0.27 12.7	0.38 9.6	0.78 9.1	0.06 28.0	0 41.2	0 46.8	0 48.7	0 50
0	0 0	0 0	0 0	0 0	0 0		0 0	0 0	0 0	0 0	0 0

~~Table 8~~

TABLE 9.

V ft/sec	$H - H_o$ lb/ft^2	$\frac{H - p_o}{\frac{1}{2}\rho V^2}$
1.9	0.021	1.5
3.1	0.020	1.18
4.4	0.028	1.12
5.6	0.027	1.07
8.4	0.017	1.02
10.6	0.021	1.016

H — Pressure on front generator of small cylinder

H_o — Total head on large pitot

p_o — Static pressure in undisturbed flow

Table 10.

Common to all	D=0.66 mm. d=0.22 V = 2.1 f/s Δθ= 9° R = 28 $\log_{10}$=1.45	D = 0.66 d = 0.22 V = 5.2 Δθ = 9° R = 70 log=1.85	D = 0.66 d = 0.22 V = 18.6 Δθ = 9° R = 250 log=2.40	D = 0.66 d = 0.17 V = 18.6 Δθ = 7° R = 250 log=2.40	D = 0.66 d = 0.17 V = 35.7 Δθ = 7° R = 484 log=2.68	D = 3.2 d = 0.13 V = 2.2 Δθ = 1° R = 144 log=2.16	D = 3.2 d = 0.39 V = 5.5 Δθ =3.5 R = 360 log=2.56	D = 3.2 d = 0.13 V = 5.5 Δθ = 1 R = 360 log=2.56	D = 3.2 d = 0.13 V = 18.3 Δθ = 1 R = 1240 log=3.09	D = 3.2 d = 0.39 V = 19.0 Δθ = 3.5 R = 1250 log=3.10
θ_o	θ p_1	θ p_1	θ p_1	θ p_1	θ p_1	θ p_1	θ p_1	θ p_1	θ p_1	θ p_1
0	0 1.46	0 1.12	0 1.00	0 1.00	0 1.00	0 1.00	0 1.00	0 1.00	0 1.00	0 1.00
10				3 0.93			6.5 0.92	9 0.91	9 0.92	6.5 0.95
20	11 1.16	11 0.98	11 0.82	13 0.80	13 0.81	19 0.71	16.5 0.71	19 0.66	19 0.67	16.5 0.74
30				23 0.48		29 0.38	26.5 0.35	29 0.29	29 0.30	26.5 0.38
40	31 0.43	31 0.32	31 0.21	33 0.11	33 0.08	39 -0.10	36.5 -0.03	39 -0.18	39 -0.15	36.5 -0.03
50				43 -0.40			46.5 -0.46	49 -0.59	49 -0.59	46.5 -0.46
60	51 -0.20	51 -0.50	51 -0.63	53 -0.77	53 -0.72	59 -0.71	66.5 -0.83	59 -0.95	59 -0.92	56.5 -0.80
70				63 -1.03		69 -1.03	66.5 -1.11	69 -0.13	69 -1.05	66.5 -1.02
80	71 -0.72	71 -0.91	71 -1.17	73 -1.18	73 -1.04	79 -1.09	76.5 -1.16	79 -1.17	79 -1.02	76.5 -1.05
90				83 -1.17		89 -1.05	86.5 -1.13	89 -1.13	89 -0.89	86.5 -0.89
100	91 -0.81	91 -0.96	91 -1.09	93 -1.12	93 -0.95	99 -0.97	96.5 -1.02	99 -1.02	99 -0.80	96.5 -0.80
120	111 -0.89	111 -0.81	111 -0.97	113 -0.96	113 -0.87	119 -0.87	116.5 -0.88	119 -0.85	119 -0.75	113.5 -0.77
140	131 -0.58	131 -0.65	131 -0.90	133 -0.90	133 -0.84	139 -0.81	136.5 -0.87	139 -0.85	139 -0.75	133.5 -0.76
160	151 -0.56	151 -0.62	151 -0.87	153 -0.91	153 -0.82	159 -0.88	156.5 -0.88	159 -0.87	159 -0.75	156.5 -0.76
180	180 -0.47	180 -0.53	180 -0.87	173 -0.89	180 -0.8	180 -0.80	180.0 -0.86	180 -0.87	180 -0.75	180.0 -0.76

Contd .....

Table 10. (Contd.)

Common to all	D = 3.2 d = 0.39 V = 39 $\Delta\theta$ = 3°5 R = 2560 $\log_{10}$=3.41		D = 3.2 d = 0.1 V = 37 $\Delta\theta$ = 1° R = 2480 log= 3.39		D = 22.2 d = 0.4 V = 6.3 $\Delta\theta$ = 0°5 R = 2900 log= 3.46		D = 22.2 d = 0.4 V = 18.6 $\Delta\theta$ = 0°5 R = 8500 log= 3.93		D = 22.2 d = 1.0 V = 18.6 $\Delta\theta$ = 1°3 R = 8500 log= 3.93		D = 22.2 d = 3.2 V = 18.5 $\Delta\theta$ = 4°2 R = 8500 log= 3.93		D = 22.2. d = 6.1 V = 18.5 $\Delta\theta$ = 7°7 R = 8500 log= 3.93		D = 22.2 d = 0.4 V = 37.3 $\Delta\theta$ = 0°5 R = 17000 log= 4.23		D = 22.2 d = 1.0 V = 36.6 $\Delta\theta$ = 1°3 R = 16700 log= 4.22	
θ_0	θ	p_1	θ	p_1	θ	p_1	θ	p_1	θ	p_1	θ	p_1	θ	p_1	θ	p_1	θ	p_1
0	0	1.00	0	1.00	0	1.00	0	1.000	0	1.000	0	1.000	0	0.99	0	1.00	0	1.00
10	6.5	0.96	9	0.92	9.5	0.93	9.5	0.905	8.7	0.941	5.8	0.965	2	0.98	9.5	0.91	8.7	
20	16.5	0.76	19	0.68	19.5	0.69	19.5	0.650	18.7	0.684	15.8	0.764	12	0.83	19.5	0.65	18.7	0.69
30	26.5	0.38	29	0.30	29.5	0.33	29.5	0.235	28.7	0.293	25.8	0.388	22	0.50	29.5	0.23	28.7	
40	36.5	-0.05	39	-0.17	39.5	-0.14	39.5	-0.265	38.7	-0.198	35.8	-0.098	32	0.04	39.5	-0.25	38.7	-0.20
50	46.5	-0.51	49	-0.61	49.5	-0.56	49.5	-0.760	48.7	-0.718	45.8	-0.603	42	-0.45	49.5	-0.75	48.7	
60	56.5	-0.88	59	-0.96	59.5	-0.87	59.5	-1.130	58.7	-1.058	55.8	-1.010	52	-0.90	59.5	-1.13	58.7	-1.11
70	66.5	-1.09	69	-1.10	69.5	-0.97	69.5	-1.297	68.7	-1.311	65.8	-1.255	62	-1.27	69.7	-1.30	68.7	
80	76.5	-1.04	79	-1.03	79.5	-0.90	79.5	-1.204	78.7	-1.168	75.8	-1.240	72	-1.39	79.5	-1.16	78.7	-1.20
90	86.5	-0.88	89	-0.90	89.5	-0.76	89.5	-1.067	88.7	-1.041	85.8	-1.091	82	-1.08	89.5	-1.07	88.7	
100	96.5	-0.82	99	-0.83	99.5	-0.71	99.5	-1.022	98.7	-1.019	95.8	-1.008	92	-1.02	99.5	-1.06	98.7	-1.07
120	116.5	-0.80	119	-0.80	119.5	-0.72	119.5	-1.038	118.7	-1.030	115.8	-1.020	112	-1.07	119.5	-1.09	118.7	-1.09
140	136.5	-0.80	139	-0.82	139.5	-0.68	139.5	-1.098	138.7	-1.062	135.8	-1.076	132	-1.07	139.5	-1.15	138.7	-1.16
160	156.5	-0.80	159	-0.82	159.5	-0.71	159.5	-1.141	158.7	-1.093	155.8	-1.094	152	-1.11	159.5	-1.18	158.7	-1.18
180	180.0	-0.80	180	-0.81	180.0	-0.70	180.0	-1.150	180.0	-1.115	180.0	-0.137	180	-1.05	180.0	-1.21	180.0	-1.23

Table 11.

Cylinder diameter	Wind Speed	VD/ν	Normal pressure Drag Coefficient.
mm.	ft./sec.		
0.66	2.1	28	0.51
0.66	5.2	70	0.44
0.66	18.6	250	0.50
0.66	35.7	484	0.47
3.2	2.2	144	0.52
3.2	5.5	360	0.48
3.2	18.5	1240	0.438
3.2	39.2	2500	0.456
22.2	6.3	2900	0.43
22.2	18.6	8500	0.561
22.2	37.3	17000	0.600

M.

TABLE 13

Pressure distribution on a rotating cylinder. *Cylinder diameter* = 8 *cm.* *Length* 61·7 *cm.* *Speed* 1,400 *r./m.*

29·5 cm. from end. $V = 9{\cdot}6$ f/s. $v/V = 2$. Prob. Acc. $\pm 0{\cdot}25$			16·2 cm. from end. $V = 9{\cdot}6$ f/s. $v/V = 2$. Prob. Acc. $\pm 0{\cdot}3$			9·7 cm. from end. $V = 9{\cdot}6$ f/s. $v/V = 2$. Prob. Acc. $\pm 0{\cdot}3$			1·2 cm. from end. $V = 9{\cdot}6$ f/s. $v/V = 2$. Prob. Acc. $\pm 0{\cdot}3$			29·5 cm. from end. $V = 19{\cdot}2$ f/s. $v/V = 1$. Prob. Acc. $\pm 0{\cdot}1$			29·5 cm. from end. $V = 6{\cdot}4$ f/s. $v/V = 3$. Prob. Acc. $\pm 0{\cdot}4$			29·5 cm. from end. $V = 4{\cdot}8$ f/s. $v/V = 4$. Prob. Acc. $\pm 0{\cdot}6$			29·5 cm. from end. Stationary Cylinder		
																							$V =$	12·5	24 f/s.
$\theta_1+14°$	p'	No.	$\theta_1+14°$	p'	No.	$\theta_1+12°$	p'	No.	$\theta_1+13°$	p'	No.	$\theta_1+13°$	p'	No.	$\theta_1+14°$	p'	No.	$\theta_1+14°$	p'	No.	θ	p'	p'
12°	−0·09	1	19°	−0·61	3	9°	+0·1	2	20°	−0·5	1	13°	+0·65	1	14°	−2·0	2	9°	− 2·8	1	0°	+1·02	+1·02
25	−1·59	1	34	−1·87	1	20	−0·5	3	32	−0·9	1	33	−0·38	1	34	−4·5	2	30	− 4·2	2	10	0·89	0·94
35	−2·33	1	41	−2·78	1	38	−2·0	1	54	−2·0	2	53	−1·91	1	56	−7·7	2	49	− 7·1	1	20	0·68	0·68
56	−4·32	3	65	−4·38	1	54	−2·3	1	72	−8·7	1	72	−2·80	2	71	−8·7	3	68	−10·4	2	30	0·24	0·25
70	−5·72	2	85	−5·98	2	74	−5·3	1	92	−2·3	3	92	−2·81	2	93	−8·8	1	81	−10·2	1	40	−0·24	−0·25
72	−5·65	1	94	−6·02	1	89	−5·4	2	103	−1·7	1	102	−2·13	1	104	−7·9	1	91	−10·4	1	50	−0·71	−0·72
80	−6·04	1	110	−4·22	1	104	−5·6	2	110	−1·3	1	116	−0·96	1	116	−4·7	2	106	− 9·7	1	60	−1·09	−1·11
89	−6·09	2	133	−2·33	1	129	−4·1	1	119	−1·2	2	135	−0·94	1	136	−2·7	2	113	− 8·9	1	80	−1·04	−1·05
97	−5·19	1	154	−1·88	1	140	−2·8	1	127	−1·2	1	153	−0·73	1	154	−1·8	2	124	− 6·2	1	100	−0·96	−1·00
105	−4·79	3	174	−1·29	1	150	−2·4	1	138	−1·2	2	172	−0·63	1	174	−1·5	2	140	− 3·2	1	120	−0·97	−1·01
111	−4·04	1	194	−0·85	1	164	−1·6	1	167	−1·0	1	196	−0·66	1	196	−1·3	2	161	− 1·8	1	140	−0·99	−1·01
124	−2·59	1	214	−0·24	1	184	−1·2	1	190	−1·0	1	216	−0·68	1	214	−0·8	3	179	− 2·2	1	160	−1·00	−1·00
135	−2·20	2	233	−0·24	1	203	−1·2	1	211	−1·0	2	236	−0·70	1	237	−0·5	2	197	− 1·2	1	180	−0·96	−1·00
146	−1·83	1	252	−0·46	2	218	−0·8	1	227	−0·9	1	255	−0·75	1	256	+0·5	3	210	− 1·0	1			
166	−1·62	1	274	+0·40	2	222	−1·3	1	263	−0·6	1	274	−0·83	1	275	0·6	1	239	− 1·0	2			
186	−1·26	1	295	0·16	2	231	−0·7	2	296	−0·1	1	292	−1·04	1	291	1·1	2	260	0	2			
194	−1·12	1	316	0·33	1	243	−0·7	1	323	+0·7	1	312	−0·35	1	313	1·1	3	280	+ 1·0	1			
200	−0·65	2	336	0·74	1	262	−0·7	1	344	0·6	1	315	−0·39	1	335	+0·7	1	288	0·8	1			
205	−0·28	1	356	+0·56	1	279	−0·4	1	359	+0·5	1	334	+0·57	1	354	−0·4	1	309	+ 1·3	1			
210	−0·25	1				300	+0·1	1	69	−2·8	1	353	+0·94	1				329	− 0·2	1			
227	−0·10	1				317	0·5	2										349	− 0·7	1			
245	−0·12	1				338	0·9	1															
263	−0·01	1				353	+0·9	1															
282	+0·04	1																					
303	0·60	1																					
333	1·03	2																					
343	1·07	1																					
352	+1·03	1																					

NOTE.—p' = pressure $\div \frac{1}{2}\rho V^2$, No. = Number of observations.

For Table 12 see Page 49

TABLE 14.

Determination of Angle of Lag from Pressure Integrations, and K_L, K_D, etc. for various sections.
n = 1,400 r./m. V = 9·6 ft./sec. Length = 7·73 × Diameter = 61·7 cm.

Sect.	Dist. from end.	k_L	k_D	K_R	φ_1	Mean $\Delta\theta$	Lag	$\varphi=\varphi_1+$lag	K_L	K_D	k'_d	k_d	K_d
					°	°	°	°					
1	29·5	2·02	−0·18	2·03	85	5·0	14	99	2·00	0·32	0·22	0·07	0·25
2	16·2	1·88	−0·13	1·88	86	4·9	14	100	1·86	0·33	0·25	0·08	0·25
3	9·7	1·90	+0·28	1·92	98	4·2	12	110	1·80	0·65	0·42	0·15	0·50
4	1·2	0·73	+0·18	0·75	104	4·7	13	117	0·65	0·34	0·13	−0·18	0·50
Mean	or total	1·84	+0·015	1·84	90·5	4·7	13·5	104*	1·78	0·44	0·28	0·08	0·36

k_L, k_D and φ_1 refer to the axis uncorrected for lag.
K_L, K_D and φ refer to the true wind axis.

k'_d = induced drag estimated by neglecting channel walls.
k_d = induced drag estimated by Lock's method.
K_d = profile drag estimated by Lock's method.

* The direction of the total resultant (104°) was obtained from balance measurements. (R. & M. 1018.) It is used here to fix the mean angle of lag.

TABLE 15.

Channel velocity V ft./sec.	v/V	Resultant.		K_L	Accuracy.	K_D	Accuracy.	k_d Induced drag.*	K_d Profile drag $=K_D-k_d$	Balance results on complete cylinder.	
		K_R	φ							K_L	K_D
			°								
12·5 & 24	0	0·54	180	0	—	0·54	±0·02	0	0·54	0	0·60
19·2	1	0·60	122	0·51	±0·05	0·32	±0·02	0·0	0·32	0·56	0·37
9·6	2	2·03	99	2·00	±0·1	0·32	±0·07	0·07	+0·25	2·00	0·50
6·4	3	3·1	89	3·1	±0·2	−0·1	±0·15	0·17	−0·3	3·75	1·1
4·8	4	3·7	91	3·7	±0·4	+0·1	±0·2	0·24	−0·1	4·6	1·8

* k_d, induced drag; assumed proportional to K_L^2.

VELOCITIES NEAR A CYLINDER ROTATING IN STILL AIR AS DETERMINED BY PITOT AND STATIC TUBES.

DIAMETER OF CYLINDER = 114 MM., R = 57 MM.

TABLE 16

Dist. from Surface n mm	$100\frac{n}{R}$ %	q/v = Speed at Pitot / Surface Speed.			
		410 R/M	820 R/M	1230 R/M	2060 R/M
0·44	0·76	0·50	0·72	0·67	
0·70	1·22	·58	·51	·51	
0·97	1·7	·48	·41	·40	
1·20	2·1	·44	·40	·38	
1·82	3·2	·38	·33	·31	
2·46	4·3		·31	·28	
3·7	6·5		·26	·25	
4·8	8·5		·26	·21	·20
7·4	12·9	·28	·19	·17	·16
9·9	17·3		·20		·14
20·0	35		·18		·10
28	50		·15		·08

TOTAL HEAD NEAR A CYLINDER ROTATING IN ~~air~~ STILL AIR AT 820 REVS. PER MINUTE.

n = DISTANCE OF TUBE FROM SURFACE (MM.)
H = TOTAL HEAD LBS/FT^2

TABLE 17

n	H		n	H
0·18	0·191		1·12	0·040
·28	·160		1·50	·029
·32	·118		2·20	·019
·38	·106		3·47	·012
·43	·073		6·15	·010
·54	·064		7·5	·007
·66	·058			
·93	·043			

DETAILS OF CALCULATION OF STATIC PRESSURE AND ~~FLOW~~ VELOCITY NEAR CYLINDER FROM THE OBSERVATIONS OF TOTAL HEAD.

TABLE 18

n (mm)	5–4	4–3	3–2	2–1·5	1·5–1	1–0·7	0·7–0·4	0·4–0·2	0·2–0·1	0·1–0
n_1 ft.	·20410	·20085	·19760	·19435	·19272	·19109	·19010	·18911	·18844	·18810
δn ft.	·00325	·00325	·00325	·00163	·00163	·00099	·00099	·00066	·00033	·00033
q_1 ft/sec	3·99	4·16	4·43	5·12	5·77	6·65	7·58	9·35	13·0	14·93
P_1 lbs/ft^2	−·0084	−·0095	−·0102	−·0111	−·0117	−·0125	−·0132	−·0139	−·015	−·016
H_2 lbs/ft^2	·011	·013	·020	·028	·040	·055	·070	·165	·250	
q_2 ft/sec	4·16	4·43	5·12	5·77	6·65	7·58	9·35	12·96	14·93	16·3
P_2 lbs/ft^2	−·0095	−·0102	−·0111	−·0117	−·0125	−·0132	−·0139	−·015	−·016	−·016

MEASUREMENTS OF TOTAL HEAD — TABLE 19

n = DISTANCE FROM SURFACE
H = TOTAL HEAD AT SMALL PITOT
H_0 = TOTAL HEAD IN FREE STREAM
ΔH = CORRECTION FOR SMALL PITOT (SEE FIG. 28A)

$\theta = 0°$

n	OBSD. $H-H_0$ lbs/ft²	ΔH	$H-H_0$ lbs/ft²
0·18	+0·166	0·006	0·160
·32	·100	·009	·091
·46	·065	·009	·056
·60	·046	·009	·037
·75	·033	·009	·024
1·17	·014	·009	·005
1·6	·008	·008	·000
2·3	·002	·001	·001
3·0	·001	000	·001
4·4	·001	000	·001
5·8	·001	000	·001

$\theta = 20°$

n	OBSD $H-H_0$	ΔH	$H-H_0$
0·18	0·127	0·002	0·125
·32	·089	·003	·086
·46	·066	·005	·061
·60	·047	·005	·042
·75	·031	·006	·025
·89	·019	·007	·012
1·17	·015	·008	·007
1·6	·004	·009	−0·005
2·3	·006	·009	−0·003
3·0	·001	·009	−0·008
4·4	·003	·009	−0·006

$\theta = 40°$

n	OBSD $H-H_0$	ΔH	$H-H_0$
0·18	0·052	0·001	0·051
·28	·049	·001	·048
·38	·044	·001	·043
·59	·029	·001	·028
·79	·016	·001	·015
·99	·017	·001	·016
1·40	·007	·001	·006
1·8	·007	·001	·006
2·2	·011	·001	·010
4·1	·000	·001	−0·001
6·3	·005	·002	+0·003

$\theta = 60°$

n	OBSD $H-H_0$	ΔH	$H-H_0$
0·18	−0·053	0	−0·053
·38	+0·003	0	+0·003
·59	·022	0	·022
·79	·022	0	·022
·99	·023	0	·023
1·40	·019	0	·019
2·2	·015	0	·015
3·2	·008	0	·008
4·3	·006	0	·006
6·3	·006	0	·006
0·28	−0·028	0	−0·028

$\theta = 80°$

n	OBSD $H-H_0$	ΔH	$H-H_0$
0·18	−0·141	0	−0·141
·28	−0·087	0	−0·087
·38	−0·052	0	−0·052
·59	−0·012	0	−0·012
·79	+0·002	0	+0·002
1·20	·004	0	·004
2·2	·005	0	·005
4·3	·004	0	·004
6·3	·005	0	·005

$\theta = 90°$

n	OBSD. $H-H_0$	ΔH	$H-H_0$
0·18	−0·100	0·001	−0·101
·28	−0·083	0	−0·083
·38	−0·055	0	−0·055
·59	−0·025	0	−0·025
·79	−0·005	0	−0·005
1·00	−0·002	0	−0·002
1·40	+0·001	0	+0·001
1·8	+0·003	0	+0·003
2·2	−0·001	0	−0·001
4·3	−0·003	0	−0·003

TABLE 19 CONTD.

	$\theta = 100°$			$\theta = 120°$			
n mm.	OBSD $H-H_0$	ΔH	$H-H_0$ lbs/ft²	n	OBSD. $H-H_0$	ΔH	$H-H_0$
0·18	−0·086	0·001	−0·089	0·18	−0·097	0·010	−0·107
·28	−0·081	0·001	−0·084	·20	−0·088	0·010	−0·098
·38	−0·082	0·001	−0·083	·28	−0·085	0·010	−0·095
·59	−0·032	0	−0·032	·48	−0·080	0·010	−0·090
·79	−0·012	0	−0·012	·56	−0·060	0·009	−0·069
1·20	0·000	0	0·000	·93	−0·035	0·006	−0·041
1·6	+0·003	0	+0·003	1·47	−0·017	0·005	−0·022
2·0	+0·003	0	+0·003	2·4	−0·017	0·001	−0·018
2·4	+0·001	0	+0·001	4·2	−0·020	0	−0·020
3·0	−0·001	0	−0·001	6·0	−0·021	0	−0·021

	$\theta = 160°$			$\theta = 200°$			
n	OBSD $H-H_0$	ΔH	$H-H_0$	n	OBSD $H-H_0$	ΔH	$H-H_0$
0·18	+0·076	0·008	+0·068	0·19	+0·138	·004	+0·134
·27	+0·025	·010	+0·015	·25	·102	·006	·096
·36	−0·015	·009	−0·024	·32	·082	·009	·073
·54	−0·051	·009	−0·060	·46	+0·027	·010	+0·017
·73	−0·064	·009	−0·073	·60	−0·009	·010	−0·019
1·09	−0·067	·008	−0·075	·82	−0·031	·008	−0·039
1·99	−0·052	·009	−0·061	1·6	−0·067	·002	−0·069
3·8	−0·009	·010	−0·019	3·0	−0·074	·002	−0·076
5·6	+0·003	·010	−0·007	4·4	−0·074	·002	−0·076
7·4	+0·004	·010	−0·006	5·8	−0·076	·002	−0·078

	$\theta = 240°$			$\theta = 280°$			
n	OBSD $H-H_0$	ΔH	$H-H_0$	n	OBSD $H-H_0$	ΔH	$H-H_0$
0·18	+0·096	0·007	0·089	0·18	+0·095	·009	+0·086
·31	·058	·010	·048	·31	+0·049	·010	+0·039
·43	·032	·010	·022	·43	+0·025	·009	+0·016
·56	+0·011	·010	·001	·56	+0·019	·009	+0·010
·68	−0·011	·009	−·020	·81	−0·028	·008	−0·036
·94	−0·033	·008	−·041	1·19	−0·042	·005	−0·047
1·32	−0·041	·007	−·048	1·44	−0·053	·004	−0·057
1·94	−0·053	·006	−·059	1·82	−0·051	·004	−0·055
				2·4	−0·044	·003	−0·052
				3·1	−0·054	·002	−0·056

	$\theta = 320°$		
n	OBSD $H-H_0$	ΔH	$H-H_0$
0·18	0·172	0·007	0·165
·32	·114	·010	·104
·43	·059	·009	·050
·56	·026	·008	·018
·68	+0·008	·005	0·003
·94	−0·009	·000	−0·009
1·32	−0·012	——	−0·012
2·6	−0·015	——	−0·015

TOTAL HEAD.

TABLE 20

TUBE REVERSED

$\theta = 240°$			
y	OBSD. $H-H_0$	ΔH	$H-H_0$
0·39	−0·087	—	−0·087
1·17	−0·084	—	−0·084
1·6	−0·085	—	−0·085
2·3	−0·078	—	−0·078
3·0	−0·082	—	−0·082
4·4	−0·076	·0·000	−0·076
5·8	−0·075	0·002	−0·077
7·4	−0·076	0·002	−0·078

$\theta = 280°$			
y	OBSD. $H-H_0$	ΔH	$H-H_0$
0·46	−0·064	—	−0·064
·75	−0·065	—	−0·065
1·6	−0·064	—	−0·064
3·0	−0·061	—	−0·061
4·4	−0·062	—	−0·062
5·8	−0·041	0·000	−0·041
7·9	−0·019	·001	−0·019
10·1	−0·005	·003	−0·005

$\theta = 320°$			
y	OBSD. $H-H_0$	ΔH	$H-H_0$
0·39	−0·009	—	−0·009
·89	−0·007	—	−0·007
1·17	−0·008	—	−0·008
1·6	+0·002	·003	−0·000
2·3	+0·001	·004	−0·003
3·0	+0·008	·004	+0·004
4·4	+0·004	·004	0·000
5·8	+0·004	·004	0·000
7·4	0·000	·003	−0·003

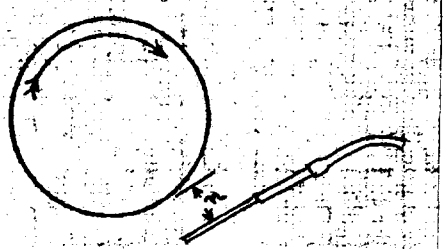

REVERSED TUBE.

TABLE 21

OBSERVATIONS OF STATIC PRESSURE NEAR A ROTATING CYLINDER IN AN AIR STREAM.

V = 8 FT/SEC. SURFACE VELOCITY = U = 16 FT/SEC.

θ	n mm.	STATIC PRESSURE p − H₀ lbs/ft²
0°	0.47	−0.036
	2.4	−0.037
	4.2	−0.036
	6.0	−0.033
20°	0.47	−0.148
	3.3	−0.128
	6.1	−0.115
40°	0.47	−0.295
	1.40	−0.289
	4.2	−0.267
	7.9	−0.236
60°	0.47	−0.436
	1.40	−0.424
	4.2	−0.397
	7.9	−0.357
80°	0.47	−0.483
	1.40	−0.449
	2.4	−0.477
	3.5	−0.494
	5.1	−0.474
	7.0	−0.455
90°	0.47	−0.405
	1.40	−0.375
	2.4	−0.404
	3.3	−0.468
	4.2	−0.502
	5.1	−0.483
	6.0	−0.474
	7.9	−0.456
100°	0.47	−0.383
	1.40	−0.339
	2.4	−0.396
	3.3	−0.430
	4.2	−0.481
	5.1	−0.487
	7.9	−0.453
120°	0.47	−0.204
	1.40	−0.219
	2.4	−0.263
	3.3	−0.341
	4.2	−0.395
	5.1	−0.420
	7.5	−0.390
160°	0.47	−0.101
	1.40	−0.189
	4.2	−0.128
	7.9	−0.132
200°	0.47	−0.080
	1.40	−0.075
	4.2	−0.073
	7.9	−0.073
240°	0.47	−0.081
	.75	−0.070
	1.17	−0.079
	1.88	−0.081
	3.3	−0.078
	4.7	−0.060
	7.5	−0.079
280°	0.47	−0.053
	1.17	−0.057
	4.7	−0.057
	8.9	−0.054
320°	0.47	−0.004
	3.3	−0.006
	7.5	−0.008

VELOCITY NEAR ROTATING CYLINDER IN AN AIR STREAM.

r = DISTANCE FROM SURFACE (MM)
VELOCITIES ARE GIVEN IN FEET/SEC.

TABLE 22

θ \ r	0·2	0·5	1·0	2·0	3·0	4·0	6·0
0°	12·3	8·6	6·3	5·8	5·8	5·8	5·5
20°	14·9	13·0	11·6	10·7	10·3	10·1	9·6
40	17·1	16·7	16·1	15·7	15·5	15·1	14·7
60	18·1	19·5	19·4	19·1	18·8	18·3	17·9
80	18·2	19·5	19·4	19·9	20·6	20·4	19·9
90	16·9	17·6	17·6	18·1	19·4	20·4	19·9
100	16·4	16·4	16·8	17·8	18·8	19·8	—
120	9·6	10·8	11·9	13·8	15·9	17·6	18·1
160	11·3	6·9	5·7	7·3	8·8	9·8	10·2
200	13·1	8·6	4·7	2·0	1·8	1·3	1·6
240	11·5	8·9	5·6	4·1	—	—	—
280	10·1	7·4	4·5	1·7	1·7	0	−4·0
320	11·6	5·1	0	−2·0	−2·2	−2·5	−2·3

VORTICITY NEAR ROTATING CYLINDER IN AN AIR STREAM.

AS GIVEN BY :- $\zeta = -\frac{\partial H}{\partial n} \div 2\rho v$

H — Total Head
v — Velocity

TABLE 23

θ \ n	0·2	0·5	1·0	2·0	4·0	6·0
0	-2500	-1300	-350	- 50	0	
20	-1300	- 850	-180	- 20	0	
40	- 60	-260	- 60	- 20	- 5	0
60	+1000	+250	- 10	- 20	-4	0
80	+1900	+600	+ 50	- 10	-0	0
90	+ 650	+580	+ 35	- 4	-13	
100	+ 320	+970	+110	- 8	-10	
120	+ 350	+620	+320	0	- 7	-7
160	-2600	-1600	+ 60	+180	+150	0
200	-1600	-1700	-800	-200	0	0
240	-1400	-1200	-460	-200	-	-
280	-1550	-1250	-800	- 55		
320	-2500	-2500	-750	0	0	+70